

**MECHANISTIC STUDIES OF PROTEIN LIPIDATION:
YEAST PALMITOYLTRANSFERASE AKR1P
AND PROTEIN FARNESYLTRANSFERASE**

by

Xiaomu Guan

A dissertation submitted in partial fulfillment
of the requirements for the degree of
Doctor of Philosophy
(Chemistry)
in The University of Michigan
2011

Doctoral Committee:

Professor Carol A. Fierke, Chair
Professor Ayyalusamy Ramamoorthy
Associate Professor Kristina I. Hakansson
Associate Professor Bruce A. Palfey

© Xiaomu Guan 2011

ACKNOWLEDGEMENTS

Many people have helped me get to this point. Foremost, I would like to thank my advisor, Prof. Carol Fierke, for her great guidance and continuous support during my Ph.D. study. Her encouragement and patience brought me confidence and helped me get through the hardest time in my research. To me, Carol is not just a knowledgeable and brilliant mentor, but also a role model in every aspect of life. I also want to thank the Fierke group members, both past and present, for many useful scientific discussions as well as friendships. Working with them has been a real pleasure. I want to express my sincere thank to my thesis committee members, Professors Ayyalusamy Ramamoorthy, Kristina Hakansson, and Bruce Palfey, for taking their time to evaluate my thesis work and to give me valuable suggestions.

Deepest gratitude also goes to my collaborators. Prof. Nicholas Davis and Dr. Amy Roth from Wayne State University provided me plasmids and yeast strains, helped me set up experiments at the initial stage of my palmitoylation project, and offered a great deal of comments and suggestions along the way. I feel very lucky to have such brilliant and kind people to collaborate with, and without them all of the accomplishments in this project would not even be possible. I must also thank Hangtian Song and Prof. Kristina Hakansson for

their contribution on the mass spectrometry experiment. Dr. Eric Simon and Prof. Philip Andrews also provided lots of help and insight in developing mass-spec conditions, which I am very grateful for.

Lastly, I want to express my utmost gratitude to my parents, who brought me to this world and raised me up to who I am today with endless love and support. I would also like to thank Yaorong Zheng, the love of my life; I cannot imagine how I could get to this point without your support and patience. I look forward to an exciting journey together with you in the rest of my life.

Thank you all.

TABLE OF CONTENTS

ACKNOWLEDGEMENTS	ii
LIST OF FIGURES	vi
LIST OF TABLES	ix
ABSTRACT	x
CHAPTER I	
INTRODUCTION	1
General Introduction of Protein Lipidation	1
Biological Significance of Protein Palmitoylation	4
DHHC Protein Family and Palmitoyltransferases (PATs)	8
Akr1p as a palmitoyltransferase	11
Methods used for studying PATs	13
Biological significance of protein prenylation	20
Structural characterization of prenyltransferases	24
Substrate recognition and catalytic mechanism of protein prenyltransferase	26
References	29
CHAPTER II	
CATALYTIC CHARACTERIZATION OF YEAST PALMITOYLTRANSFERASE AKR1P USING THE NEWLY IDENTIFIED SUBSTRATE YPL199C	48
Introduction	48
Experimental Procedures	51
Result	55
Discussion	66
References	70
CHAPTER III	
IDENTIFICATION OF PALMITOYLATION SITE(S) IN YEAST PALMITOYLTRANSFERASE AKR1P	76
Introduction	76
Experimental Procedures	79
Result	85
Discussion	98

References.....	102
CHAPTER IV	
CONSERVED AMINO ACIDS IN PROTEIN FARNESYLTRANSFERASE MODULATE PEPTIDE SUBSTRATE SELECTIVITY	
	107
Introduction	107
Experimental procedures	110
Results	113
Discussion.....	121
References.....	125
CHAPTER V	
SUMMARY, CONCLUSIONS, AND FUTURE DIRECTIONS	
	132
Summary and Conclusions.....	132
Future Directions.....	137
References.....	142

LIST OF FIGURES

Figure

1.1: Inter-compartment protein shuttling through palmitoylation-depalmitoylation cycles.	5
1.2: Schematic representation of the Akr1p sequence.	12
1.3: Prenylation pathway of substrate proteins in vivo.	23
1.4: Crystal structure of mammalian FTase.	25
1.5: Kinetic mechanism of mammalian FTase.	29
2.1: Sequence alignment of the identified yeast and human PATs.	50
2.2: Flow chart of the anti-FLAG affinity purification of Akr1p.	56
2.3: SYPRO® Ruby protein gel stain for the determination of the Akr1p concentration.	57
2.4: Analysis of reactivity of Akr1p with a new protein substrate Ypl199c.	60
2.5: Identification of the palmitoylation site(s) in the substrate Ypl199c.	61
2.6: pH profile of Akr1p palmitoylation activity.	62
2.7: Akr1p activity is not metal dependent.	63
2.8: Zinc inhibits rather than activates the Akr1p activity.	64
2.9: D, H, and C residues in the D497H498Y499C500 motif are crucial for the Akr1p palmitoylation activity.	65
2.10. The DHYC motif functions as a catalytic triad.	69
2.11: Scheme of the proposed Akr1p palmitoylation mechanism showing the first auto-palmitoylation step.	70

3.1: Schematic representation of Akrlp membrane topology showing the position of all its 12 cysteines.....	86
3.2: C663/667A double mutant abolishes the Akrlp auto-palmitoylation activity.	88
3.3: C667A mutant abolishes the Akrlp auto-palmitoylation activity but maintains the trans-palmitoylation activity, while C663A has no observable effect on catalysis.	88
3.4: Schematic procedure of the acyl-biotinyl exchange (ABE) chemistry for the characterization of the Akrlp auto-palmitoylation site(s).	91
3.5: Extracted ion chromatograms of the doubly positively charged peptide FDHYCPWIFNDVGLK from HPLC-ESI-FTICR-MS of the EXP (red) and CON (blue) samples.	93
3.6: Extracted ion chromatograms of the doubly positively charged peptide TC(NEM)FGVCYAVTGMDQWLAVIK from the HPLC-ESI-FTICR-MS spectra of the EXP (red) and CON (blue) samples.	94
3.7: In vivo labeling of WT and mutant Akrlp with 17-ODYA to analyze auto-palmitoylation.	96
3.8: Palmitoylation assay of C667A Akrlp with and without substrate Ypl199c.	97
3.9: Scheme of the proposed Akrlp palmitoylation mechanism.	99
4.1: W102 β A and W106 β A FTase activity with peptide substrates dansyl-GCva ₂ S.	114
4.2: SDS-PAGE analysis of the lysates of FTase mutants.	116
4.3: W102 β A and W106 β A FTase activity with peptide substrates dansyl-GCva ₂ S using the cell lysate-based assay.	117
4.4: Validation of the cell lysate-based assay.	117
4.5: W102 β F and W106 β F FTase activity with peptide substrates dansyl-GCva ₂ S.	119
4.6: Overlay of W102 β X and W106 β X FTase activity with peptide substrates dansyl-GCva ₂ S.	120

4.7: Crystal structure of FTase α_2 residue binding pocket.....	123
5.1: Schematic representation of the HIP14 sequence.	140
5.2: pReceiver-B13 vector information for HIP14 and substrate PSD-95.....	141

LIST OF TABLES

Table

1.1: Structures, signals, and corresponding enzymes of three types of lipid modifications.....	4
1.2: Four different types of palmitoylation with correlated substrate proteins...7	
2.1: Akr1p substrate candidates based on the global analysis of protein palmitoylation in yeast.	67
5.1: Peptide library designing criteria and sequence examples for studying the substrate recognition of Akr1p.....	138

ABSTRACT

MECHANISTIC STUDIES OF PROTEIN LIPIDATION: YEAST

PALMITOYLTRANSFERASE AKR1P AND PROTEIN

FARNESYLTRANSFERASE

by

Xiaomu Guan

Chair: Carol A. Fierke

Protein palmitoylation is a widespread lipid modification in which cysteine thiols on a substrate protein are modified with a palmitoyl group. Mutations in palmitoyltransferases responsible for this modification are associated with a number of neurological diseases and cancer progression. Defining the active site and catalytic mechanism of palmitoyltransferases represents a key step towards understanding its biological significance. Akr1p, one of the first identified protein palmitoyltransferases, is an 86 kDa yeast integral membrane protein. Mutagenesis studies of Akr1p suggest that a conserved DHYC motif serves as a potential active site; the hypothesized mechanism is a two-step mechanism where the palmitoyl group is transferred from palmitoyl-CoA to Akr1p, and finally from Akr1p to the substrate protein. A covalent intermediate has been detected using radioactive assays. In this study, we elucidated the

role of each amino acid in the DHYC motif using mutagenesis. In addition, mutagenesis of all of the cysteine residues in Akr1p along with mass spectrometric analysis demonstrated that the DHYC cysteine is the site in Akr1p where a covalent thioester intermediate forms. Based on these data, we propose a detailed mechanism for palmitoylation catalyzed by Akr1p, which may shed light on the mechanism of other palmitoyltransferases within the DHHC protein family.

Protein farnesylation is another important lipid modification in which the cysteine of a substrate protein is modified by attachment of a 15-carbon farnesyl group which results in membrane localization of the protein. Protein farnesyltransferase (FTase) catalyzes farnesylation of a specific C-terminal “Ca₁a₂X” sequence of substrate proteins. Here we analyze the determinants of recognition of the a₂ residue by FTase, demonstrating that completely conserved tryptophan residues in FTase, although not essential for maintaining the farnesylation activity, play an important role in modulating the substrate selectivity of FTase. Mutagenesis studies demonstrate that the conserved W102 β and W106 β residues modulate both the reactivity of FTase and substrate selectivity based on the size of the binding pocket. The complete conservation of these two amino acids suggests that maintenance of the exact substrate selectivity of FTase is crucial for the *in vivo* activity.

CHAPTER I

INTRODUCTION

General Introduction of Protein Lipidation

As many as 25-40% of eukaryotic cellular proteins are estimated to be membrane-associated proteins (1). To interact with the hydrophobic lipid bilayer environment of cell membranes, proteins require hydrophobic surfaces formed by structures such as α -helices or β -sheets. In addition to that, permanent cotranslational additions or posttranslational modifications under dynamic enzymatic control also allow proteins to be attached to the membrane by lipid anchors, which serve as the hydrophobic interface to interact with the hydrocarbon core of the lipid bilayer. These lipid modifications are increasingly recognized as important mechanisms for membrane targeting and subcellular protein trafficking which allow proteins to obtain a variety of functions. To date hundreds of proteins have been shown to be covalently modified with lipid groups, many of which are important for the cellular function of these proteins. For example, the lipidated forms of receptors, monomeric and trimeric G-proteins (2-5) and protein tyrosine kinases (6-11) play crucial roles in a variety of cell signaling events.

Protein lipid modifications can be broadly divided into two categories. The

first category includes modifications that orient the protein to the outside of the cell such as glycosylphosphatidylinositol (GPI) anchoring (12-20) and cholesterolation (21-23). GPI moiety is important for the trafficking of proteins through the secretory pathway from the endoplasmic reticulum (ER) to the Golgi apparatus, and finally to the extracellular face of the plasma membrane. The second category of lipidation includes modifications that orient the protein to the cytoplasmic side of the plasma membrane, which is what this work will be focusing on. These modifications can be further divided into 3 types: N-myristoylation (24-28), prenylation (4, 29-35), and palmitoylation (36-44) (Table 1.1). N-myristoylation entails formation of an amide bond between the N-terminal amino group of a protein and a 14-carbon saturated fatty acid (myristate). This is a large category among lipid modifications, as about 5% of eukaryotic proteins are N-myristoylated. N-myristoylation occurs on proteins with an N-terminal sequence of Met-Gly-. First the N-terminal methionine is cleaved, catalyzed by methionine aminopeptidase and then the N-terminal glycine reacts with myristoyl-CoA to form an amide linkage, catalyzed by N-myristoyltransferase (25). Another type of modification, protein prenylation, includes both farnesylation (45-52) and geranylgeranylation (53-55). In this case, a cysteine thiol side chain near the C-terminus of a substrate protein reacts with a prenyl diphosphate to form a thioester with either a 15-carbon (farnesyl) or 20-carbon (geranylgeranyl) isoprenoid group. The enzymes that catalyze these modifications, protein farnesyltransferase (FTase) and

geranylgeranyltransferase type-I (GGTase-I) recognize canonical protein substrates containing a C-terminal 'CaaX' box, in which 'C' refers to the prenylated cysteine residue, while 'a' refers to any aliphatic amino acids, and X is proposed to be a set of amino acids that determine the type of lipid group added to the protein (either farnesyl or geranylgeranyl) (46, 56-58). Once the protein is prenylated on the cysteine, the terminal 'aaX' sequence can be cleaved catalyzed by CaaX protease Rce1, followed by carboxymethylation of the terminal prenyl cysteine catalyzed by protein S-isoprenylcysteine O-methyltransferase (ICMT) (59-61). The protein can then be trafficked to the Golgi apparatus for additional modifications, processing, and trafficking to the plasma membrane. Protein geranylgeranyltransferase type-II (GGTase-II) prenylates Rab proteins using a similar catalysis mechanism by recognizing the cysteines at or near their C-terminus (55). Lastly, palmitoylation involves the formation of a thioester bond between a cysteine thiol side chain and a saturated 16-carbon fatty acid (36-44). The major unique feature of this modification is that it is readily reversible due to the lability of the thioester bond. Therefore rapid palmitoylation and depalmitoylation allow modified proteins to be readily shuttled between the plasma membrane and the Golgi complex to regulate many cellular functions (62-68). Palmitoylation is catalyzed by protein palmitoyltransferases (PATs). Although many PATs have been recently identified using sequence homology, the motifs they recognize in the substrate proteins are still poorly defined. A summary of the structures,

recognition signals, and the corresponding enzymes that catalyze each lipid modification are listed in Table 1.1. Studies conducted over the past decades have substantially advanced our understanding of not only the molecular mechanisms and the functional consequences of these modifications, but also disclosed important implications for biomedical research and drug development. This thesis will focus on studying the catalytic mechanism and molecular recognition of the enzymes responsible for catalyzing two of the most important lipidation reactions, palmitoylation and farnesylation.

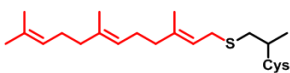
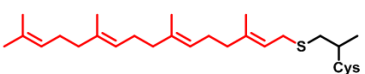
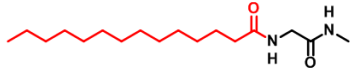
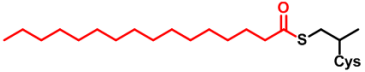
	Lipid Modifications	Signals	Enzymes
Prenylation	Farnesylation 	—CaaX	Farnesyltransferase Geranylgeranyltransferase I
	Geranylgeranylation 	—CC or —CXC (Rab proteins only)	Geranylgeranyltransferase II
N-myristoylation		MGxxS—	N-myristoyltransferase
Palmitoylation		Poorly defined	Palmitoyltransferase

Table 1.1: Structures, signals, and corresponding enzymes of three types of lipid modifications. The lipid portion of each modification in the structures is highlighted in red. The recognizing signals for both prenylation and N-myristoylation have been well identified, while there has not been a consensus signal for palmitoylation.

Biological Significance of Protein Palmitoylation

As described earlier, palmitoylation is an important reversible lipid modification (62, 63, 65-68). However, palmitoylation functions in the cell are more than just a lipid anchor. The reversibility of palmitoylation differentiates it

from the other two types of lipid modifications, and allows proteins to be shuttled among cellular compartments. A scheme of this process is shown in Figure 1.1, where proteins are continually relocalized in the cell or within different regions of the membrane through palmitoylation and depalmitoylation (69). Therefore, in addition to enhancing the membrane association of proteins, palmitoylation also helps target proteins in neurons, recruit proteins into lipid rafts, regulate cell signaling processes, etc. (65-67). Defining the active site and catalytic mechanism of palmitoyltransferases responsible for this modification represents a key step towards understanding its biological significance and developing active site-directed inhibitors.

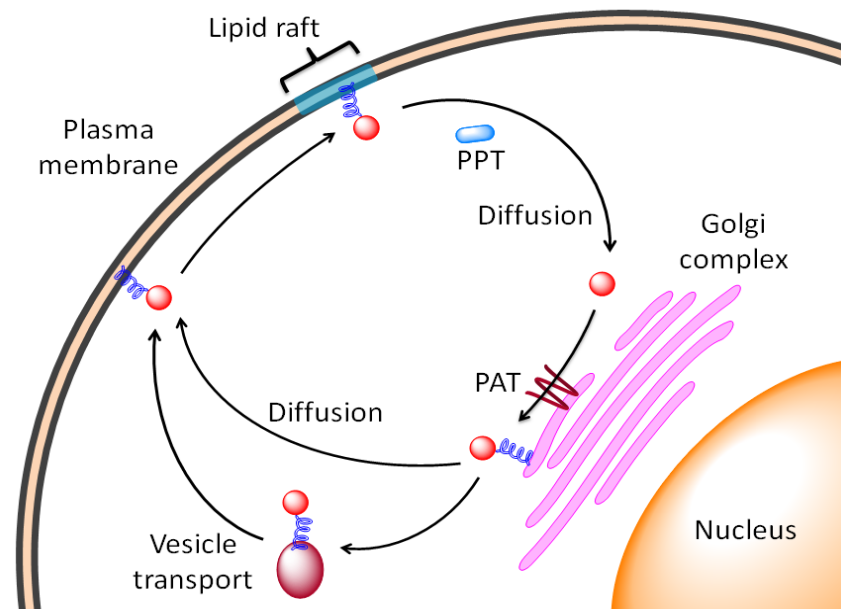


Figure 1.1: Inter-compartment protein shuttling through palmitoylation-depalmitoylation cycles. Palmitoylated proteins (shown as a red circle with an attached blue fatty acid chain) is trafficked to the plasma membrane through either diffusion or vesicle transport, and is then targeted to lipid rafts. Depalmitoylation is catalyzed by putative palmitoyl protein thioesterase (PPT, shown as a blue oval), leading to a palmitoylated half-time of 20 min to 2 h. The depalmitoylated protein diffuses back to the Golgi complex where it can be palmitoylated for another cycle.

The major function of palmitoylation is likely to promote protein membrane association. Palmitoylation required for membrane localization can be divided into 4 types of substrate proteins (70-77), which are shown in Table 1.2. Proteins can also be dually lipidated with a palmitoyl group and either a prenyl group or a myristoyl group. For example, mammalian Ras proteins are farnesylated for interacting with cell membrane but additional interactions are needed to enhance membrane localization, which is palmitoylation for H-Ras and N-Ras, while K-Ras membrane association is enhanced by the electrostatic interaction between its positively charged basic sequence and the negatively charged plasma membrane (46, 78-80). The first modification in the dually lipid modification model (e.g. prenylation and myristoylation) is proposed to provide substrate proteins with a weak membrane interaction, while the subsequent palmitoylation generates sufficient hydrophobicity for strong membrane affinity (81, 82). However, there are a number of proteins that are only modified with a palmitoyl group. A good example is the G-protein α subunits, which are palmitoylated to enhance the interaction with $G_{\beta\gamma}$ subunits, an essential step in cell signaling cycles (43). Regulators of G-protein signaling (RGS) also go through a single palmitoylation mechanism, which regulates membrane localization and inactivation of G proteins to turn off the G protein-coupled receptor signaling pathways (43, 68, 83).

Furthermore, numerous neuronal proteins are palmitoylated, including synaptic scaffolding proteins, G-protein-coupled receptors (GPCRs) and

synaptic vesicle proteins (68). Palmitoylation of these proteins is vital for regulating proper neuronal development and function, including neuronal differentiation, neurotransmission, and neurotransmitter release (84-86). One of the first neuronal proteins that was demonstrated to be palmitoylated is rhodopsin, in which two cysteines proximal to the transmembrane domain are modified with palmitoyl groups (87). Similarly, many GPCRs are palmitoylated on analogous cysteines (85). A second example is the dendritic postsynaptic density protein 95 (PSD-95) that requires palmitoylation to enhance clustering of AMPA receptors at excitatory synapses; furthermore, palmitate cycling of PSD-95 also regulates synaptic plasticity (88-90). Palmitoylation of the SNARE

palmitoylation type	substrate proteins
palmitoylation + prenylation -CXC*aaX ¹	Ras proteins, Rho Proteins, G _γ subunits
palmitoylation + myristoylation MGC*- ¹	G _α subunits, Src family kinases (Yes, Fyn, Lck)
proximal to TMDs ²	GPCRs ² , viral-envelope proteins (HIV, influenza)
palmitoylation alone	G _α subunits, GRKs ² , RGS ² , SNAP-25, PSD-95

Table 1.2: Four different types of palmitoylation with correlated substrate proteins. Although many proteins have been identified to be palmitoylated, the recognition signal in the protein is still poorly defined. Palmitoylation could happen alone, with the presence of transmembrane domains, or with the combination of other lipid modifications.

¹ Palmitoylation sites are identified with a *.

² Abbreviations used: TMD = transmembrane domain; GPCR = G protein-coupled receptor; GRK = G protein-coupled receptor kinase; RGS = regulator of G protein signaling.

protein (soluble *N*-ethylmaleimide-sensitive fusion protein-attachment protein receptor) SNAP-25 (25 kDa synaptosome-associated protein) is also important for neuronal functions (91). SNAP-25 is located at presynaptic axon terminals, and is essential for neurotransmitter release (92). Palmitoylation of SNAP-25 is proposed to help regulate aspects of synaptic vesicle fusion, and to target synaptic vesicles to the site of transmitter release (93).

Palmitoylation also functions to target proteins to lipid rafts. Lipid rafts are dynamic nanoscale assemblies in the cell membrane that are enriched in sphingolipid, cholesterol, and GPI-anchored proteins (94, 95). Studies have shown that proteins no longer localize to lipid rafts if palmitoylation is blocked by either mutagenesis or inhibition of PATs (28, 96-99). The localization of proteins to the lipid rafts is especially important for signaling proteins. The best-studied examples are nonreceptor tyrosine kinases (NRTKs) and linker for activation of T cells (LAT) which are involved in T cell signaling events where mutations of the palmitoylated cysteine residues in these proteins disrupt the lipid raft structure, and lead to attenuated T-cell responses (100-102). These studies assert the important role that palmitoylation plays in localizing proteins to functional membrane subdomains, such as lipid rafts.

DHHC Protein Family and Palmitoyltransferases (PATs)

Even though palmitoylation of protein thiols can occur nonenzymatically *in vitro* upon incubation with palmitoyl-CoA within a few hours (103), protein palmitoylation in the cell is catalyzed by palmitoylating enzymes, namely,

protein palmitoyltransferases (PATs) (78). PATs catalyze the thioesterification of cysteines in the substrate protein with a palmitoyl group using palmitoyl-CoA as a co-substrate. One of the first identified PATs is the *Saccharomyces cerevisiae* Ras palmitoyltransferase Erf2p/Erf4p (effectors of Ras function) (104). As mentioned earlier, Ras proteins are first prenylated on a C-terminal cysteine within the CaaX sequence which enhances their localization to the ER membrane. Here the Erf2p/Erf4p PAT catalyzes palmitoylation of an upstream cysteine which enhances the interaction with the membrane. The two proteins in the Erf2p/Erf4p co-purify and are both required for Ras palmitoylation activity. Deletions of the *ERF2* or *ERF4* gene in yeast lead to a decrease in palmitoylation and mislocalization of Ras in the cell (105). Phenotypic analysis leads to the identification of a second palmitoyltransferase, Akr1p (ankyrin-repeat-containing protein), in yeast. This enzyme catalyzes palmitoylation of Yck2p (yeast casein kinase 2) both *in vivo* and *in vitro*. In the *AKR1Δ* strain, Yck2p localizes diffusely in the cytosol rather than associating with the membrane (106).

Both Erf2p and Akr1p are integral membrane proteins that contain several transmembrane domains (TMDs), and share a common DHH/YC-CRD (Asp-His-His/Tyr-Cys-cysteine rich domain) positioned between two TMDs (78, 107). For the majority of PATs the consensus sequence is DHHC, while this sequence is DHYC in Akr1p. For both enzymes, mutations in this motif abolish the palmitoyltransferase activity, suggesting that this motif is involved in the

palmitoylation catalytic mechanism.

Based on the prediction that the DHHC motif is important for catalytic activity of PAT, a search of the yeast genome for the DHHC-containing proteins was carried out, leading to the discovery of five other putative PATs, including Akr2p, Swf1p, Pfa3p, Pfa4p, and Pfa5p (73, 108-110). All of these proteins catalyze palmitoylation reactions with varying substrate recognition. These results further confirmed the importance of the DHHC-CRD sequence for PAT activity. Similar research has been extended to other organisms as well; there are now 23 mammalian DHHC proteins identified and they all possess palmitoyltransferase activity. In addition, 15 genes from *Caenorhabditis elegans* and 22 genes from *Drosophila melanogaster* are also predicted to have PAT activity from their conserved DHHC sequence (111).

Among the 23 mammalian PATs, several are suggested to have biomedical relevance as their palmitoylated substrates are involved in the pathogenesis of neurological disorders, such as Huntington's disease (DHHC17) (112), schizophrenia (DHHC8) (113), and X-linked mental retardation (DHHC9 and DHHC15) (114). One of the most notable example is DHHC17, better known as HIP14 (huntingtin interacting protein 14) (112, 115, 116). HIP14 catalyzes the palmitoylation of several neuronal proteins, including huntingtin, PSD-95 (88, 89, 117, 118), and SNAP-25 (91). Furthermore, HIP14 activity regulates the subcellular trafficking and function of huntingtin, leading to the suggestion that it is involved in the pathogenesis of

Huntington's disease (116). Consistent with this, studies have indicated that the N-terminal polyglutamine (polyQ) expansion of the huntingtin protein prevents interaction with HIP14, and therefore leads to a decrease in its palmitoylation level, which enhances aggregation of the protein (116). Further studies on the palmitoylation mechanism of HIP14 as well as other DHHC proteins may disclose their exact pathophysiological roles in neurological disorders (119).

Akr1p as a palmitoyltransferase

Akr1p, the yeast homologue of HIP14, is an 86-kDa integral membrane protein with six transmembrane domains. The N-terminal hydrophilic domain contains six ankyrin repeat sequences. The topology of Akrlp in the membrane indicates that the conserved DHHC-CRD sequence is located on the cytosolic side of the membrane between transmembrane domains four and five (120). A scheme of the Akrlp domains is shown in Figure 1.2.

Davis and colleagues have carried out multiple studies demonstrating that Akrlp is a palmitoyltransferase that catalyzes the palmitoylation of yeast casein kinase (Yck2p) both *in vivo* and *in vitro*. In the wild-type (*AKR1*⁺) yeast cells Yck2p is exclusively trafficked to the cell membrane, whereas in *akr1Δ* cells Yck2p is diffusely localized in the cytoplasm (106). This finding is consistent with the role of palmitoylation tethering proteins to the membrane. In addition, the C-terminus of Yck2p contains two cysteines that are hypothesized as the palmitoylation sites. Consistent with this, mutations of the

two C-terminal cysteines (-CC) to serines (-SS), leads to the relocalization of Yck2p from the membrane to the cytoplasm, as observed for WT Yck2p in *akr1Δ* cells (106).

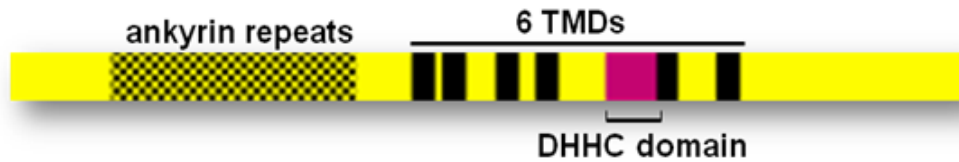


Figure 1.2: Schematic representation of the Akr1p sequence. Ankyrin repeats are shown in the shaded region; the six transmembrane domains are indicated in black and the DHHC domain is highlighted in magenta.

Furthermore, the DHHC motif of Akr1p is important for catalytic activity as observed for Erf2p, mutations in the DHYC motif disable the Akr1p catalytic activity; mutation of DH to AA, or C to A eliminates labeling of Yck2p with palmitate both *in vivo* and *in vitro* (106).

To search for palmitoylated proteins in yeast, the Davis lab carried out a global analysis of yeast membrane proteins using MudPIT (multi-dimensional protein identification technology) tandem-MS-based proteomic methodology (108). Forty-seven palmitoylated proteins, including Akr1p, were identified by MS/MS data. To identify the substrate proteins palmitoylated by each of the DHHC-containing palmitoyltransferases, including Akr1p, this proteomic method was applied to mutant yeast strains deficient for one of more DHHC proteins. To identify the putative substrates of Akr1p, MudPIT analysis was carried out on proteins isolated from the *akr1Δ* strain. Akr1p substrates were identified with a decreased representation in the MS/MS data. Based on this experiment six yeast proteins were identified as potential Akr1p substrates:

Yck1p, Yck2p, Akr1p, Ypl199c, Yki047w, and Meh1p.

It is worth noting that Akr1p is palmitoylated upon incubation with palmitoyl-CoA, which is known as auto-palmitoylation (106). Interestingly, this phenomenon has been observed in many other DHHC protein palmitoyltransferases as well. The auto-palmitoylation is proposed to be enzyme catalyzed since the DHHC sequence is required. Alanine mutations of DH or C in the conserved DHYC sequence abolish both the auto-palmitoylation and trans-palmitoylation both *in vivo* and *in vitro*. The cysteine in the DHHC motif has been proposed as the site of auto-palmitoylation in PATs; however this has not yet been demonstrated. In this work, we use mass spectrometric analysis to demonstrate that the cysteine in the DHHC motif is palmitoylated in Akr1p.

In fact, the auto-palmitoylated enzyme has been hypothesized to be a covalent intermediate that occurs during catalysis. In this proposed mechanism, a palmitoyl group is first transferred to covalently label an amino acid side chain in the PAT, followed by transfer of the palmitoyl group from the enzyme to the substrate protein in a second step. Kinetic measurements of the Erf2p/Erf4p PAT are consistent with the formation of an intermediate, providing support for this mechanism (121).

Methods used for studying PATs

Palmitoyltransferases are integral membrane proteins that contain several transmembrane domains. Therefore these proteins are difficult to overexpress

and purify in large quantities which presents a big challenge to the characterization of PATs. In this section, some current methods used to express, purify, and characterize of yeast PATs will be presented.

Expression and purification of yeast PATs

The largest quantities of active yeast PATs have been obtained using galactose inducible yeast expression systems. Active Akr1p has not yet been obtained by recombinant expression in *E. coli*. This is likely due to both the difficulty of expression of eukaryotic membrane proteins in bacteria and the lack of necessary posttranslational modifications.

Deschenes and colleagues have optimized the expression of yeast PATs, including Erf2p, Akr1p, Pfa3p, Pfa4p, and Pfa5p (122). The FLAG-tagged version of these protein genes encoded on a yeast plasmid were transformed into yeast strain YPH499, and the cells were grown on selective media. The culture was then induced for 16 h by adding galactose at the OD₆₀₀ of 0.4-0.6. The cells were harvested by centrifugation at 1000 × *g* and lysed by vigorous vortexing with glass beads. The unbroken cells were removed by gentle centrifugation and the membrane fractions were collected using ultracentrifugation at 200,000 × *g*. Membrane-based PAT assays were also performed with the diluted membrane fractions of each protein. It was shown that the membrane fractions containing PATs were sufficient to palmitoylate their corresponding protein substrates, suggesting that the PATs expressed well using this system.

Purification of PATs was developed using Erf2p/Erf4p as an example. The membrane fractions were first solubilized by adding 0.75% (w/v) detergent. A few different detergents were tried including dodecylmaltoside (DDM), deoxycholic acid (DCA), Triton X-100, octylglucoside, and CHAPS. DDM turned out to be the most effective detergent in solubilizing the PAT Erf2p/Erf4p, which was tested by immunoblotting for 6×His-Erf2p and FLAG-Erf4p with anti-His and anti-FLAG antibodies. Triton X-100 and DCA also provide good results in solubilizing the PAT but are less effective in maintaining the palmitoylation activity (122). Following protein solubilization, Erf2p/Erf4p was then purified using nickel affinity and anion exchange chromatography, with DDM present in all wash buffers and the elution buffer. The purified active protein was obtained based on UV₂₈₀, SDS-PAGE, and PAT activity assay.

To sum up, the expression of the yeast PATs can be best achieved by using the galactose inducible yeast expression system, and to extract the maximum amount of PAT from the membrane fraction while maintaining the most activity, a suitable detergent needs to be added during purification.

Palmitoylation assays

To study catalysis of palmitoylation and obtain a better understanding of its biological significance, and therefore assisting the drug discovery in treating neurological diseases, a robust palmitoylation assay is required. Several palmitoylation assays have been developed and used to study PATs; each assay has both advantages and disadvantages (123).

The first developed and most frequently used assay is the *in vivo* metabolic labeling of proteins using radiolabeled palmitate, most commonly [³H]palmitate (89, 104, 124-126). The radiolabeled palmitate is added to the cell culture during growth, where the palmitoyl moiety is incorporated onto target proteins. The labeling of proteins is evaluated by fractionation of the proteins by SDS-PAGE of the cell lysate followed by exposing the dried gel to high-sensitivity films. This method provides an efficient way to identify palmitoylated proteins and to assess the palmitoylation level of a certain protein in living cells. In a pulse-chase format this assay can also be used to measure both the palmitoylation and depalmitoylation rates. Disadvantages of this method are: low sensitivity requiring long hours of labeling and exposure time for detection of the radioactive signal and difficulty with accurately quantifying the result, since the *in vivo* labeling process is affected by many cellular factors. Therefore, this method is useful for the initial identification of PATs but is not suitable for further mechanistic characterization of the enzymes.

A similar assay labels palmitoylated proteins with ω -azido-fatty acids. In this method synthetic ω -azido-fatty acid is added to the cell culture during growth, so the target proteins was labeled with a palmitoyl group containing an azido group at the end of the fatty acid chain (127). Following *in vivo* labeling, proteins can be extracted and subjected to click chemistry (127, 128) to label the proteins with a detectable chemical probes, such as biotin or a fluorophore,

to quantify the palmitoylated proteins. This method is both safer and more sensitive than labeling with radiolabeled palmitate; however, it requires multiple steps and presents challenges for quantification and measurement of the time-dependence of the reactions.

Another commonly used assay is the *in vitro* palmitoylation assay, in which peptides mimicking the protein palmitoylation motif or whole proteins are used as substrates, and PATs catalyze palmitoylation upon addition of exogenous palmitoyl-CoA (129). When using peptides as substrates, fluorescent labeling enhances the sensitivity of the assay and the palmitoylated peptides can be separated from the non-palmitoylated peptides by high performance liquid chromatography (HPLC). However, not all PATs react readily with peptide substrates. When using whole proteins as substrates, the radiolabeled palmitoyl-CoA is used so that palmitoylation is detected by autoradiography after separation by SDS-PAGE. This method is more quantitative, requires less reaction handling for signal detection, and can be used to measure time-dependent reactions. This assay has also been applied in a cell-based assay format, in which intact cells are incubated with fluorescently-labeled peptides and endogenous palmitoyl-CoA. This assay has the advantage of speed and simplicity and can be used to study the intracellular trafficking of the palmitoylated peptides. The *in vitro* palmitoylation assay has been widely used to study the catalytic mechanism of PATs.

In a recent kinetic study of Erf2p/Erf4p, the Ras PAT, Deschenes and

colleagues introduced a coupled fluorescence-based assay to indirectly monitor the rate of CoASH release from palmitoyl-CoA in the palmitoylation reaction (121). A standard curve between NADH production and CoASH concentration in control reactions with various CoASH amounts was plotted, and the PAT activity was determined based on the standard curve. Based on the kinetics data obtained using this assay, they concluded that palmitoylation by Erf2p/Erf4p is proceeded by a two-step mechanism: the enzyme is first auto-palmitoylated to form a palmitoyl-Erf2p intermediate, followed by the transfer of the palmitoyl moiety to the Ras2p substrate. This assay does not require using the radioactive material, and can be performed on a 96-well plate which makes it potential for high-throughput inhibitor screening. The challenge is that it is not as sensitive as the radioactive assay, and therefore needs sufficient amount of active enzyme and substrate protein to generate detectable signal from CoASH.

Besides the traditional biochemical assays, mass spectrometry has become an important tool for studying the posttranslational modifications of proteins, including lipidation (126, 130, 131). In this case, the palmitoylated proteins are subjected to protease digestion and the resulting peptides are separated by chromatography. By comparing the sample spectrum with the control (no modification), the peptides with the palmitoyl group are easily identified by matrix-assisted laser desorption ionization time-of-flight mass spectrometry (MALDI-TOF MS) based on the 272 Da mass shift for the

palmitoyl group (132). This method is not quantitative but is a versatile tool to identify palmitoylated proteins. However, this method has some complications. For example, the thioester linkage is not stable so that the palmitoyl moiety can get lost during sample preparation, especially at high or low pH in the presence of exogenous thiols. In addition, peptides containing a hydrophobic fatty acid chain, like palmitoyl, have low solubility, can stick to separation columns and may have poor ionization efficiency. Based on these difficulties, this method was optimized by performing an additional step, called fatty acyl exchange chemistry, before mass spectral analysis (108, 133-135). This method has three basic steps which replace the labile thioester bond with a more stable thioether linkage. The first step involves blocking of all of the unlabeled free cysteine thiols by reaction with N-ethylmaleimide (NEM). In the second step, the thioester bond with the palmitoyl group is cleaved by the addition of hydroxylamine, exposing the palmitoylated cysteines. Last, the exposed cysteine thiols are reacted with thiol-specific reagents with detectable function groups, such as 1-biotinamido-4-[4'-(maleimidomethyl) cyclohexanecarbox-amido] butane (Biotin-BMCC) and biotin-HPDP. After these steps, the labeled peptide is purified and analyzed by mass spectrometry. This optimized method has been successfully used to identify palmitoylated proteins in several biological systems. For example, Davis and colleagues have successfully identified most of the palmitoylated proteins in yeast (108), and Freeman and colleagues identified palmitoylated proteins and their sites of modification in

lipid raft-enriched and non-raft membranes of mammalian cells (135). This method can generate false positives, due to the non-specific nature of the reactions; therefore, careful controls and confirmation of the results using other biological tools are essential. Overall, this method has great advantages for discovering novel palmitoylated proteins but may not be suitable for detailed mechanistic studies of the enzymatic reactions.

To sum up, there are a number of assays that have been developed to study protein palmitoylation, with each having their own advantages and disadvantages. Using these assays, many novel palmitoylated proteins have been identified, some of which have been further mechanistically characterized. However, to obtain an in-depth picture of the palmitoylation mechanism, faster, more sensitive, and higher-throughput assays are desired.

Biological significance of protein prenylation

Protein prenylation is another important lipid modification that tether proteins to membranes (4, 29-35, 136). This modification has been shown to be essential for the proper biological function of more than 100 proteins, by serving as membrane anchors or acting as sites for protein-protein interactions. Protein prenylation was first discovered in 1978, when prenylated peptides was isolated from secreted yeast sex hormones as part of a yeast mating factor (137). Since then, prenylation has been widely studied to illuminate its function, structure, and catalytic mechanism.

Protein prenylation can be divided into three subfamilies: farnesylation

(45-52), geranylgeranylation I (35, 138-142), and geranylgeranylation II (Rab geranylgeranylation) (53, 55, 143, 144). Farnesylation involves the addition of a 15-carbon farnesyl group from farnesyl diphosphate (FPP) onto the cysteine thiol of a protein substrate, and this reaction is catalyzed by protein farnesyltransferase (FTase). Geranylgeranylation I, catalyzed by protein geranylgeranyltransferase type I (GGTase-I), recruits a 20-carbon geranylgeranyl group from geranylgeranyl diphosphate (GGPP) to form a thioether bond with a protein substrate. Both FTase and GGTase are $\alpha\beta$ heterodimers and they share a common 48 kDa α subunit with different β subunits (35). Mechanistic studies have shown that they both recognize a canonical C-terminal CaaX sequence of the substrate protein, with “C” as the cysteine that is modified with the farnesyl / geranylgeranyl group, “a” being an aliphatic amino acid, and “X” being a certain set of amino acids that determines the substrate specificity of the enzyme recognizing either FPP or GGPP (145). Later studies have demonstrated broader substrate recognition (146). Geranylgeranyltransferase type II (Rab GGTase), modifies Rab proteins with the 20-carbon geranylgeranyl group from GGPP using a similar catalytic mechanism. However, rather than the CaaX sequence of the substrate protein, it recognizes the whole structure of Rab proteins is recognized (147, 148). Therefore, Rab GGTase is usually categorized separately and will not be further discussed here.

Protein prenylation has received great interest ever since its discovery

due to the potential significant implications for medical research since it has been suggested to be involved in many diseases (48, 50, 149-154). For example, a large portion of the characterized prenylated proteins are small GTPases that belong to the Ras superfamily, including Ras, Rho, Cdc42, Rac, Rap, and Rab proteins (153-155). A prenylation pathway of Ras proteins is shown in Figure 1.3, and prenylation is indispensable for them to be properly processed and trafficked to the plasma membrane for appropriate functions in the cell. Mutations of these proteins occur in 30% of all human cancers (156). Farnesyltransferase inhibitors (FTIs) have been characterized and are being tested in clinical trials as anticancer drugs (157, 158). In addition to inhibition of tumor growth, FTIs have also been implicated for the treatment of a rapid aging genetic disease, Hutchinson-Gilford progeria, in animal models, which is caused by mutations in protein lamin A (159). Lamin A contains a C-terminal CaaX motif which is farnesylated and subsequently the C-terminus is proteolyzed to dissociate the protein from the nuclear membrane for proper function in the nucleus. The mutated form of lamin A, however, lacks the protease site and is therefore not processed appropriately. Hence, the farnesylated lamin A accumulates in the nuclear membrane which is very likely the cause of the symptom. FTI treatment allows lamin A to localize normally to the nucleus and releases many of the disease symptoms in animal models. Recently, FTIs with specificity for inhibition of parasitic FTases have shown promising results in the treatment of parasitic infections. For example, FTIs

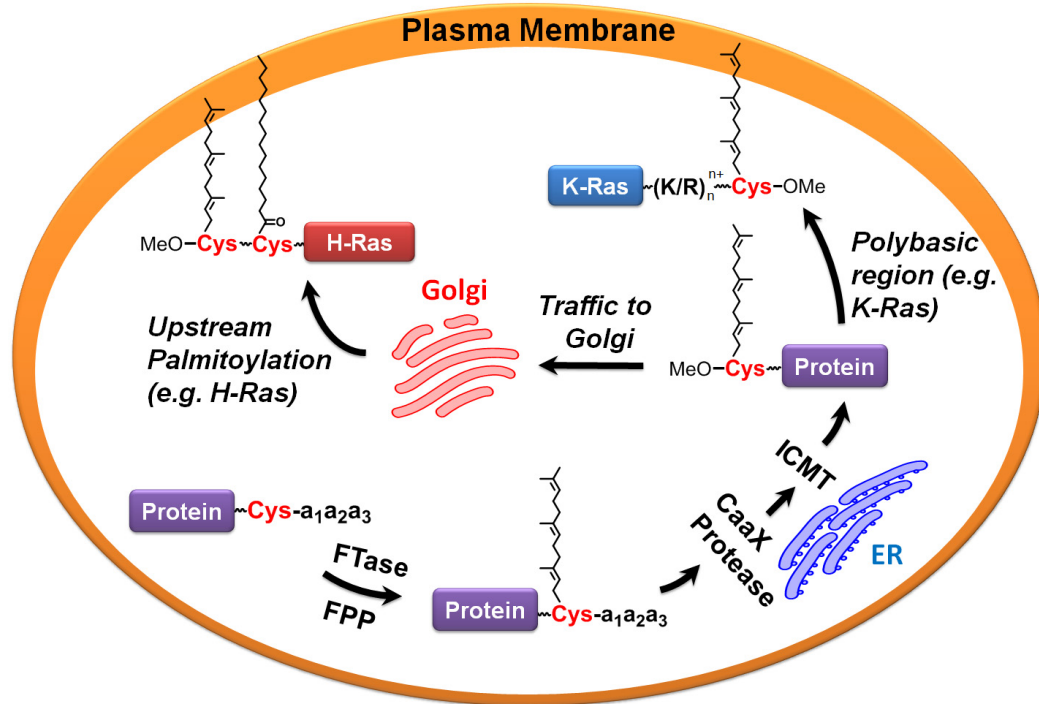


Figure 1.3: Prenylation pathway of substrate proteins in vivo. With Ras protein as an example, the pathway starts with farnesylation on the C-terminal cysteine of the protein (highlighted in red), followed by processing with CaaX protease and ICMT, generating a new carboxyl methyl group on the modified protein. The protein can then be recognized, and further localized to the plasma membrane with the assist of either its polybasic region (K-Ras) or upstream palmitoylation occurred in Golgi (H-Ras).

have been reported to inhibit the growth of the Malaria parasite *Plasmodium falciparum* both *in vivo* and *in vitro*, and inhibitors of the *Trypanosoma brucei* FTase also inhibits the *Trypanosoma brucei* cell growth, suggesting the development of novel therapeutics against African Sleeping Sickness (160-163). Similar to FTIs, GGTase-I inhibitors (GGTIs) also inhibit tumor growth. In addition, they have been shown to promote the activity of statins in the cholesterol biosynthesis pathway and therefore benefit cardiovascular health (164). GGTase I is also a potential targets for antifungal therapies. GGTIs have been reported to have antifungal activity for *Candida albicans*,

which is a causing agent of systemic fungal infections in immunocompromised individuals (165-167). Finally, the recent observation of host-catalyzed prenylation of proteins from bacterial pathogens, such as *Legionella pneumophila* (168), suggests the possibility that FTIs could serve as antibacterial agents as well.

Structural characterization of prenyltransferases

FTase and GGTase-I are $\alpha\beta$ heterodimers, and they contain a common 48 kDa α subunit, and a homologous β subunit, which is 46 kDa for FTase and 42 kDa for GGTase-I (142, 169). Both subunits are composed primarily of α helices, and the crescent-shaped α subunit is arranged around the barrel-shaped β subunits, with a catalytic zinc ion bound to the β subunit near the subunit interface. A picture of the overall structure of FTase complexed with a peptide substrate and FPP analogue is shown in Figure 1.4.

The α subunit of these prenyltransferases is composed of a set of seven pairs of α helices that form a superhelix. The N-terminal domain is a proline-rich domain that is not essential for either the catalytic activity (170) or stabilizing the protein structure (171) and has been suggested to interact with other cellular factors for directing enzyme localization. The β subunits are composed of 14 (for FTase) or 13 (for GGTase-I) helices with very similar structures. It has a barrel shape, with six core α helices forming the bottom of the barrel, and the other six antiparallel α helices forming the side of the barrel. The β subunit is crucial for the catalytic activity of these enzymes as the active

site is located within the cavity shaped by the barrel. This cavity contains many conserved hydrophobic residues, which interact with FPP or GGPP and the CaaX sequence of the protein substrate. These residues are not only important for regulating the prenylation activity, but they also determine the substrate selectivity of the enzymes, which will be discussed in detail in chapter 4.

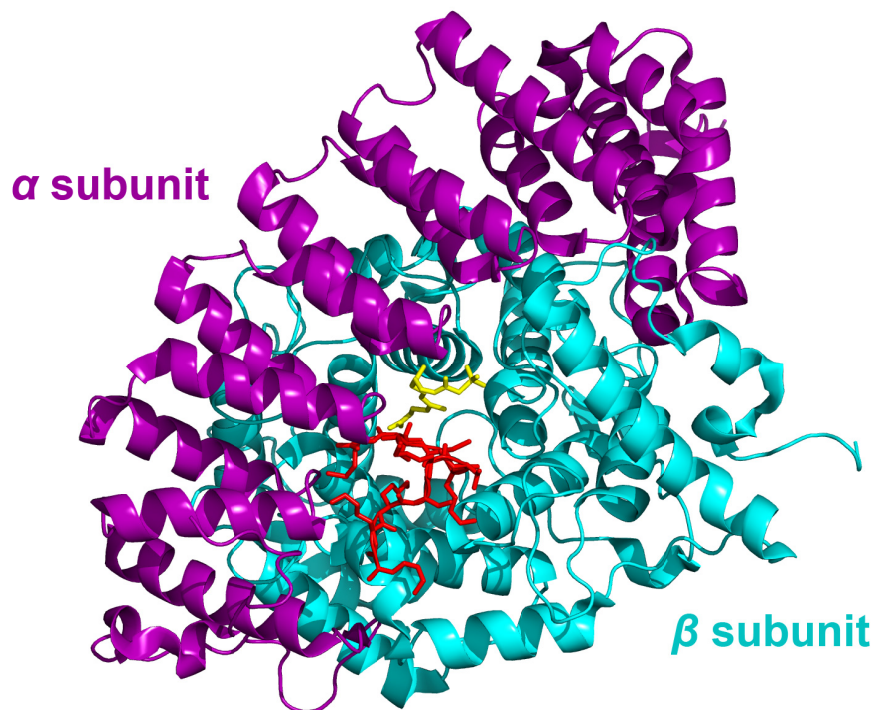


Figure 1.4: Crystal structure of mammalian FTase. The protein is a heterodimer containing a crescent-shaped α subunit (purple) and a barrel-shaped β subunit (cyan). The structure also includes a peptide substrate KKSKTKCVIM resembling K-Ras (red) and an FPP analogue inhibitor FPT-II (yellow). This figure is derived from PDB ID 1D8D and adapted from ref (142, 172).

FTase and GGTase-I are both metalloenzymes, containing a catalytic zinc ion bound to the β subunit (142, 169). The zinc ion is coordinated by three conserved residues D297 β , C299 β , and H362 β in FTase and D269 β , C271 β ,

and H321 β in GGTase-I. In addition, the zinc ion also coordinates the cysteine thiolate of the CaaX sequence in the substrate, but does not affect the affinity of the prenyl diphosphate substrate (31, 173). Moreover, the catalytic activity of FTase is activated by magnesium (174). The magnesium ion stabilizes both the reactive conformation of the bound substrate and the pyrophosphate leaving group from FPP. Although GGTase-I shares many similarities with FTase in terms of structure and mechanism, a lysine side chain replaces the magnesium ion for stabilizing product formation (174, 175).

Substrate recognition and catalytic mechanism of protein prenyltransferase

It has been widely accepted that FTase and GGTase-I recognize the protein substrates based on their C-terminal Ca₁a₂X motif (176-181). The first aliphatic a₁ residue has been shown from the structure to be solvent-exposed and not interact with the enzyme (172). Consistent with this, reactivity of FTase with peptide libraries indicate little selectivity at the a₁ position. However, the a₂ side chain of the Ca₁a₂X motif interacts with the hydrophobic cavity of the β subunit barrel. Mechanistic studies using peptides containing the Ca₁a₂X motif with varying a₂ residues suggest that this position is important for substrate recognition (182). These data demonstrate that both hydrophobicity and side chain volume are important determinants of reactivity; in particular the binding cavity is optimized to bind a side chain with a volume of $\sim 140 \text{ \AA}^3$ (i.e. Leu, Ile, Val) (182). The last residue in the motif, X, refers to a series of amino acids that

determine the substrate specificity of the prenyltransferase. FTase prefers methionine, serine, glutamine, and alanine, while GGTase-I prefers leucine, phenylalanine, and methionine (183). Although the definition of the above CaaX paradigm has been accepted for many years, recent computational analysis and biochemical studies have shown that many noncanonical amino acids could be accepted at the a₁, a₂, and X position, suggesting the possibility of a large number of additional protein substrates of prenyltransferases (146).

The reaction mechanism of prenylation has been extensively studied in the past few decades. Based on the biochemical, structural, and computational studies, a model of the catalytic mechanism has been proposed, as shown in Figure 1.5. The substrate binding is functionally ordered with FPP binding prior to the peptide substrate (35, 58, 169, 184-187). Once the two substrates are bound to the enzyme, structural and biochemical analysis indicates that the bound substrates undergo a conformational change in which the last isoprene unit of the isoprenoid moiety rotates to bring the C1 atom of FPP (or GGPP) close to the reactive cysteine, to assist in forming the new covalent bond (52). The pK_a of the cysteine thiol is lowered by the stabilizing effect of coordination to the zinc metal ion in the active site. The thiolate functions as a nucleophile to attack the alpha carbon of the prenyl diphosphate to form an associative transition state with carbocation character. This results in the formation of a thioether bond between the peptide and the prenyl group with the release of the pyrophosphate. In FTase, the negatively charged diphosphate group is

stabilized with magnesium ion, and in GGTase-I the leaving group interacts with a conserved lysine residue so magnesium is no longer required (174, 175). After the chemical step occurs, the product release step is slow and is the rate-limiting step of the overall reaction under saturating substrate conditions (188, 189). An additional isoprenoid substrate binding to the enzyme-product complex facilitates the dissociation of the product (52, 138). However, under the subsaturating substrate conditions, where the FPP/GGPP concentration is low, the reaction stops at the E•F-Spep complex (at the end of the black portion of scheme 1). Under single turnover conditions ($[E] > [FPP]$) where product dissociation is not observed, the rate-limiting step is either the conformational change or the chemical step (182).

Elucidation of the structure and catalytic and kinetic mechanism of protein prenylation have enhanced the rational design of prenylation inhibitors for the possible treatment of a number of diseases (48, 149, 190-194). Hundreds of compounds have been identified as potential farnesyltransferase inhibitors (FTIs) in preclinical studies for use as anticancer, antiparasitic, or antifungal agents, and some of these are in phase II or phase III clinical trials (48, 50, 149-151, 190, 193-195). The current inhibitors fall into three categories: FPP analogues; peptide-competitive inhibitors; and bisubstrate mimics (142). The peptide-competitive inhibitors can be further divided into peptidomimetics and nonpeptide inhibitors (196-198). Peptide-competitive inhibitors are by far the most promising and prevalent inhibitors among all three types (142); therefore,

understanding the substrate recognition and selectivity of the enzyme as well as how this process is regulated will provide important information for the development of novel peptide-competitive FTIs.

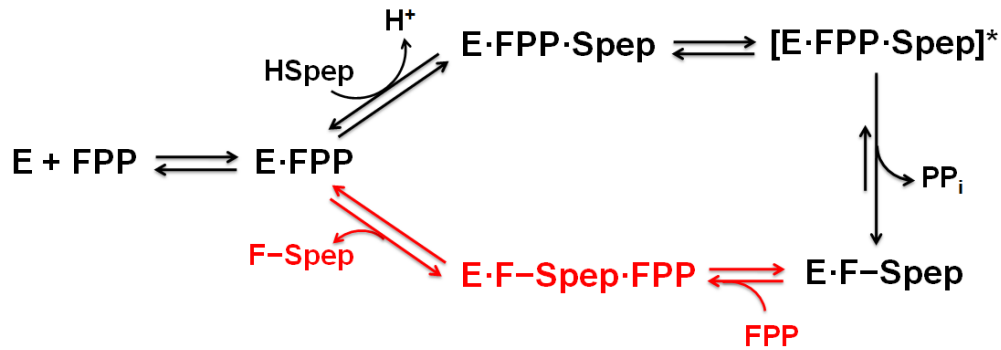


Figure 1.5: Kinetic mechanism of mammalian FTase. Substrate binding is functionally ordered with FPP binding before the peptide. $E \cdot FPP \cdot Spep$ in the ternary complex undergoes a conformational change followed by formation of the thioether bond. Dissociation of the diphosphate product is rapid while dissociation of the farnesylated peptide is slow. This step is activated by binding of FPP.

References

1. Stevens, T. J., and Arkin, I. T. (2000) Do more complex organisms have a greater proportion of membrane proteins in their genomes?, *Proteins: Struct., Funct., Genet.* **39**, 417-420.
2. Terry, K. L., Casey, P. J., and Beese, L. S. (2006) Conversion of protein farnesyltransferase to a geranylgeranyltransferase, *Biochemistry* **45**, 9746-9755.
3. Fields, T. A., and Casey, P. J. (1997) Signalling functions and biochemical properties of pertussis toxin-resistant G-proteins, *Biochem. J.* **321**, 561-571.
4. Higgins, J. B., and Casey, P. J. (1996) The role of prenylation in G-protein assembly and function, *Cell. Signaling* **8**, 433-437.
5. Thomason, P. A., James, S. R., Casey, P. J., and Downes, C. P. (1994) A G-protein beta gamma-subunit-responsive phosphoinositide 3-kinase activity in human platelet cytosol, *J. Biol. Chem.* **269**, 16525-16528.
6. Kurosaki, T., and Hikida, M. (2009) Tyrosine kinases and their

substrates in B lymphocytes, *Immunol. Rev.* 228, 132-148.

7. Chiarugi, P., and Fiaschi, T. (2007) Redox signalling in anchorage-dependent cell growth, *Cell. Signalling* 19, 672-682.
8. Latour, S., and Veillette, A. (2001) Proximal protein tyrosine kinases in immunoreceptor signaling, *Curr. Opin. Immunol.* 13, 299-306.
9. Ellery, J. M., Kempshall, S. J., and Nicholls, P. J. (2000) Activation of the interleukin 2 receptor: a possible role for tyrosine phosphatases, *Cell. Signalling* 12, 367-373.
10. Kamata, H., and Hirata, H. (1998) Redox regulation of cellular signaling, *Cell. Signalling* 11, 1-14.
11. Neel, B. G., and Tonks, N. K. (1997) Protein tyrosine phosphatases in signal transduction, *Curr. Opin. Cell Biol.* 9, 193-204.
12. VanZanten, T. S., Cambi, A., Koopman, M., Joosten, B., Figdor, C. G., and Garcia-Parajo, M. F. (2009) Hotspots of GPI-anchored proteins and integrin nanoclusters function as nucleation sites for cell adhesion, *Proc. Natl. Acad. Sci. U. S. A.* 106, 18557-18562
13. Sharma, P., Varma, R., Sarasij, R. C., Ira, Gousset, K., Krishnamoorthy, G., Rao, M., and Mayor, S. (2004) Nanoscale organization of multiple GPI-anchored proteins in living cell membranes, *Cell* 116, 577-589.
14. Chatterjee, S., and Mayor, S. (2001) The GPI-anchor and protein sorting, *Cell. Mol. Life Sci.* 58, 1969-1987.
15. Benting, J., Rietveld, A., Ansorge, I., and Simons, K. (1999) Acyl and alkyl chain length of GPI-anchors is critical for raft association in vitro, *FEBS Lett.* 462, 47-50.
16. Varma, R., and Mayor, S. (1998) GPI-anchored proteins are organized in submicron domains at the cell surface, *Nature* 394, 798-801.
17. Friedrichson, T., and Kurzchalia, T. V. (1998) Microdomains of GPI-anchored proteins in living cells revealed by crosslinking, *Nature* 394, 802-805.
18. Sheets, E. D., Lee, G. M., Simson, R., and Jacobson, K. (1997) Transient confinement of a glycosylphosphatidylinositol-anchored protein in the plasma membrane, *Biochemistry* 36, 12449-12458.
19. Brown, D. A., and Rose, J. K. (1992) Sorting of GPI-anchored proteins to glycolipid-enriched membrane subdomains during transport to the

apical cell surface, *Cell* 68, 533-544.

20. Lisanti, M. P., Le, B. A., Saltiel, A. R., and Rodriguez-Boulan, E. (1990) Preferred apical distribution of glycosyl-phosphatidylinositol (GPI) anchored proteins: a highly conserved feature of the polarized epithelial cell phenotype, *J. Membr. Biol.* 113, 155-167.
21. Jeong, J., and McMahon, A. P. (2002) Cholesterol modification of Hedgehog family proteins, *J. Clin. Invest.* 110, 591-596.
22. Mann, R. K., and Beachy, P. A. (2000) Cholesterol modification of proteins, *Biochim. Biophys. Acta* 1529, 188-202.
23. Porter, J. A., Young, K. E., and Beachy, P. A. (1996) Cholesterol modification of hedgehog signaling proteins in animal development, *Science* 274, 255-259.
24. Selvakumar, P., Lakshmikuttyamma, A., Shrivastav, A., Dimmock, J. R., and Sharma, R. K. (2005) Myristoylation and cell signaling: involvement of heat shock protein 70 family, *Recent Res. Dev. Life Sci.* 3, 75-82.
25. Farazi, T. A., Waksman, G., and Gordon, J. I. (2001) The biology and enzymology of protein N-myristoylation, *J. Biol. Chem.* 276, 39501-39504.
26. Taniguchi, H. (1999) Protein myristoylation in protein-lipid and protein-protein interactions, *Biophys. Chem.* 82, 129-137.
27. Lindwasser, O. W., and Resh, M. D. (2002) Myristoylation as a target for inhibiting HIV assembly: unsaturated fatty acids block viral budding, *Proc. Natl. Acad. Sci. U. S. A.* 99, 13037-13042.
28. Robbins, S. M., Quintrell, N. A., and Bishop, J. M. (1995) Myristoylation and differential palmitoylation of the HCK protein-tyrosine kinases govern their attachment to membranes and association with caveolae, *Mol. Cell. Biol.* 15, 3507-3515.
29. Winter-Vann, A. M., and Casey, P. J. (2005) Post-prenylation-processing enzymes as new targets in oncogenesis, *Nat. Rev. Cancer* 5, 405-412.
30. Thissen, J. A., Gross, J. M., Subramanian, K., Meyer, T., and Casey, P. J. (1997) Prenylation-dependent association of Ki-Ras with microtubules. Evidence for a role in subcellular trafficking, *J. Biol. Chem.* 272, 30362-30370.
31. Casey, P. J., and Seabra, M. C. (1996) Protein prenyltransferases, *J.*

Biol. Chem. 271, 5289-5292.

32. Thissen, J. A., Barrett, M. G., and Casey, P. J. (1995) Prenylated peptides in identification of specific binding proteins, *Methods Enzymol.* 250, 158-168.
33. Casey, P. J., Moomaw, J. F., Zhang, F. L., Higgins, Y. B., and Thissen, J. A. (1994) Prenylation and G protein signaling, *Recent Prog. Horm. Res.* 49, 215-238.
34. Casey, P. J. (1992) Biochemistry of protein prenylation, *J. Lipid. Res.* 33, 1731-1740.
35. Casey, P. J., and Seabra, M. C. (1996) Protein Prenyltransferases, *J. Biol. Chem.* 271, 5289-5292.
36. Greaves, J., and Chamberlain, L. H. (2011) DHHC palmitoyl transferases: substrate interactions and (patho)physiology, *Trends Biochem. Sci.* 36, 245-253.
37. Planey, S. L., and Zacharias, D. A. (2009) Palmitoyl acyltransferases, their substrates, and novel assays to connect them, *Mol. Membr. Biol.* 26, 14-31.
38. Baekkeskov, S., and Kanaani, J. (2009) Palmitoylation cycles and regulation of protein function, *Mol. Membr. Biol.* 26, 42-54.
39. Wan, J., Roth, A. F., Bailey, A. O., and Davis, N. G. (2007) Palmitoylated proteins: purification and identification, *Nat. Protoc.* 2, 1573-1584.
40. Linder, M. E., and Deschenes, R. J. (2007) Palmitoylation: policing protein stability and traffic, *Nat. Rev. Mol. Cell Biol.* 8, 74-84.
41. Chakrabandhu, K., Herincs, Z., Huault, S., Dost, B., Peng, L., Conchonaud, F., Marguet, D., He, H.-T., and Hueber, A.-O. (2007) Palmitoylation is required for efficient Fas cell death signaling, *EMBO J.* 26, 209-220.
42. Smotrys, J. E., and Linder, M. E. (2004) Palmitoylation of intracellular signaling proteins: Regulation and function, *Annu. Rev. Biochem.* 73, 559-587.
43. Osterhout, J. L., Waheed, A. A., Hiol, A., Ward, R. J., Davey, P. C., Nini, L., Wang, J., Milligan, G., Jones, T. L. Z., and Druey, K. M. (2003) Palmitoylation Regulates Regulator of G-protein Signaling (RGS) 16 Function: II. Palmitoylation of a cysteine residue in the RGS box is critical for RGS16 GTPase accelerating activity and regulation of

Gi-coupled signaling, *J. Biol. Chem.* 278, 19309-19316.

44. Mumby, S. M., Kleuss, C., and Gilman, A. G. (1994) Receptor regulation of G-protein palmitoylation, *Proc. Natl. Acad. Sci. U. S. A.* 91, 2800-2804.
45. Young, S. G., Meta, M., Yang, S. H., and Fong, L. G. (2006) Prelamin A Farnesylation and Progeroid Syndromes, *J. Biol. Chem.* 281, 39741-39745.
46. Wright, L. P., and Philips, M. R. (2006) CAAX modification and membrane targeting of Ras, *J. Lipid Res.* 47, 883-891.
47. Eastman, R. T., Buckner, F. S., Yokoyama, K., Gelb, M. H., and Van, V. W. C. (2006) Fighting parasitic disease by blocking protein farnesylation, *J. Lipid Res.* 47, 233-240.
48. Sebti, S. M. (2005) Protein farnesylation: Implications for normal physiology, malignant transformation, and cancer therapy, *Cancer Cell* 7, 297-300.
49. Galichet, A., and Gruissem, W. (2003) Protein farnesylation in plants: Conserved mechanisms but different targets, *Curr. Opin. Plant Biol.* 6, 530-535.
50. Tamanoi, F., Gau, C. L., Jiang, C., Edamatsu, H., and Kato-Stankiewicz, J. (2001) Protein farnesylation in mammalian cells: effects of farnesyltransferase inhibitors on cancer cells, *Cell. Mol. Life Sci.* 58, 1636-1649.
51. Nambara, E., and McCourt, P. (1999) Protein farnesylation in plants: a greasy tale, *Curr. Opin. Plant Biol.* 2, 388-392.
52. Long, S. B., Casey, P. J., and Beese, L. S. (2002) Reaction path of protein farnesyltransferase at atomic resolution, *Nature* 419, 645-650.
53. Leung, K. F., Baron, R., and Seabra, M. C. (2006) Thematic review series: lipid posttranslational modifications. geranylgeranylation of Rab GTPases, *J Lipid Res* 47, 467-475.
54. Leung, K. F., Baron, R., and Seabra, M. C. (2006) Geranylgeranylation of Rab GTPases, *J. Lipid Res.* 47, 467-475.
55. Desnoyers, L., Anant, J. S., and Seabra, M. C. (1996) Geranylgeranylation of Rab proteins, *Biochem. Soc. Trans.* 24, 699-703.

56. Bergo, M. O., Lieu, H. D., Gavino, B. J., Ambroziak, P., Otto, J. C., Casey, P. J., Walker, Q. M., and Young, S. G. (2004) On the physiological importance of endoproteolysis of CAAX proteins: heart-specific RCE1 knockout mice develop a lethal cardiomyopathy, *J. Biol. Chem.* 279, 4729-4736.
57. Bergo, M. O., Ambroziak, P., Gregory, C., George, A., Otto, J. C., Kim, E., Nagase, H., Casey, P. J., Balmain, A., and Young, S. G. (2002) Absence of the CAAX endoprotease Rce1: effects on cell growth and transformation, *Mol. Cell Biol.* 22, 171-181.
58. Fu, H. W., and Casey, P. J. (1999) Enzymology and biology of CaaX protein prenylation, *Recent Prog. Horm. Res.* 54, 315-342
59. Volker, C., Pillinger, M. H., Philips, M. R., and Stock, J. B. (1995) Prenylcysteine analogs to study function of carboxymethylation in signal transduction, *Methods Enzymol.* 250, 216-225.
60. Fukada, Y. (1995) Prenylation and carboxymethylation of G-protein gamma subunit, *Methods Enzymol.* 250, 91-105.
61. Billingsley, M. L., and Lovenberg, W. (1985) Protein carboxymethylation and nervous system function, *Neurochem. Int.* 7, 575-587.
62. Greaves, J., Carmichael, J. A., and Chamberlain, L. H. (2011) The palmitoyl transferase DHHC2 targets a dynamic membrane cycling pathway: regulation by a C-terminal domain, *Mol. Biol. Cell* 22, 1887-1895.
63. Zhang, M. M., Tsou, L. K., Charron, G., Raghavan, A. S., and Hang, H. C. (2010) Tandem fluorescence imaging of dynamic S-acylation and protein turnover, *Proc. Natl. Acad. Sci. U. S. A.* 107, 8627-8632.
64. Salaun, C., Greaves, J., and Chamberlain, L. H. (2010) The intracellular dynamic of protein palmitoylation, *J. Cell Biol.* 191, 1229-1238.
65. Conibear, E., and Davis, N. G. (2010) Palmitoylation and depalmitoylation dynamics at a glance, *J. Cell Sci.* 123, 4007-4010.
66. Iwanaga, T., Tsutsumi, R., Noritake, J., Fukata, Y., and Fukata, M. (2009) Dynamic protein palmitoylation in cellular signaling, *Prog. Lipid Res.* 48, 117-127.
67. Basu, J. (2004) Protein palmitoylation and dynamic modulation of protein function, *Curr. Sci.* 87, 212-217.
68. Qanbar, R., and Bouvier, M. (2003) Role of

palmitoylation/depalmitoylation reactions in G-protein-coupled receptor function, *Pharmacol. Ther.* 97, 1-33.

69. Fukata, Y., and Fukata, M. Protein palmitoylation in neuronal development and synaptic plasticity, *Nat. Rev. Neurosci.* 11, 161-175.
70. Tsutsumi, R., Fukata, Y., Noritake, J., Iwanaga, T., Perez, F., and Fukata, M. (2009) Identification of G protein α subunit-palmitoylating enzyme, *Mol. Cell. Biol.* 29, 435-447.
71. Masuda, K., Itoh, H., Sakihama, T., Akiyama, C., Takahashi, K., Fukuda, R., Yokomizo, T., Shimizu, T., Kodama, T., and Hamakubo, T. (2003) A combinatorial G protein-coupled receptor reconstitution system on budded baculovirus. Evidence for Gai and Gao coupling to a human leukotriene B4 receptor, *J. Biol. Chem.* 278, 24552-24562.
72. Sandilands, E., Brunton, V. G., and Frame, M. C. (2007) The membrane targeting and spatial activation of Src, Yes and Fyn is influenced by palmitoylation and distinct RhoB/RhoD endosome requirements, *J Cell Sci* 120, 2555-2564.
73. Dighe, S. A., and Kozminski, K. G. (2008) Swf1p, a member of the DHHC-CRD family of palmitoyltransferases, regulates the actin cytoskeleton and polarized secretion independently of its DHHC motif, *Mol. Biol. Cell* 19, 4454-4468.
74. Wang, D.-A., and Sebt, S. M. (2005) Palmitoylated cysteine 192 is required for RhoB tumor-suppressive and apoptotic activities, *J Biol Chem* 280, 19243-19249.
75. Bhattacharyya, R., and Wedegaertner, P. B. (2000) G α 13 requires palmitoylation for plasma membrane localization, Rho-dependent signaling, and promotion of p115-RhoGEF membrane binding, *J Biol Chem* 275, 14992-14999.
76. Bhattacharyya, R., and Wedegaertner, P. B. (2000) G α 13 requires palmitoylation for plasma membrane localization, Rho-dependent signaling, and promotion of p115-RhoGEF membrane binding, *J. Biol. Chem.* 275, 14992-14999.
77. Patterson, S. I., and Skene, J. H. P. (1999) A shift in protein S-palmitoylation, with persistence of growth-associated substrates, marks a critical period for synaptic plasticity in developing brain, *J. Neurobiol.* 39, 423-437.
78. Mitchell, D. A., Vasudevan, A., Linder, M. E., and Deschenes, R. J. (2006) Protein palmitoylation by a family of DHHC protein

S-acyltransferases, *J. Lipid Res.* 47, 1118-1127.

79. Pechlivanis, M., and Kuhlmann, J. (2006) Hydrophobic modifications of Ras proteins by isoprenoid groups and fatty acids--More than just membrane anchoring, *Biochim Biophys Acta* 1764, 1914-1931.
80. Resh, M. D. (2004) Membrane targeting of lipid modified signal transduction proteins, *Subcell. Biochem.* 37, 217-232.
81. Peitzsch, R. M., and McLaughlin, S. (1993) Binding of acylated peptides and fatty acids to phospholipid vesicles: Pertinence to myristoylated proteins, *Biochemistry* 32, 10436-10443.
82. Shahinian, S., and Silviu, J. R. (1995) Doubly-lipid-modified protein sequence motifs exhibit long-lived anchorage to lipid bilayer membranes, *Biochemistry* 34, 3813-3822.
83. Wang, J., Xie, Y., Wolff, D. W., Abel, P. W., and Tu, Y. (2010) DHHC protein-dependent palmitoylation protects regulator of G-protein signaling 4 from proteasome degradation, *FEBS Lett.* 584, 4570-4574.
84. Morello, J. P., and Bouvier, M. (1996) Palmitoylation: a post-translational modification that regulates signalling from G-protein coupled receptors, *Biochem. Cell. Biol.* 74, 449-457.
85. Bouvier, M., Moffett, S., Loisel, T. P., Mouillac, B., Hebert, T., and Chidiac, P. (1995) Palmitoylation of G-protein-coupled receptors: a dynamic modification with functional consequences, *Biochem. Soc. Trans.* 23, 116-120.
86. Bouvier, M., Chidiac, P., Hebert, T. E., Loisel, T. P., Moffett, S., and Mouillac, B. (1995) Dynamic palmitoylation of G-protein-coupled receptors in eukaryotic cells, *Methods Enzymol.* 250, 300-314.
87. O'Brien, P. J., and Zatz, M. (1984) Acylation of bovine rhodopsin by [3H]palmitic acid, *J. Biol. Chem.* 8, 5054-5057.
88. Noritake, J., Fukata, Y., Iwanaga, T., Hosomi, N., Tsutsumi, R., Matsuda, N., Tani, H., Iwanari, H., Mochizuki, Y., Kodama, T., Matsuura, Y., Brecht, D. S., Hamakubo, T., and Fukata, M. (2009) Mobile DHHC palmitoylating enzyme mediates activity-sensitive synaptic targeting of PSD-95, *J. Cell Biol.* 186, 147-160.
89. Fukata, M., Fukata, Y., Adesnik, H., Nicoll, R. A., and Brecht, D. S. (2004) Identification of PSD-95 Palmitoylating enzymes, *Neuron* 44, 987-996.
90. Topinka, J. R., and Brecht, D. S. (1998) N-terminal palmitoylation of

PSD-95 regulates association with cell membranes and interaction with K⁺ channel Kv1.4, *Neuron* 20, 125-134.

91. Gonzalo, S., Greentree, W. K., and Linder, M. E. (1999) SNAP-25 is targeted to the plasma membrane through a novel membrane-binding domain, *J. Biol. Chem.* 274, 21313-21318.
92. Greaves, J., Gorleku, O. A., Salaun, C., and Chamberlain, L. H. (2010) Palmitoylation of the SNAP25 protein family: specificity and regulation by DHHC palmitoyl transferases, *J. Biol. Chem.* 285, 24629-24638.
93. Kang, R., Wan, J., Arstikaitis, P., Takahashi, H., Huang, K., Bailey, A. O., Thompson, J. X., Roth, A. F., Drisdell, R. C., Mastro, R., Green, W. N., Yates, J. R., III, Davis, N. G., and El-Husseini, A. (2008) Neural palmitoyl-proteomics reveals dynamic synaptic palmitoylation, *Nature* 456, 904-909.
94. Edidin, M. (2003) The state of lipid rafts: From model membranes to cells, *Annu. Rev. Biophys. Biomol. Struct.* 32, 257-283.
95. Brown, D. A., and London, E. (1998) Functions of lipid rafts in biological membranes, *Annu. Rev. Cell Dev. Biol.* 14, 111-136.
96. Shenoy-Scaria, A. M., Dietzen, D. J., Kwong, J., Link, D. C., and Lublin, D. M. (1994) Cysteine3 of Src family protein tyrosine kinase determines palmitoylation and localization in caveolae, *J. Cell Biol.* 126, 353-363.
97. Guzzi, F., Zanchetta, D., Chini, B., and Parenti, M. (2001) Thioacylation is required for targeting G-protein subunit Go1 α to detergent-insoluble caveolin-containing membrane domains, *Biochem. J.* 355, 323-331.
98. Arni, S., Keilbaugh, S. A., Ostermeyer, A. G., and Brown, D. A. (1998) Association of GAP-43 with detergent-resistant membranes requires two palmitoylated cysteine residues, *J. Biol. Chem.* 273, 28478-28485.
99. Webb, Y., Hermida-Matsumoto, L., and Resh, M. D. (2000) Inhibition of protein palmitoylation, raft localization, and T cell signaling by 2-bromopalmitate and polyunsaturated fatty acids, *J. Biol. Chem.* 275, 261-270.
100. Kabouridis, P. S., Magee, A. I., and Ley, S. C. (1997) S-acylation of LCK protein tyrosine kinase is essential for its signaling function in T lymphocytes, *EMBO J.* 16, 4983-4998.
101. Zhang, W., Triple, R. P., and Samelson, L. E. (1998) LAT palmitoylation: its essential role in membrane microdomain targeting and tyrosine phosphorylation during T cell activation, *Immunity.* 9, 239-246.

102. Lin, J., Weiss, A., and Finco, T. S. (1999) Localization of LAT in glycolipid-enriched microdomains is required for T cell activation, *J. Biol. Chem.* 274, 28861-28864.
103. Duncan, J. A., and Gilman, A. G. (1996) Autoacylation of G protein subunits, *J. Biol. Chem.* 271, 23594-23600.
104. Lobo, S., Greentree, W. K., Linder, M. E., and Deschenes, R. J. (2002) Identification of a Ras Palmitoyltransferase in *Saccharomyces cerevisiae*, *J. Biol. Chem.* 277, 41268-41273.
105. Bartels, D. J., Mitchell, D. A., Dong, X., and Deschenes, R. J. (1999) Erf2, a novel gene product that affects the localization and palmitoylation of Ras2 in *Saccharomyces cerevisiae*, *Mol. Cell. Biol.* 19, 6775-6787.
106. Roth, A. F., Feng, Y., Chen, L., and Davis, N. G. (2002) The yeast DHHC cysteine-rich domain protein Akr1p is a palmitoyl transferase, *J. Cell. Biol.* 159, 23-28.
107. Greaves, J., and Chamberlain, L. H. (2010) S-acylation by the DHHC protein family, *Biochem. Soc. Trans.* 38, 522-524.
108. Roth, A. F., Wan, J., Bailey, A. O., Sun, B., Kuchar, J. A., Green, W. N., Phinney, B. S., Yates, J. R., III, and Davis, N. G. (2006) Global analysis of protein palmitoylation in yeast, *Cell* 125, 1003-1013.
109. Smotrýs, J. E., Schoenfish, M. J., Stutz, M. A., and Linder, M. E. (2005) The vacuolar DHHC-CRD protein Pfa3p is a protein acyltransferase for Vac8p, *J. Cell. Biol.* 170, 1091-1099.
110. Hou, H., John Peter, A. T., Meiringer, C., Subramanian, K., and Ungermann, C. (2009) Analysis of DHHC acyltransferases implies overlapping substrate specificity and a two-step reaction mechanism, *Traffic* 10, 1061-1073.
111. Bannan, B. A., Van Etten, J., Kohler, J. A., Tsoi, Y., Hansen, N. M., Sigmon, S., Fowler, E., Buff, H., Williams, T. S., Ault, J. G., Glaser, R. L., and Corey, C. A. (2008) The *Drosophila* protein palmitoylome: characterizing palmitoyl-thioesterases and DHHC palmitoyl-transferases, *Fly* 2, 198-214.
112. Ducker, C. E., Stettler, E. M., French, K. J., Upson, J. J., and Smith, C. D. (2004) Huntingtin interacting protein 14 is an oncogenic human protein: palmitoyl acyltransferase, *Oncogene* 23, 9230-9237.
113. Mukai, J., Dhillia, A., Drew, L. J., Stark, K. L., Cao, L., MacDermott, A. B.,

- Karayiorgou, M., and Gogos, J. A. (2008) Palmitoylation-dependent neurodevelopmental deficits in a mouse model of 22q11 microdeletion, *Nat. Neurosci.* *11*, 1302-1310.
114. Raymond, F. L., Tarpey, P. S., Edkins, S., Tofts, C., O'Meara, S., Teague, J., Butler, A., Stevens, C., Barthorpe, S., Buck, G., Cole, J., Dicks, E., Gray, K., Halliday, K., Hills, K., Hinton, J., Jones, D., Menzies, A., Perry, J., Raine, K., Shepherd, R., Small, A., Varian, J., Widaa, S., Mallya, U., Moon, J., Luo, Y., Shaw, M., Boyle, J., Kerr, B., Turner, G., Quarrell, O., Cole, T., Easton, D. F., Wooster, R., Bobrow, M., Schwartz, C. E., Gecz, J., Stratton, M. R., and Futreal, P. A. (2007) Mutations in ZDHHC9, which encodes a palmitoyltransferase of NRAS and HRAS, cause X-linked mental retardation associated with a marfanoid habitus, *Am. J. Hum. Genet.* *80*, 982-987.
115. Ohyama, T., Verstreken, P., Ly, C. V., Rosenmund, T., Rajan, A., Tien, A.-C., Haueter, C., Schulze, K. L., and Bellen, H. J. (2007) Huntingtin-interacting protein 14, a palmitoyl transferase required for exocytosis and targeting of CSP to synaptic vesicles, *J. Cell Biol.* *179*, 1481-1496.
116. Yanai, A., Huang, K., Kang, R., Singaraja, R. R., Arstikaitis, P., Gan, L., Orban, P. C., Mullard, A., Cowan, C. M., Raymond, L. A., Drisdell, R. C., Green, W. N., Ravikumar, B., Rubinsztein, D. C., El-Husseini, A., and Hayden, M. R. (2006) Palmitoylation of huntingtin by HIP14 is essential for its trafficking and function, *Nat. Neurosci.* *9*, 824-831.
117. El-Husseini, A. E.-D., Schnell, E., Dakoji, S., Sweeney, N., Zhou, Q., Prange, O., Gauthier-Campbell, C., Aguilera-Moreno, A., Nicoll, R. A., and Brecht, D. S. (2002) Synaptic strength regulated by palmitate cycling on PSD-95, *Cell* *108*, 849-863.
118. El-Husseini, A. E., Craven, S. E., Chetkovich, D. M., Firestein, B. L., Schnell, E., Aoki, C., and Brecht, D. S. (2000) Dual palmitoylation of PSD-95 mediates its vesiculotubular sorting, postsynaptic targeting, and ion channel clustering, *J. Cell Biol.* *148*, 159-171.
119. Singaraja, R. R., Hadano, S., Metzler, M., Givan, S., Wellington, C. L., Warby, S., Yanai, A., Gutekunst, C.-A., Leavitt, B. R., Yi, H., Fichter, K., Gan, L., McCutcheon, K., Chopra, V., Michel, J., Hersch, S. M., Ikeda, J.-E., and Hayden, M. R. (2002) HIP14, a novel ankyrin domain-containing protein, links huntingtin to intracellular trafficking and endocytosis, *Hum. Mol. Genet.* *11*, 2815-2828.
120. Politis, E. G., Roth, A. F., and Davis, N. G. (2005) Transmembrane topology of the protein palmitoyl transferase Akr1, *J. Biol. Chem.* *280*,

10156-10163.

121. Mitchell, D. A., Mitchell, G., Ling, Y., Budde, C., and Deschenes, R. J. (2010) Mutational analysis of *Saccharomyces cerevisiae* Erf2 reveals a two-step reaction mechanism for protein palmitoylation by DHHC enzymes, *J. Biol. Chem.* **285**, 38104-38114.
122. Budde, C., Schoenfish, M. J., Linder, M. E., and Deschenes, R. J. (2006) Purification and characterization of recombinant protein acyltransferases, *Methods* **40**, 143-150.
123. Draper, J. M., and Smith, C. D. (2009) Palmitoyl acyltransferase assays and inhibitors, *Mol Membr Biol* **26**, 5-13.
124. Fernandez-Hernando, C., Fukata, M., Bernatchez, P. N., Fukata, Y., Lin, M. I., Bredt, D. S., and Sessa, W. C. (2006) Identification of Golgi-localized acyl transferases that palmitoylate and regulate endothelial nitric oxide synthase, *J. Cell Biol.* **174**, 369-377.
125. Resh, M. D. (2006) Palmitoylation of ligands, receptors, and intracellular signaling molecules, *Sci. STKE* **2006**, re14.
126. Drisdell, R. C., Alexander, J. K., Sayeed, A., and Green, W. N. (2006) Assays of protein palmitoylation, *Methods* **40**, 127-134.
127. Hang, H. C., Geutjes, E.-J., Grotenbreg, G., Pollington, A. M., Bijlmakers, M. J., and Ploegh, H. L. (2007) Chemical Probes for the Rapid Detection of Fatty-Acylated Proteins in Mammalian Cells, *J. Am. Chem. Soc.* **129**, 2744-2745.
128. Martin, B. R., and Cravatt, B. F. (2009) Large-scale profiling of protein palmitoylation in mammalian cells, *Nat. Methods* **6**, 135-138.
129. Draper, J. M., Xia, Z., and Smith, C. D. (2007) Cellular palmitoylation and trafficking of lipidated peptides, *J. Lipid Res.* **48**, 1873-1884.
130. Hensel, J., Hintz, M., Karas, M., Linder, D., Stahl, B., and Geyer, R. (1995) Localization of the palmitoylation site in the transmembrane protein p12E of Friend murine leukemia virus, *Eur. J. Biochem.* **232**, 373-380.
131. Liang, X., Nazarian, A., Erdjument-Bromage, H., Bornmann, W., Tempst, P., and Resh, M. D. (2001) Heterogeneous fatty acylation of Src family kinases with polyunsaturated fatty acids regulates raft localization and signal transduction, *J. Biol. Chem.* **276**, 30987-30994.
132. Hoffman, M. D., and Kast, J. (2006) Mass spectrometric

characterization of lipid-modified peptides for the analysis of acylated proteins, *J. Mass. Spectrom.* 41, 229-241.

133. Zhao, Z., Hou, J., Xie, Z., Deng, J., Wang, X., Chen, D., Yang, F., and Gong, W. (2010) Acyl-biotinyl exchange chemistry and mass spectrometry-based analysis of palmitoylation sites of in vitro palmitoylated rat brain tubulin, *Protein J.* 29, 531-537.
134. Drisdell, R. C., and Green, W. N. (2004) Labeling and quantifying sites of protein palmitoylation, *BioTechniques* 36, 276-282,284-285.
135. Yang, W., Di Vizio, D., Kirchner, M., Steen, H., and Freeman, M. R. (2010) Proteome scale characterization of human S-acylated proteins in lipid raft-enriched and non-raft membranes, *Mol. Cell. Proteomics* 9, 54-70.
136. Zhang, F. L., and Casey, P. J. (1996) Protein prenylation: molecular mechanisms and functional consequences, *Annu. Rev. Biochem.* 65, 241-269.
137. Kamiya, Y., Sakurai, A., Tamura, S., and Takahashi, N. (1978) Structure of rhodotorucine A, a novel lipopeptide, inducing mating tube formation in *Rhodospiridium toruloides*, *Biochem. Biophys. Res. Commun.* 83, 1077-1083.
138. Taylor, J. S., Reid, T. S., Terry, K. L., Casey, P. J., and Beese, L. S. (2003) Structure of mammalian protein geranylgeranyltransferase type-I, *EMBO J* 22, 5963-5974.
139. Stirtan, W. G., and Poulter, C. D. (1997) Yeast protein geranylgeranyltransferase type-I: steady-state kinetics and substrate binding, *Biochemistry* 36, 4552-4557.
140. Stirtan, W. G., and Poulter, C. D. (1995) Yeast protein geranylgeranyltransferase type-I: overproduction, purification, and characterization, *Arch. Biochem. Biophys.* 321, 182-190.
141. Zhang, F. L., Moomaw, J. F., and Casey, P. J. (1994) Properties and kinetic mechanism of recombinant mammalian protein geranylgeranyltransferase type I, *J. Biol. Chem.* 269, 23465-23470.
142. Lane, K. T., and Beese, L. S. (2006) Structural biology of protein farnesyltransferase and geranylgeranyltransferase type I, *J. Lipid Res.* 47, 681-699.
143. Leung, K. F., Baron, R., and Seabra, M. C. (2006) Thematic review series: lipid posttranslational modifications. geranylgeranylation of Rab

GTPases, *J. Lipid Res.* 47, 467-475.

144. Jiang, Y., Rossi, G., and Ferro-Novick, S. (1995) Characterization of yeast type-II geranylgeranyltransferase, *Methods Enzymol.* 257, 21-29.
145. Del, V. K., Dorin, D., Sattler, I., Urano, J., Pouillet, P., Robinson, N., Mitsuzawa, H., and Tamanoi, F. (1996) C-terminal motifs found in Ras-superfamily G-proteins: CAAX and C-seven motifs, *Biochem. Soc. Trans.* 24, 709-713.
146. Houglund, J. L., Hicks, K. A., Hartman, H. L., Kelly, R. A., Watt, T. J., and Fierke, C. A. Identification of Novel Peptide Substrates for Protein Farnesyltransferase Reveals Two Substrate Classes with Distinct Sequence Selectivities, *J. Mol. Biol.* 395, 176-190.
147. Andres, D. A., Seabra, M. C., Brown, M. S., Armstrong, S. A., Smeland, T. E., Cremers, F. P. M., and Goldstein, J. L. (1993) cDNA cloning of component A of Rab geranylgeranyl transferase and demonstration of its role as a Rab escort protein, *Cell* 73, 1091-1099.
148. Rak, A., Pylypenko, O., Niculae, A., Pyatkov, K., Goody, R. S., and Alexandrov, K. (2004) Structure of the Rab7:REP-1 Complex: Insights into the Mechanism of Rab Prenylation and Choroideremia Disease, *Cell* 117, 749-760.
149. Sousa, S. F., Fernandes, P. A., and Ramos, M. J. (2008) Farnesyltransferase inhibitors: a detailed chemical view on an elusive biological problem, *Curr. Med. Chem.* 15, 1478-1492.
150. Sebti, S. M., and Hamilton, A. D. (2000) Farnesyltransferase and geranylgeranyltransferase I inhibitors in cancer therapy: important mechanistic and bench to bedside issues, *Expert Opin. Invest. Drugs* 9, 2767-2782.
151. Sebti, S. M., and Hamilton, A. D. (2000) Farnesyltransferase and geranylgeranyltransferase I inhibitors and cancer therapy: lessons from mechanism and bench-to-bedside translational studies, *Oncogene* 19, 6584-6593.
152. Hooff, G. P., Wood, W. G., Muller, W. E., and Eckert, G. P. (2010) Isoprenoids, small GTPases and Alzheimer's disease, *Biochim. Biophys. Acta* 1801, 896-905.
153. Caraglia, M., Budillon, A., Tagliaferri, P., Marra, M., Abbruzzese, A., and Caponigro, F. (2005) Isoprenylation of intracellular proteins as a new target for the therapy of human neoplasms: preclinical and clinical implications, *Curr. Drug Targets* 6, 301-323.

154. McTaggart, S. J. (2006) Isoprenylated proteins, *Cell. Mol. Life Sci.* **63**, 255-267.
155. Nguyen, U. T., Wu, Y., Goodall, A., and Alexandrov, K. (2010) Analysis of protein prenylation in vitro and in vivo using functionalized phosphoisoprenoids, *Curr. Protoc. Protein Sci.* **62**:14.3.1–14.3.15.
156. Appels, N. M., Bolijn, M. J., Chan, K., Stephens, T. C., Hocht-Boes, G., Middleton, M., Beijnen, J. H., de Bono, J. S., Harris, A. L., and Schellens, J. H. (2008) Phase I pharmacokinetic and pharmacodynamic study of the prenyl transferase inhibitor AZD3409 in patients with advanced cancer, *Br. J. Cancer* **98**, 1951-1958.
157. Dinsmore, C. J., and Bell, I. M. (2003) Inhibitors of farnesyltransferase and geranylgeranyltransferase-I for antitumor therapy: Substrate-based design, conformational constraint and biological activity, *Curr. Top. Med. Chem.* **3**, 1075-1093.
158. Caponigro, F., Casale, M., and Bryce, J. (2003) Farnesyl transferase inhibitors in clinical development, *Expert Opinion on Investigational Drugs* **12**, 943-954.
159. Capell, B. C., Erdos, M. R., Madigan, J. P., Fiordalisi, J. J., Varga, R., Conneely, K. N., Gordon, L. B., Der, C. J., Cox, A. D., and Collins, F. S. (2005) Inhibiting farnesylation of progerin prevents the characteristic nuclear blebbing of Hutchinson-Gilford progeria syndrome, *Proc. Natl. Acad. Sci. U. S. A.* **102**, 12879-12884.
160. Crowther, G. J., Napuli, A. J., Gilligan, J. H., Gagaring, K., Borboa, R., Francek, C., Chen, Z., Dagostino, E. F., Stockmyer, J. B., Wang, Y., Rodenbough, P. P., Castaneda, L. J., Leibly, D. J., Bhandari, J., Gelb, M. H., Brinker, A., Engels, I. H., Taylor, J., Chatterjee, A. K., Fantauzzi, P., Glynne, R. J., Van Voorhis, W. C., and Kuhlen, K. L. (2011) Identification of inhibitors for putative malaria drug targets among novel antimalarial compounds, *Mol. Biochem. Parasitol* **175**, 21-29.
161. Olepu, S., Suryadevara, P. K., Rivas, K., Yokoyama, K., Verlinde, C. L., Chakrabarti, D., Van Voorhis, W. C., and Gelb, M. H. (2008) 2-Oxo-tetrahydro-1,8-naphthyridines as selective inhibitors of malarial protein farnesyltransferase and as anti-malarials, *Bioorg. Med. Chem. Lett.* **18**, 494-497.
162. Cammerer, S. B., Jimenez, C., Jones, S., Gros, L., Lorente, S. O., Rodrigues, C., Rodrigues, J. C., Caldera, A., Ruiz Perez, L. M., da Souza, W., Kaiser, M., Brun, R., Urbina, J. A., Gonzalez Pacanowska, D., and Gilbert, I. H. (2007) Quinuclidine derivatives as potential

antiparasitics, *Antimicrob. Agents Chemother.* **51**, 4049-4061.

163. Ohkanda, J., Lockman, J. W., Yokoyama, K., Gelb, M. H., Croft, S. L., Kendrick, H., Harrell, M. I., Feagin, J. E., Blaskovich, M. A., Sebti, S. M., and Hamilton, A. D. (2001) Peptidomimetic inhibitors of protein farnesyltransferase show potent antimalarial activity, *Bioorg. Med. Chem. Lett.* **11**, 761-764.
164. van de Donk, N. W., Kamphuis, M. M., van Kessel, B., Lokhorst, H. M., and Bloem, A. C. (2003) Inhibition of protein geranylgeranylation induces apoptosis in myeloma plasma cells by reducing Mcl-1 protein levels, *Blood* **102**, 3354-3362.
165. Hast, M. A., and Beese, L. S. (2008) Structure of protein geranylgeranyltransferase-I from the human pathogen *Candida albicans* complexed with a lipid substrate, *J. Biol. Chem.* **283**, 31933-31940.
166. Murthi, K. K., Smith, S. E., Kluge, A. F., Bergnes, G., Bureau, P., and Berlin, V. (2003) Antifungal activity of a *Candida albicans* GGase I inhibitor-alanine conjugate. Inhibition of Rho1p prenylation in *C. albicans*, *Bioorg. Med. Chem. Lett.* **13**, 1935-1937.
167. Song, J. L., and White, T. C. (2003) RAM2: an essential gene in the prenylation pathway of *Candida albicans*, *Microbiology* **149**, 249-259.
168. Price, C. T. D., Al-Quadani, T., Santic, M., Jones, S. C., and Abu Kwaik, Y. Exploitation of conserved eukaryotic host cell farnesylation machinery by an F-box effector of *Legionella pneumophila*, *J. Cell. Biol.* **190**, 1713-1726.
169. Liang, P. H., Ko, T. P., and Wang, A. H. (2002) Structure, mechanism and function of prenyltransferases, *Eur. J. Biochem.* **269**, 3339-3354.
170. Andres, D. A., Goldstein, J. L., Ho, Y. K., and Brown, M. S. (1993) Mutational analysis of alpha-subunit of protein farnesyltransferase. Evidence for a catalytic role, *J. Biol. Chem.* **268**, 1383-1390.
171. Dunten, P., Kammlott, U., Crowther, R., Weber, D., Palermo, R., and Birkoft, J. (1998) Protein Farnesyltransferase: Structure and Implications for Substrate Binding, *Biochemistry* **37**, 7907-7912.
172. Long, S. B., Casey, P. J., and Beese, L. S. (2000) The basis for K-Ras4B binding specificity to protein farnesyltransferase revealed by 2 A resolution ternary complex structures, *Structure* **8**, 209-222.
173. Moomaw, J. F., and Casey, P. J. (1992) Mammalian protein

- geranylgeranyltransferase. Subunit composition and metal requirements, *J Biol Chem* 267, 17438-17443.
174. Reiss, Y., Seabra, M. C., Brown, M. S., and Goldstein, J. L. (1992) p21ras farnesyltransferase: purification and properties of the enzyme, *Biochem. Soc. Trans.* 20, 487-488.
 175. Hartman, H. L., Bowers, K. E., and Fierke, C. A. (2004) Lysine beta311 of protein geranylgeranyltransferase type I partially replaces magnesium, *J. Biol. Chem.* 279, 30546-30553.
 176. Caplin, B. E., Hettich, L. A., and Marshall, M. S. (1994) Substrate characterization of the *Saccharomyces cerevisiae* protein farnesyltransferase and type-I protein geranylgeranyltransferase, *Biochim. Biophys. Acta, Protein Struct. Mol. Enzymol.* 1205, 39-48.
 177. Omer, C. A., Kral, A. M., Diehl, R. E., Prendergast, G. C., Powers, S., Allen, C. M., Gibbs, J. B., and Kohl, N. E. (1993) Characterization of recombinant human farnesyl-protein transferase: Cloning, expression, farnesyl diphosphate binding, and functional homology with yeast prenyl-protein transferases, *Biochemistry* 32, 5167-5176.
 178. Reiss, Y., Seabra, M. C., Armstrong, S. A., Slaughter, C. A., Goldstein, J. L., and Brown, M. S. (1991) Nonidentical subunits of p21H-ras farnesyltransferase. Peptide binding and farnesyl pyrophosphate carrier functions, *J. Biol. Chem.* 266, 10672-10677.
 179. Moores, S. L., Schaber, M. D., Mosser, S. D., Rands, E., O'Hara, M. B., Garsky, V. M., Marshall, M. S., Pompliano, D. L., and Gibbs, J. B. (1991) Sequence dependence of protein isoprenylation, *J. Biol. Chem.* 266, 14603-14610.
 180. Yokoyama, K., Goodwin, G. W., Chomashchi, F., Glomset, J. A., and Gelb, M. H. (1991) A protein geranylgeranyltransferase from bovine brain: implications for protein prenylation specificity, *Proc. Natl. Acad. Sci. U. S. A.* 88, 5302-5306.
 181. Casey, P. J., Thissen, J. A., and Moomaw, J. F. (1991) Enzymic modification of proteins with a geranylgeranyl isoprenoid, *Proc. Natl. Acad. Sci. U. S. A.* 88, 8631-8635.
 182. Lamphear, C. L., Scott, S. A., Gibbs, R. A., and Fierke, C. A. (2009) Context-Dependent Substrate Recognition by Protein Farnesyltransferase, *Biochemistry* 48, 1691-1701.
 183. Reid, T. S., Terry, K. L., Casey, P. J., and Beese, L. S. (2004) Crystallographic analysis of CaaX prenyltransferases complexed with

- substrates defines rules of protein substrate selectivity, *J. Mol. Biol.* **343**, 417-433.
184. Casey, P. J. (1995) Mechanisms of protein prenylation and role in G protein function, *Biochem. Soc. Trans.* **23**, 161-166.
 185. Liang, P. H. (2009) Reaction kinetics, catalytic mechanisms, conformational changes, and inhibitor design for prenyltransferases, *Biochemistry* **48**, 6562-6570.
 186. Pickett, J. S., Bowers, K. E., Hartman, H. L., Fu, H.-W., Embry, A. C., Casey, P. J., and Fierke, C. A. (2003) Kinetic studies of protein farnesyltransferase mutants establish active substrate conformation, *Biochemistry* **42**, 9741-9748.
 187. Huang, C., Hightower, K. E., and Fierke, C. A. (2000) Mechanistic studies of rat protein farnesyltransferase indicate an associative transition state, *Biochemistry* **39**, 2593-2602.
 188. Furfine, E. S., Leban, J. J., Landavazo, A., Moomaw, J. F., and Casey, P. J. (1995) Protein farnesyltransferase: kinetics of farnesyl pyrophosphate binding and product release, *Biochemistry* **34**, 6857-6862.
 189. Pais, J. E., Bowers, K. E., Stoddard, A. K., and Fierke, C. A. (2005) A continuous fluorescent assay for protein prenyltransferases measuring diphosphate release, *Anal. Biochem.* **345**, 302-311.
 190. Banerjee, S., and McGeady, P. (2005) Inhibitors of protein prenylation, *Curr. Enzyme Inhib.* **1**, 183-206.
 191. Cohen, L. H., Pieterman, E., van, L. R. E. W., Overhand, M., Burm, B. E. A., van, d. M. G. A., and van, B. J. H. (2000) Inhibitors of prenylation of Ras and other G-proteins and their application as therapeutics, *Biochem. Pharmacol.* **60**, 1061-1068.
 192. Lebowitz, P. F., Casey, P. J., Prendergast, G. C., and Thissen, J. A. (1997) Farnesyltransferase inhibitors alter the prenylation and growth-stimulating function of RhoB, *J. Biol. Chem.* **272**, 15591-15594.
 193. Sebti, S. M., and Hamilton, A. D. (2000) Farnesyltransferase and geranylgeranyltransferase I inhibitors and cancer therapy: lessons from mechanism and bench-to-bedside translational studies, *Oncogene* **19**, 6584-6593.
 194. Oliff, A. (1999) Farnesyltransferase inhibitors: targeting the molecular basis of cancer, *Biochim. Biophys. Acta* **1423**, C19-30.

195. Ohkanda, J., Knowles, D. B., Blaskovich, M. A., Sebti, S. M., and Hamilton, A. D. (2002) Inhibitors of protein farnesyltransferase as novel anticancer agents, *Curr. Top. Med. Chem.* 2, 303-323.
196. Reiss, Y., Goldstein, J. L., Seabra, M. C., Casey, P. J., and Brown, M. S. (1990) Inhibition of purified p21ras farnesyl:protein transferase by Cys-AAX tetrapeptides, *Cell* 62, 81-88.
197. Goldstein, J. L., Brown, M. S., Stradley, S. J., Reiss, Y., and Gierasch, L. M. (1991) Nonfarnesylated tetrapeptide inhibitors of protein farnesyltransferase, *J. Biol. Chem.* 266, 15575-15578.
198. Peruzzi, M., Parker, K. C., Long, E. O., and Malnati, M. S. (1996) Peptide sequence requirements for the recognition of HLA-B*2705 by specific natural killer cells, *J. Immunol.* 157, 3350-3356.

CHAPTER II

CATALYTIC CHARACTERIZATION OF YEAST PALMITOYLTRANSFERASE AKR1P USING THE NEWLY IDENTIFIED SUBSTRATE YPL199C

Introduction

Palmitoylation (1, 2), prenylation (3-6), and myristoylation (7, 8) represent three types of common lipid modifications that occur in the cell. During the past decade, the enzymes responsible for prenylation and myristoylation have been extensively studied, and the target sequences for these modifications have been identified. In recent years, palmitoylation has attracted great attention due to the reversibility of the thioester modification (9-16), which could allow for regulation of protein membrane localization and other lipid-dependent interactions (2, 9, 12, 17-22). However, unlike the other two common lipid modifications, both the sites of palmitoylation in substrate proteins and the catalytic mechanism of the palmitoyltransferases (PATs) are not well understood.

PATs were first identified in yeast more than a decade ago using a genetic screen against palmitoylation-dependent Ras proteins (23); afterwards a number of PATs have been identified in both yeast and mammals, with each catalyzing the palmitoylation of a different set of substrate proteins (24). Many

of these substrate proteins are involved in important biological pathways. For example, the PAT complex Erf2p/Erf4p (25-28) catalyzes the palmitoylation of Ras proteins to enhance membrane association (29), and the PAT HIP14 (18, 30-32) modifies many neuronal proteins, including PSD-95, SNAP-25 (31) and huntingtin protein (htt) (24). Akr1p, an integral membrane protein which is a homologue of HIP14 from yeast, catalyzes the palmitoylation of yeast casein kinase 2 (Yck2p) to regulate endocytic trafficking (33-36). Davis and colleagues have demonstrated that Yck2p is exclusively localized at the plasma membrane in cells expressing Akr1p (*AKR1*⁺ cells) while diffusely localized in the cytosol in *akr1Δ* cells. Mutation of the two C-terminal cysteines of Yck2p to serine also results in cytosolic localization. These data suggest that palmitoylation of Yck2p, catalyzed by Akr1p, enhances membrane association (35).

Even though significant effort has been expended to identify palmitoylated proteins, the lack of a consensus motif for palmitoylation has made prediction of substrate proteins difficult (37). This difficulty is underscored by the large variety of protein contexts observed for palmitoylation. In contrast, sequence alignment of the PATs reveals a conserved DHHC (Asp-His-His-Cys) cysteine-rich domain (38), a sequence reminiscent of a zinc finger-like motif. In several of the PATs including Akr1p, tyrosine is substituted for the second histidine of the DHHC motif (Figure 2.1) (39). Among the DHHC protein family, there are 7 proteins from yeast and 23 proteins from humans that have

palmitoylation activity (2). Mutations in the DHHC sequence of Akr1p abolish the palmitoylation activity (40), implicating this region as a possible active site candidate. However, the *in vitro* observation of DHHC protein-independent palmitoylation activity suggests that this domain may not be essential for palmitoylation within the cell (37). Thus, identifying the role, if any, that the DHHC motif plays in the palmitoylation reaction is an important topic to address to understand *in vivo* palmitoylation.

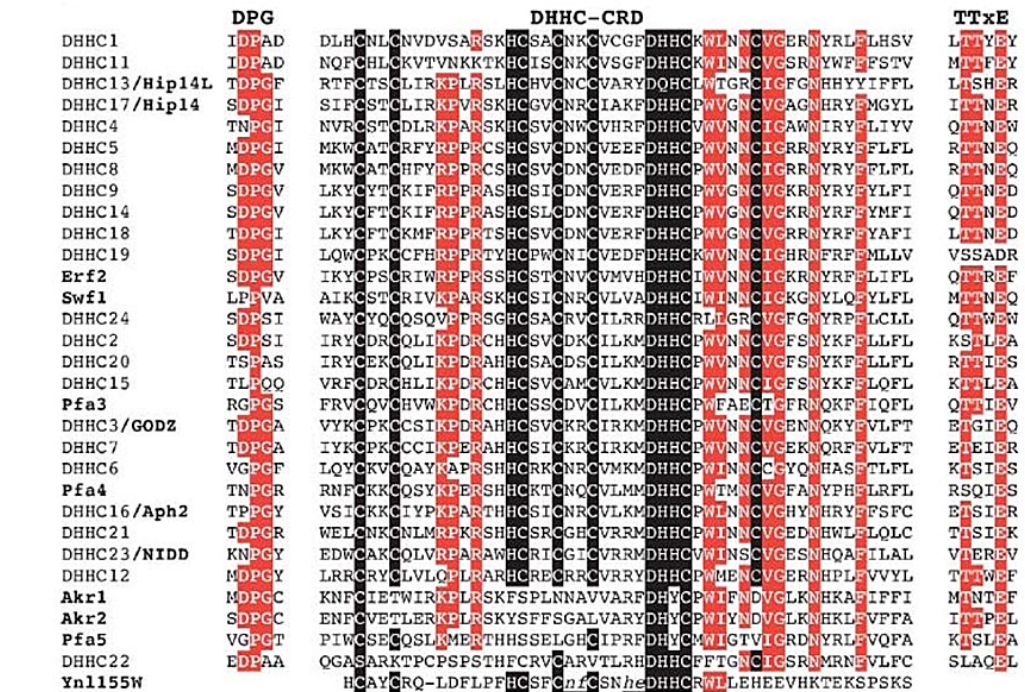


Figure 2.1: Sequence alignment of the identified yeast and human PATs. All of these proteins belong to the DHHC protein family and have palmitoylation activity. The consensus motif at the bottom shows that they all contain the DHHC-cysteine rich domain (CRD). In Akr1p DHHC is replaced by DHYC. Additionally, several of the conserved cysteines are absent in Akr1p.

Akr1p is an 86 kDa yeast integral membrane protein containing 6 transmembrane domains (TMD) and 6 ankyrin repeat sequences; the DHHC motif (DHYC in Akr1p) is located between TMD 4 and 5 (41). Since it is a yeast membrane protein, overexpression, purification, and stability of the activity in detergents represent significant challenges to mechanistic studies of Akr1p. In this chapter I will describe the optimization of Akr1p expression and purification methods to obtain ~50 µg Akr1p per liter of yeast culture. In addition, this chapter describes preliminary characterization of the catalytic properties and analysis of the reactivity of Akr1p with a novel substrate that is better suited for mechanistic studies. These developments provide useful tools for studying Akr1p, as well as other PATs implicated in disease development, such as HIP14.

Experimental Procedures

Akr1p expression and purification

The plasmid encoding the *AKR1* gene and the expressing yeast strain were obtained from the Davis lab at Wayne State University as generous gifts. The C-terminal 3xHA/FLAG/6xHis-tagged Akr1p encoded on pRS316 vector was transformed into *akr1Δ pep4Δ* NDY1547 yeast cells, and Akr1p was expressed under the control of the *GAL1* promoter. Cells were grown in SRC-Ura (synthetic raffinose complete-uracil) medium at 30°C to late log-phase with $\sim 2 \times 10^8$ cells/mL, pelleted by centrifugation and resuspended in 20 mL cold TBS (Tris-Buffered Saline) containing 1 mM Dithiothreitol (DTT)

and 2x protease inhibitors (Buffer 1). The suspension was slowly dripped into liquid nitrogen to form frozen droplets and lysed by 15 min of grinding with a mortar and pestle in the presence of liquid nitrogen. The lysate was thawed on ice, and the membrane mixture was solubilized by incubation with 1% Triton X-100 using end-over-end mixing for 30 min at 4 °C. The undissolved fraction was removed by centrifugation at 20,000 × *g* for 20 min. The supernatant was incubated with 4 mL anti-FLAG M2 mAb-agarose (Sigma-Aldrich) for 2 h at 4 °C, and washed with buffer containing 50 mM HEPES, 150 mM NaCl, 140 mM sucrose, 1 mM DTT, 0.5 mg/ml bovine liver lipids (Avanti Polar Lipids), 1% Triton X-100, pH 8.0. Akr1p was eluted by addition of buffer containing 0.3% Triton X-100 and 300 g/ml FLAG peptide (Sigma-Aldrich) to the wash buffer.

SYPRO® Ruby protein gel staining

SYPRO® Ruby protein gel stain was purchased from Molecular Probes. After electrophoresis, the SDS-PAGE gel was incubated two times with 100 mL of fix solution (50% methanol, 7% acetic acid) on an orbital shaker for 15 min. The gel was then placed into 60 mL of SYPRO® Ruby stain with 3 cycles of heating in a microwave (30 sec) followed by agitation on a shaker (30 sec, 5 min, and 23 min). After staining, the gel was transferred to a new container and washed in 100 mL of wash solution (10% methanol, 7% acetic acid) for 30 min. Finally, the gel was rinsed in ultrapure water and visualized on a Typhoon 9410 phosphorimager with excitation at 457 nm and emission at 610 nm.

In vitro palmitoylation assay

The *in vitro* palmitoylation reaction contained 5 μ Ci of [3 H]palmitoyl-CoA (PerkinElmer), 10 μ M Ypl199c substrate protein, 100 mM MES, pH 6.4, 0.2 mg/ml bovine liver lipids (Avanti), 1 mM DTT, and Akr1p (~30–40 nM). After incubation at 30 °C for various time, the reactions were stopped by the addition of 400 μ L methanol and 150 μ L chloroform, and the proteins were pelleted by methanol-chloroform precipitation and subjected to SDS-PAGE. The gel was fixed by incubation with 4% isopropanol, 10% acetic acid, 0.2% formaldehyde and incubated with 20% 2, 5-diphenyloxazole (PPO) in DMSO and dried with a gel-dryer. The gel was then exposed to Kodak high-sensitivity film for 72 h to visualize radioactive bands.

Yck2p and Ypl199c substrate proteins

The N-terminal 6xHis/FLAG/HA-tagged Yck2p (with a D218A mutation) and Ypl199c gene encoded on pET30a expression vector were gifts from the Davis lab. Both substrate proteins were overexpressed recombinantly in *E. coli* Rosetta DE3 strain transformed with expression plasmids after induction with 400 μ M Isopropyl β -D-1-thiogalactopyranoside (IPTG) at 15 °C for 8 h. The cells were pelleted by centrifugation and resuspended in 20 mM Tris, pH 8.0, 300 mM NaCl, 10 mM imidazole with protease inhibitors. The cells were lysed by sonication on ice and the target proteins were purified using Ni-NTA agarose (QIAGEN) affinity chromatography. The proteins were washed and eluted from the column in a gradient imidazole format using buffer A (20 mM

Tris, pH 8.0, 300 mM NaCl, 10 mM imidazole) and buffer B (20 mM Tris, pH 8.0, 300 mM NaCl, 500 mM imidazole). The protein fractions were combined, concentrated using Amicon Ultra-15 Centrifugal Filter Units (Millipore), and buffer-exchanged to 20 mM Tris-HCl, pH 7.7, 150 mM NaCl, 10 mM DTT.

Dependence of Akr1p activity on chelators or metals

Stock aqueous solutions of 100 mM 2,6-pyridinedicarboxylic acid (DPA) and 100 mM ethylenediaminetetraacetic acid (EDTA) were prepared and base was added to neutralize the pH. Stock solutions of 5 mM N,N,N',N'-tetrakis(2-pyridylmethyl)ethylenediamine (TPEN) and 100 mM 1,10-phenanthroline stock solutions were prepared in ethanol. Purified Akr1p was incubated with 100 mM MES with 20 mM DPA, 100 μ M TPEN, 5 mM 1,10-phenanthroline, or each of these plus 5 mM EDTA on ice for 1 h. Then the enzyme was diluted into the assay mix and the palmitoylation activity was measured. For testing the effect of zinc on catalytic activity, Akr1p was incubated with various concentrations of ZnSO₄ (100 nM, 1 μ M, 10 μ M, 100 μ M, 500 μ M, 1 mM, 2 mM) for 1 h on ice before assaying activity.

Mutagenesis

All Akr1p mutations were introduced into the pRS316 plasmid using QuikChange methodology (Stratagene). Following confirmation of the desired mutation by sequencing, mutant Akr1p was expressed in yeast and purified using the same protocol as the WT enzyme. Mutations of Ypl199c were

prepared in pET30a plasmid and the mutant proteins were expressed in *E. coli* and purified similarly as described for the WT protein.

Results

Expression and in vitro purification of Akr1p

I expressed active Akr1p protein encoded on pRS316 plasmid from NDY1547 *akr1*Δ yeast strain, which prevents interference from endogenous Akr1p. Additionally, to suppress the deleterious effects of the chromosomal Akr1p deletion on growth, the -CCIIIS sequence was appended to the C-terminal of the chromosomal copy of Yck2 (*YCK2(CCIIS)*). This is a recognition sequence for farnesylation of the cysteine 4 amino acids from the C-terminus by FTase followed by palmitoylation of the upstream cysteine catalyzed by Erf2p. I first expressed Akr1p under the control of the natural Akr1p promoter; however the expression yield was very low. To enhance expression, I switched to a new plasmid with Akr1p under control of the *GAL1* promoter. In NDY1547 yeast transformed with this plasmid, the expression level of Akr1p increased ~10 fold, which is required for characterization of the enzyme mechanism.

Anti-FLAG affinity purification was performed to purify the FLAG-tagged Akr1p. The flow chart describing the procedure is shown in Figure 2.2(a), while anti-HA western blot of samples 1–4 is shown in Figure 2.2(b), indicating that Akr1p was enriched using this procedure. It is important to note that bovine liver lipids play a crucial role in reconstituting the palmitoylation activity of

Akr1p, possibly by forming a lipid bilayer membrane structure. We have shown that without adding this component, Akr1p is inactive. To sum up, after Akr1p overexpression and anti-FLAG affinity purification, 40–50 µg of purified Akr1p could be obtained from each liter of yeast culture, as indicated by SYPRO® Ruby staining of a SDS-PAGE gel (Figure 2.3).

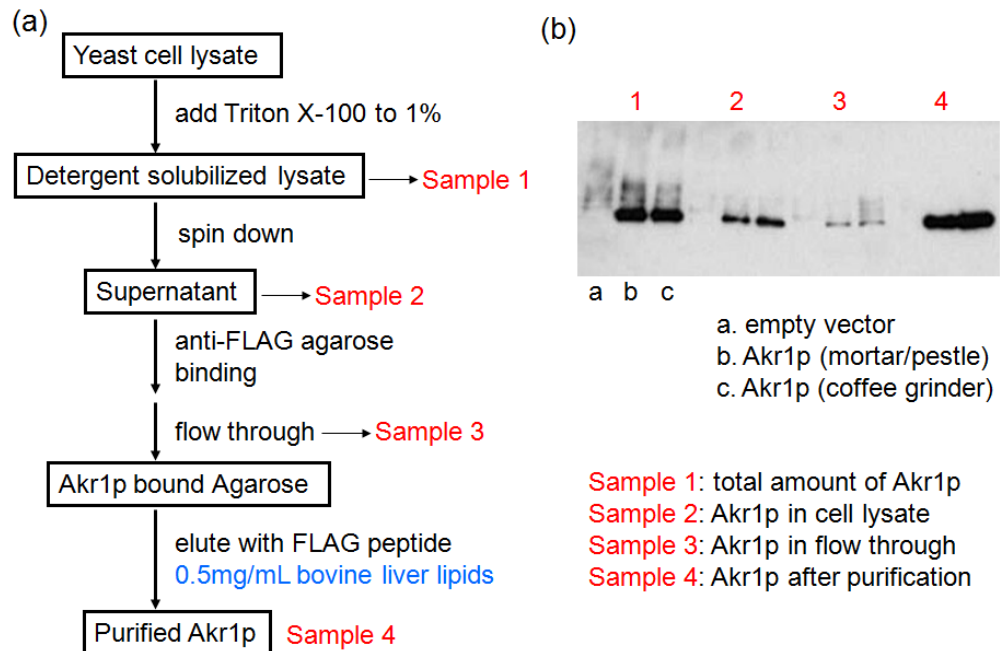


Figure 2.2: Flow chart of the anti-FLAG affinity purification of Akr1p (a). Sample 1 contains the total amount of Akr1p expressed in yeast cells, and sample 2 contains Akr1p in the crude cell lysate. Sample 3 contains Akr1p in the flow through which fails to bind to the agarose, while sample 4 is the amount of Akr1p after purification. **Anti-HA western blot of a SDS-PAGE gel containing Akr1p samples at each step in the anti-FLAG affinity purification process (b).** For each sample there are 3 lanes: a. empty vector control, b. Akr1p lysed by mortar/pestle grinding with liquid N₂, c. Akr1p lysed by a coffee grinder.

Determination of the Akr1p concentration

Akr1p expresses at a very low level in yeast; therefore it is quite a challenge to measure its concentration. UV absorbance or coomassie staining of an SDS gel is not sensitive enough to detect the protein signal, and western blotting

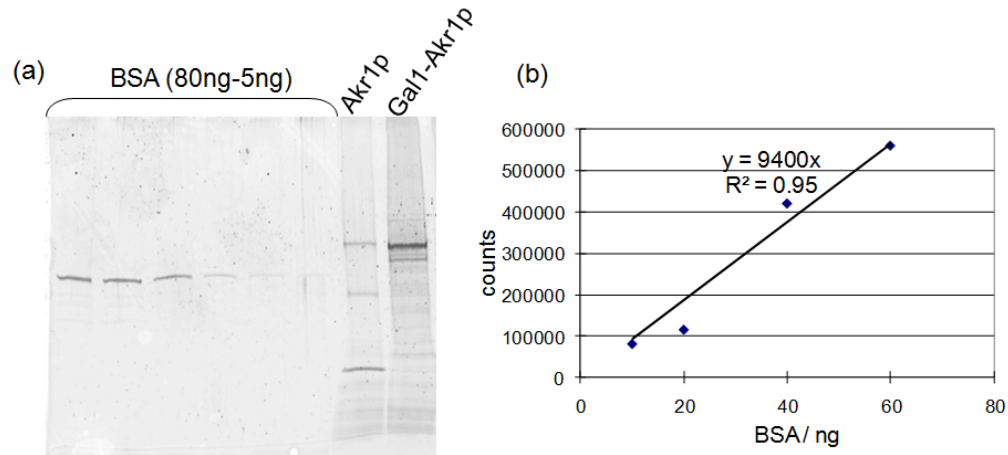


Figure 2.3: SYPRO® Ruby protein gel stain for the determination of the Akrlp concentration (a). Different amount of ultrapure BSA and anti-FLAG affinity purified Akrlp and *GAL1*-Akrlp were loaded onto the SDS-PAGE protein gel. The gel was then stained using the Ruby staining protocol and subjected to Typhoon 9410 phosphorimager analysis with excitation at 457 nm and emission at 610 nm. **Standard curve of the intensity of the BSA bands (b).** The protein band intensities were determined using the ImageQuant software and the intensities were plotted versus the amount of BSA. The amount of purified Akrlp and *GAL1*-Akrlp were then calculated based on the standard curve.

does not measure the protein concentration with sufficient accuracy or provide information about enzyme purity. Herein, I developed a method using the very sensitive SYPRO® Ruby protein gel stain to estimate the amount of purified Akrlp. Ruby stain has a sensitivity in the 1 ng protein range (42), which is even more sensitive than traditional silver stain. To quantify the Akrlp concentration, BSA was used as a protein standard, with 5-80 ng loaded lanes on the protein gel along with the Akrlp samples (Figure 2.3(a)). The gel was fixed and incubated with the Ruby stain, as described in the methods section and quantified by phosphorimager analysis of the intensity of each protein band. A standard curve was made using the BSA intensities which is reasonably linear

in the range of 10-60 ng (Figure 2.3(b)). We assume that BSA and Akr1p are stained at about the same level, as Ruby stain provides little protein-to-protein variability since it binds to both basic amino acids and the polypeptide backbone (43, 44). Figure 2.3(a) shows that switching to the *GAL1* promoter-containing plasmid increases expression level greatly and the protein purity is also enhanced. Based on the intensity of the *GAL1*-Akr1p band and the BSA standard curve, 40–50 µg purified Akr1p was obtained per liter of yeast culture.

Identification of a new Akr1p substrate Ypl199c

The proteomic study carried out by the Davis laboratory (45) identified several potential Akr1p substrates, including yeast casein kinase (Yck2p), which is a relatively well-studied substrate. However, Yck2p is a casein kinase that is heavily phosphorylated at multiple positions by cellular kinases, which complicates using this substrate to study palmitoylation. In particular, palmitoylation of Yck2p is activated by ATP, suggesting that palmitoylation is dependent on phosphorylation (35). Therefore, an alternate substrate could significantly simplify mechanistic studies of Akr1p. We therefore compared the reactivity of recombinantly expressed Yck2p and Ypl199c, a protein identified as an Akr1p substrate by the proteomic analysis (45) with unknown function. The protein substrates were incubated with [³H]palmitoyl-CoA and Akr1p purified from yeast, precipitated with methanol-chloroform, and fractionated by SDS-PAGE. Tritium-labeled proteins were detected by autoradiography. Both

Yck2p and Ypl199c are palmitoylated in an Akr1p-dependent manner under these conditions; Akr1p catalyzes palmitoylation of Ypl199c to a greater extent than Yck2p, while auto-palmitoylation of Akr1p occurs to a similar extent in both reactions (Figure 2.4(a)). Using the same assay condition, a time-dependent [³H]palmitoyl labeling of Ypl199c catalyzed by Akr1p was observed, indicating a single exponential increase of the band intensity (Figure 2.4(b)). These data demonstrate that palmitoylation of both proteins is readily catalyzed by Akr1p. Due to the enhanced reactivity of Ypl199c, we chose to use this substrate for further mechanistic studies.

Ypl199c contains two cysteines at its c-terminus (-FCNCIQSLA), which are hypothesized to be its palmitoylation sites. To explore which cysteine(s) is the palmitoylation site(s), we made the single and double cysteine mutations to serine. As shown in Figure 2.5, C233S showed the same level of palmitoylation as WT Ypl199c. Unexpectedly C235S shows a higher level of palmitoylation. These data demonstrate that palmitoylation of both cysteines can be catalyzed by Akr1p. In addition, the recognition of the palmitoylation site is not strict, as long as the cysteine is close to the C-terminus of the protein. Other cysteines in Ypl199c are not palmitoylated, as the C233/235S double mutant showed no significant labeling.

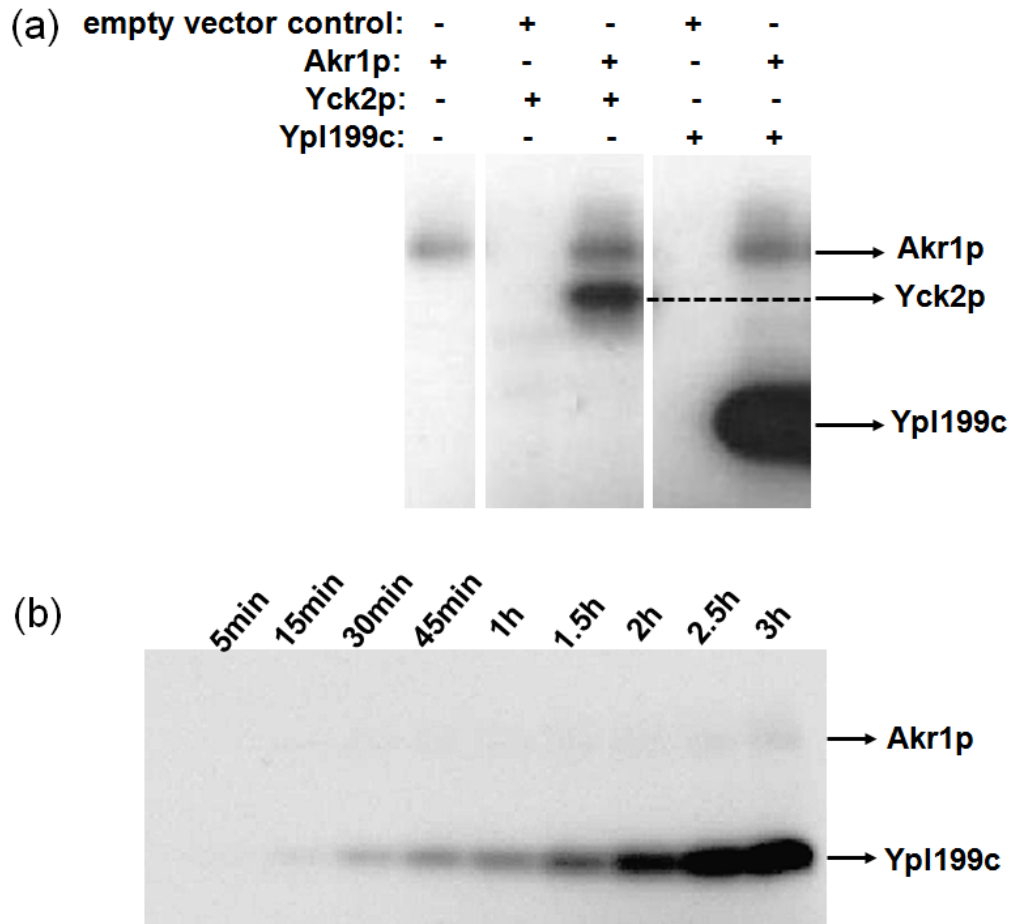


Figure 2.4: Analysis of reactivity of Akr1p with a new protein substrate Ypl199c (a). Reactions are done *in vitro* using the radioactive palmitoylation assay. Each 50 μ L reaction contains 100 mM MES, pH 6.4, 3.8 μ M [3 H]palmitoyl-CoA (31 Ci/mmol), 10 μ M Yck2p or Ypl199c, ~15 nM Akr1p (or control) purified from yeast, and 0.2 mg/mL bovine liver lipids. After 1h incubation at 30°C, the reactions were stopped by addition of methanol-chloroform. The precipitated proteins were fractionated by SDS-PAGE and radiolabeled proteins were detected by autoradiography. **Palmitoylation time course of Ypl199c catalyzed by Akr1p (b).** Reactions were carried out as described in (a) and stopped at various time points by addition of methanol-chloroform.

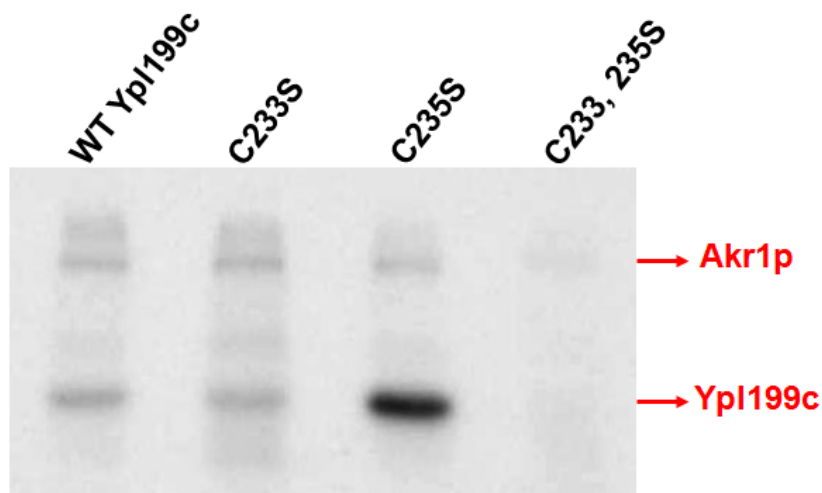


Figure 2.5: Identification of the palmitoylation site(s) in the substrate Ypl199c. Ypl199c contains 2 cysteines (C233 and C235) toward its C-terminus (-FCNCIQSLA). WT, C233S, C235S, and C233/235S Ypl199c protein were recombinantly expressed in *E. coli* and purified using Ni-NTA column. Each protein (10 μ M) was added to reactions containing 1.25 μ M [3 H]palmitoyl-CoA and \sim 60nM Akr1p enzyme purified from yeast. After 1h incubation at 30°C, reactions were methanol-chloroform precipitated, run on a SDS-PAGE gel, and then subjected to autoradiography to detect the protein labeling level.

Akr1p activity is dependent on pH but not metal ion

An important first step in mechanistic studies is identification of conditions where the enzyme is maximally active. Therefore, a pH profile of Akr1p catalyzed palmitoylation of Ypl199c was carried out at saturating palmitoyl-CoA measuring product formation within the linear range of the reaction curve. These data indicate that maximal activity occurs between pH 6.0 and 6.5, with activity decreasing substantially at both lower and higher pH values (Figure 2.6). However, the pKa of an unperturbed cysteine is 8.0. It is then reasonable to hypothesize that the cysteine thiolate is stabilized by some positively charged groups such as a metal ion or some amino acids for efficient catalysis.

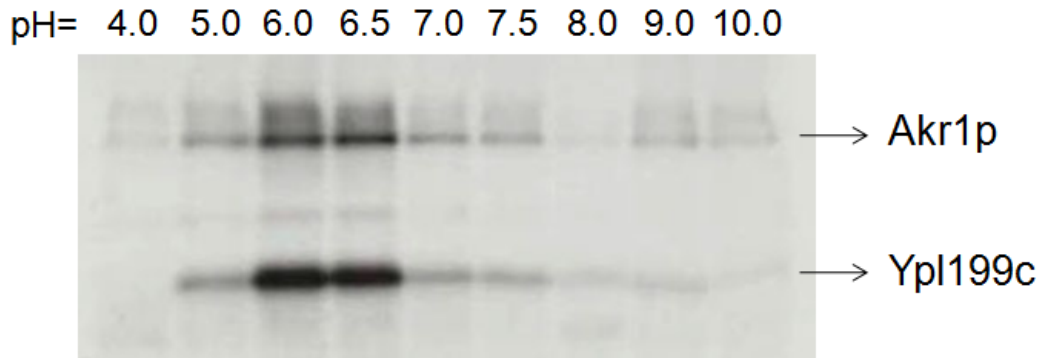


Figure 2.6: pH profile of Akkr1p palmitoylation activity. The 100 mM buffers for the pH profile were: acetate (pH 4 and 5); MES (pH 6 and 6.5); bis-Tris propane (pH 7-9) and CAPS (pH 10). All assays were done with saturating palmitoyl-CoA within the linear range of the reaction curve (1 h reaction time, 30°C). The reactions were stopped and precipitated by addition of methanol-chloroform, run on a SDS-PAGE gel, and then subjected to autoradiography to detect the level of palmitoylation.

The sequence alignment of all DHHC proteins shows a conserved DHHC-cysteine rich domain (CRD), which has some structural similarity with the C₂H₂ zinc finger domain (46). This leads to the proposal that there might be a zinc metal ion bound to Akkr1p that is important for function. I therefore tested whether Akkr1p activity is affected by incubation with metal ions or a variety of metal chelators, including EDTA and the more hydrophobic chelators, DPA, TPEN, and 1, 10-phenanthroline (structures shown in Figure 2.7). The chelators were incubated with the purified enzyme for 1 h on ice before the catalytic activity was measured. As shown in Figure 2.7, none of these chelators completely eliminated either the auto- or trans-palmitoylation activity as proposed for chelators of an essential metal ion (lane 2-7). However, 1, 10-phenanthroline may partially inhibit trans-palmitoylation (lane 4 and 7) while some chelators may enhance activity somewhat. Consistent with this,

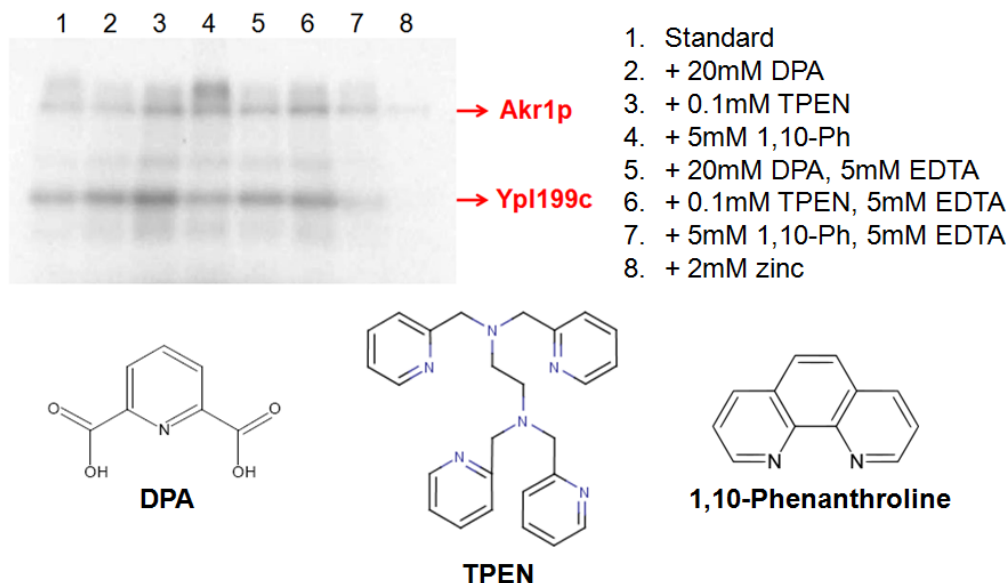


Figure 2.7: Akrl1p activity is not metal-dependent. Purified Akrl1p was incubated with different chelators (listed in the figure) for 1 h on ice before added to initiate the reactions. The reactions were stopped and proteins were precipitated by addition of methanol-chloroform. The substrate proteins were fractionated on a SDS-PAGE gel, and then subjected to autoradiography to detect the protein labeling level. The enzyme incubated with chelators (lane 2-7) showed similar amount of activities compared to the standard non-chelated enzyme (lane 1).

addition of 2 mM ZnSO₄ significantly inhibits the Akrl1p activity. To verify that Akrl1p activity is inhibited rather than activated by the zinc ion, Akrl1p activity was measured in the presence of zinc concentration varying from 100 nM to 2 mM. These data demonstrate that Akrl1p is not activated by zinc; rather inhibition is observed when the total zinc concentration is > 100 μM in the pre-incubation enzyme mix in the assay (Figure 2.8). To sum up, there is no evidence for a role of a metal in the function of Akrl1p.



Figure 2.8: Zinc inhibits rather than activates the Akkr1p activity. Different concentrations of zinc (from 100 nM to 2 mM) were incubated with Akkr1p for 1 h on ice before measuring catalytic activity. The reactions were stopped and proteins were precipitated by addition of methanol-chloroform. The substrate proteins were fractionated on a SDS-PAGE gel, and then subjected to autoradiography to detect the protein labeling level. The palmitoylation activity did not change significantly until the zinc concentration reached to 100 μ M, indicating that zinc is not involved in the catalytic site of Akkr1p.

Mutagenesis studies on the DHYC motif disclose the importance of each amino acid

As a first step in analyzing the catalytic mechanism of Akkr1p, we used mutagenesis to identify residues essential for efficient catalytic activity. The most conserved sequence in the palmitoyltransferases discovered so far, including the 23 proteins from human and 7 from yeast, is the DHHC motif (DHYC for Akkr1p), suggesting that these residues might be important for catalysis. Consistent with this, as reported by Roth et. al. (35), mutations in the DHYC motif (DH \rightarrow AA and C \rightarrow A) abolish catalysis of palmitoylation of Yck2p by Akkr1p. Furthermore, mutations in this conserved motif in other PATs, including C203S in Erf2p (34) and C468S in HIP14 (47), also abolish palmitoylation activity. To further elucidate the catalytic importance of each residue within this motif, we constructed nine single amino acid mutants:

D497A, D497N, H498A, H498N, H498K, Y499H, Y499F, C500S, and C500A. None of these mutations significantly affect the yield of Akrlp after purification (Figure 2.9). However, all of the mutations at D497, H498 or C500, which are strictly conserved across all known DHHC palmitoyltransferases, show at least a 100-fold decrease in both palmitoylation of Ypl199c and auto-palmitoylation catalyzed by Akrlp (Figure 2.9), demonstrating the catalytic importance of these side chains. In contrast, mutation of Y499 to either Phe or His, the amino acid observed in other palmitoyltransferases, causes only a 2-3-fold decrease in the activity of Akrlp, as indicated by palmitoylation of either Ypl199c and Akrlp.

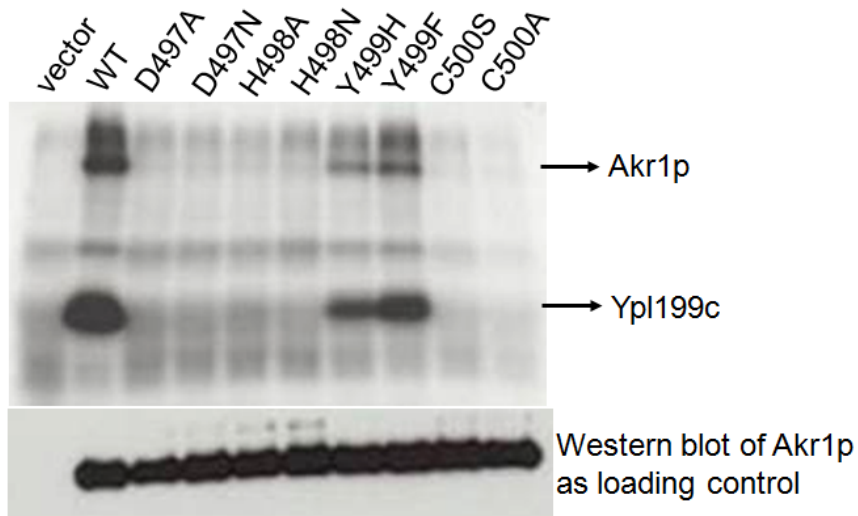


Figure 2.9: D, H, and C residues in the D497H498Y499C500 motif are crucial for the Akrlp palmitoylation activity. Reactions are done *in vitro* using the radioactive assay as described in the legend of Figure 2.4. Each reaction contains 2.5 μ M [3 H]palmitoyl-CoA, 10 μ M Ypl199c, and \sim 60 nM WT or mutant Akrlp purified from yeast. After 1h incubation at 30°C, reactions were methanol-chloroform precipitated, run on a SDS-PAGE gel, and then subjected to autoradiography to detect the protein labeling level. An anti-HA western blot, detecting HA-tagged Akrlp, is also shown indicating that similar amount of WT and mutant Akrlp were obtained after expression and purification.

Discussion

Ypl199c as a novel substrate of Akr1p

Davis and colleague carried out a global analysis of all yeast proteins in the membrane fraction to identify palmitoylated proteins using the MudPIT (multi-dimensional protein identification technology) tandem-MS-based proteomic methodology (45). They successfully detected 47 palmitoylated proteins, including 12 of the 15 proteins known at that time plus 35 new ones. In addition, to identify the substrate proteins of each DHHC-containing palmitoyltransferase, they also applied the proteomic method to mutant yeast strains deficient for one DHHC protein (for example, *akr1Δ*strain). As a result, the substrate candidates for Akr1p should be underrepresented in the MS/MS analysis of palmitoylated proteins in the *akr1Δ*strain. In this way they successfully identified 6 yeast proteins as potential Akr1p substrates, whose names, functions and localizations are listed in Table 2.1 (45).

Yck2p is a relatively well-studied substrate protein of Akr1p; however, it is a casein kinase, so that it gets heavily phosphorylated in the cell, which complicates analysis of palmitoylation. Although we used the D218A mutant that decreases the casein kinase activity, multiple bands on SDS-PAGE analysis indicate structural heterogeneity. Therefore, the mechanistic studies will be simplified by analyzing palmitoylation of an alternate substrate.

Based on the table above, we cloned the *YPL199C* and *YKL047W* gene into pET30a vector, and recombinantly expressed them in *E. coli*. Both

Ypl199c and Yki047w showed Akr1p dependent palmitoylation, while Ypl199c had much higher palmitoyl labeling. Moreover, Yki047w is a membrane protein, while Ypl199c is cytosolic, which makes Ypl199c much easier to express and purify. I therefore choose Ypl199c for our palmitoylation mechanistic studies.

Name	Function	Localization
Yck1	Type I casein kinase; roles in endocytic trafficking and cellular morphogenesis	Plasma membrane
Yck2	Type I casein kinase; roles in endocytic trafficking and cellular morphogenesis	Plasma membrane
Akr1	DHHC-type protein palmitoyltransferase	Golgi
Ypl199c	Function unknown	Plasma membrane
Yki047w	Function unknown	ER and plasma membrane
Meh1	EGO1; component of the EGO complex; regulates microautophagy	Vacuolar membrane

Table 2.1: Akr1p substrate candidates based on the global analysis of protein palmitoylation in yeast. Yck2p has long been identified as the substrate of Akr1p. Additional substrates and their cellular locations are indicated.

D, H, and C in the DHYC motif function as a catalytic triad

The conserved DHHC motif is proposed to constitute a core element responsible for the PAT activity. The mutagenesis data (Figure 2.9) confirm that the Asp, His, and Cys residues in the DHYC motif are essential for the palmitoylation activity of Akr1p. However, how this motif contributes to the catalytic mechanism of Akr1p is still unknown. Our functional data demonstrate that there is no evidence for involvement of a metal ion in Akr1p function.

Furthermore, it is likely that the cysteine thiolate on the substrate is stabilized since this is a better nucleophile than the thiol group. The pH profile suggests that the maximal activity is at ~6.5, possibly indicates a decreased thiol substrate pKa. Based on these data, the mutagenesis results and literature precedents (48), we propose a possible catalytic triad (Figure 2.10) proposing potential roles for each amino acid to catalyze palmitoylation. Cysteine proteases, like papain, contain a similar catalytic dyad with Asp and His. The mutagenesis data are consistent with similar functions of the Cys, His, Asp triad in Akr1p. The D497N abolished the activity of Akr1p, implying that either the negative charge or hydrogen bond acceptor of aspartate is crucial for the catalytic activity, perhaps by enhancing the reactivity of His, as observed in papain. Furthermore, neither H498N nor H498K retain the Akr1p palmitoylation activity, meaning that the role of histidine is not just to function as a hydrogen bond acceptor/donor. Based on the aromatic structure of histidine, we propose that it is responsible for facilitating the formation of the thiolate nucleophile on the enzyme and the protein substrate. To sum up, D497 and H498 may serve to stabilize a nucleophilic thiolate anion for formation of a covalent thiolester intermediate, similar to the thiols activation in thiol proteases (48) and N-acetyltransferases (49-51).

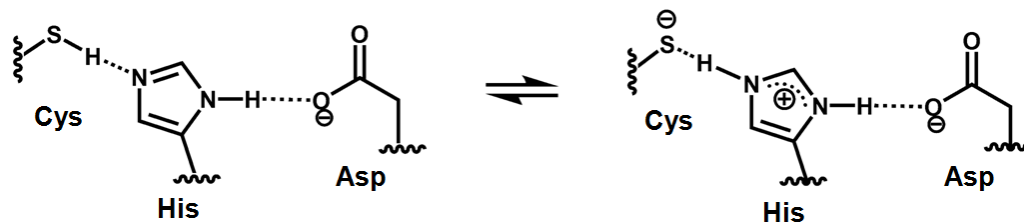


Figure 2.10. The DHYC motif functions as a catalytic triad. A model of a catalytic triad formed by D497, H498, and C500 is proposed showing the activation of the thiol group of the C500 (the DHYC cysteine), which facilitates the formation of a covalent intermediate.

Auto-palmitoylation has been suggested as a covalent thioester intermediate in the catalytic pathway. However it is also possible that auto-palmitoylation of a non-active site residue regulates the function of PATs. Akr1p mutations affect both auto- and trans-palmitoylation, consistent with a catalytic role for this intermediate. A reasonable mechanism showing the formation of the covalent enzyme intermediate, based on the mechanism of thiol proteases, is proposed in Figure 2.11. In this mechanism a reactive cysteine of Akr1p functions as a nucleophile to react with the non-covalently bound palmitoyl-CoA to form a new Akr1p-palmitoyl thioester bond with formation and dissociation of CoA. With this intermediate, the thiol of the protein substrate reacts with the Akr1p thioester to form the palmitoylated protein and regenerate Akr1p in a second step. Based on our findings, the X group in the scheme stabilizing the cysteine thiolate is composed of the Asp and His residues rather than a metal ion.

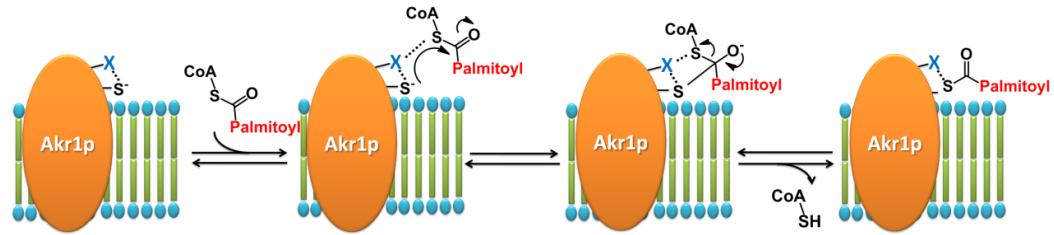


Figure 2.11: Scheme of the proposed Akkr1p palmitoylation mechanism showing the first auto-palmitoylation step. X indicates one or more groups stabilizing the cysteine thiolate, and is proposed to be the Asp and His residues. The thiolate then attacks the carbonyl carbon of palmitoyl-CoA as a nucleophile and the palmitoyl moiety from palmitoyl-CoA is modified onto the stabilized cysteine through the addition-elimination reaction. CoA-SH is then released and the structure showing on the right is the auto-palmitoylated Akkr1p, which is observed in the *in vitro* palmitoylation reaction.

References

1. Charollais, J., and Van, D. G. F. G. (2009) Palmitoylation of membrane proteins, *Mol. Membr. Biol.* 26, 55-66.
2. Fukata, Y., and Fukata, M. (2010) Protein palmitoylation in neuronal development and synaptic plasticity, *Nat. Rev. Neurosci.* 11, 161-175.
3. Zhang, F. L., and Casey, P. J. (1996) Protein prenylation: molecular mechanisms and functional consequences, *Annu. Rev. Biochem.* 65, 241-269.
4. Winter-Vann, A. M., and Casey, P. J. (2005) Opinion: Post-prenylation-processing enzymes as new targets in oncogenesis, *Nat. Rev. Cancer* 5, 405-412.
5. Sebti, S. M., and Hamilton, A. D. (2000) Farnesyltransferase and geranylgeranyltransferase I inhibitors and cancer therapy: lessons from mechanism and bench-to bedside translational studies, *Oncogene* 19, 6584-6593.
6. Magee, T., and Seabra, M. C. (2005) Fatty acylation and prenylation of proteins: what's hot in fat, *Curr. Opin. Cell Biol.* 17, 190-196.
7. Johnson, D. R., Bhatnagar, R. S., Knoll, L. J., and Gordon, J. I. (1994) Genetic and biochemical studies of protein N-myristoylation, *Annu. Rev. Biochem.* 63, 869-914.
8. Farazi, T. A., Waksman, G., and Gordon, J. I. (2001) The biology and

enzymology of protein N-myristoylation, *J. Biol. Chem.* 276, 39501-39504.

9. Smotrys, J. E., and Linder, M. E. (2004) Palmitoylation of intracellular signaling proteins: Regulation and function, *Annu. Rev. Biochem.* 73, 559-587.
10. Qanbar, R., and Bouvier, M. (2003) Role of palmitoylation/depalmitoylation reactions in G-protein-coupled receptor function, *Pharmacol. Ther.* 97, 1-33.
11. Milligan, G., Parenti, M., and Magee, A. I. (1995) The dynamic role of palmitoylation in signal transduction, *Trends Biochem. Sci.* 20, 181-186.
12. Iwanaga, T., Tsutsumi, R., Noritake, J., Fukata, Y., and Fukata, M. (2009) Dynamic protein palmitoylation in cellular signaling, *Prog. Lipid Res.* 48, 117-127.
13. Bouvier, M., Moffett, S., Loisel, T. P., Mouillac, B., Herbert, T., and Chidiac, P. (1995) Palmitoylation of G-protein-coupled receptors: a dynamic modification with functional consequences, *Biochem. Soc. Trans.* 23, 116-120.
14. Basu, J. (2004) Protein palmitoylation and dynamic modulation of protein function, *Curr. Sci.* 87, 212-217.
15. Conibear, E., and Davis, N. G. (2010) Palmitoylation and depalmitoylation dynamics at a glance, *J. Cell Sci.* 123, 4007-4010.
16. Mumby, S. M. (1997) Reversible palmitoylation of signaling proteins, *Curr. Opin. Cell Biol.* 9, 148-154.
17. El-Husseini, A. E.-D., and Bredt, D. S. (2002) Protein palmitoylation: a regulator of neuronal development and function, *Nat. Rev. Neurosci.* 3, 791-802.
18. Yanai, A., Huang, K., Kang, R., Singaraja, R. R., Arstikaitis, P., Gan, L., Orban, P. C., Mullard, A., Cowan, C. M., Raymond, L. A., Drisdell, R. C., Green, W. N., Ravikumar, B., Rubinsztein, D. C., El-Husseini, A., and Hayden, M. R. (2006) Palmitoylation of huntingtin by HIP14 is essential for its trafficking and function, *Nat Neurosci* 9, 824-831.
19. Linder, M. E., and Deschenes, R. J. (2007) Palmitoylation: policing protein stability and traffic, *Nat. Rev. Mol. Cell Biol.* 8, 74-84.

20. Baekkeskov, S., and Kanaani, J. (2009) Palmitoylation cycles and regulation of protein function, *Mol. Membr. Biol.* 26, 42-54.
21. Dalva, M. B. (2009) Neuronal activity moves protein palmitoylation into the synapse, *J. Cell Biol.* 186, 7-9.
22. Shipston, M. J. (2011) Ion Channel Regulation by Protein Palmitoylation, *J. Biol. Chem.* 286, 8709-8716.
23. Bartels, D. J., Mitchell, D. A., Dong, X., and Deschenes, R. J. (1999) Erf2, a Novel Gene Product That Affects the Localization and Palmitoylation of Ras2 in *Saccharomyces cerevisiae*, *Mol Cell Biol.* 19, 6775-6787.
24. Linder, M. E., and Deschenes, R. J. (2007) Palmitoylation: policing protein stability and traffic, *Nat. Rev. Mol. Cell Biol.* 8, 74-84.
25. Bartels, D. J., Mitchell, D. A., Dong, X., and Deschenes, R. J. (1999) Erf2, a novel gene product that affects the localization and palmitoylation of Ras2 in *Saccharomyces cerevisiae*, *Mol. Cell. Biol.* 19, 6775-6787.
26. Dong, X., Mitchell, D. A., Lobo, S., Zhao, L., Bartels, D. J., and Deschenes, R. J. (2003) Palmitoylation and plasma membrane localization of Ras2p by a nonclassical trafficking pathway in *Saccharomyces cerevisiae*, *Mol. Cell. Biol.* 23, 6574-6584.
27. Lobo, S., Greentree, W. K., Linder, M. E., and Deschenes, R. J. (2002) Identification of a Ras palmitoyltransferase in *Saccharomyces cerevisiae*, *J. Biol. Chem.* 277, 41268-41273.
28. Zhao, L., Lobo, S., Dong, X., Ault, A. D., and Deschenes, R. J. (2002) Erf4p and Erf2p form an endoplasmic reticulum-associated complex involved in the plasma membrane localization of yeast Ras proteins, *J. Biol. Chem.* 277, 49352-49359.
29. Linder, M. E., and Deschenes, R. J. (2004) Model organisms lead the way to protein palmitoyltransferases, in *J. Cell Sci.* 521-526.
30. Singaraja, R. R., Hadano, S., Metzler, M., Givan, S., Wellington, C. L., Warby, S., Yanai, A., Gutekunst, C.-A., Leavitt, B. R., Yi, H., Fichter, K., Gan, L., McCutcheon, K., Chopra, V., Michel, J., Hersch, S. M., Ikeda, J.-E., and Hayden, M. R. (2002) HIP14, a novel ankyrin

domain-containing protein, links huntingtin to intracellular trafficking and endocytosis, *Hum. Mol. Genet.* 11, 2815-2828.

31. Huang, K., Yanai, A., Kang, R., Arstikaitis, P., Singaraja, R. R., Metzler, M., Mullard, A., Haigh, B., Gauthier-Campbell, C., Gutekunst, C.-A., Hayden, M. R., and El-Husseini, A. (2004) Huntingtin-Interacting Protein HIP14 Is a Palmitoyl Transferase Involved in Palmitoylation and Trafficking of Multiple Neuronal Proteins, *Neuron* 44, 977-986.
32. Ohyama, T., Verstreken, P., Ly, C. V., Rosenmund, T., Rajan, A., Tien, A. C., Haueter, C., Schulze, K. L., and Bellen, H. J. (2007) Huntingtin-interacting protein 14, a palmitoyl transferase required for exocytosis and targeting of CSP to synaptic vesicles, *J. Cell. Biol.* 179, 1481-1496.
33. Givan, S. A., and Sprague, G. F., Jr. (1997) The ankyrin repeat-containing protein Akr1p is required for the endocytosis of yeast pheromone receptors, *Mol. Biol. Cell* 8, 1317-1327.
34. Feng, Y., and Davis, N. G. (2000) Akr1p and the type I casein kinases act prior to the ubiquitination step of yeast endocytosis: Akr1p is required for kinase localization to the plasma membrane, *Mol. Cell Biol.* 20, 5350-5359.
35. Roth, A. F., Feng, Y., Chen, L., and Davis, N. G. (2002) The yeast DHHC cysteine-rich domain protein Akr1p is a palmitoyl transferase, *J Cell Biol* 159, 23-28.
36. Babu, P., Deschenes, R. J., and Robinson, L. C. (2004) Akr1p-dependent Palmitoylation of Yck2p Yeast Casein Kinase 1 Is Necessary and Sufficient for Plasma Membrane Targeting, *J. Biol. Chem.* 279, 27138-27147.
37. Ungermann, L. E. P. D. C. (2004) On the mechanism of protein palmitoylation, *EMBO reports* 5.
38. Putilina, T., Wong, P., and Gentleman, S. (1999) The DHHC domain: A new highly conserved cysteine-rich motif, *Molecular and Cellular Biochemistry* 195, 219-226.
39. Mitchell, D. A., Vasudevan, A., Linder, M. E., and Deschenes, R. J. (2006) Thematic review series: Lipid Posttranslational Modifications. Protein palmitoylation by a family of DHHC protein S-acyltransferases, in *Journal of Lipid Research*, pp 1118-1127.

40. Roth, A. F., Feng, Y., Chen, L., and Davis, N. G. (2002) The yeast DHHC cysteine-rich domain protein Akr1p is a palmitoyl transferase, in *Journal of Cell Biology*, pp 23-28.
41. Politis, E. G., Roth, A. F., and Davis, N. G. (2005) Transmembrane Topology of the Protein Palmitoyl Transferase Akr1, in *Journal of Biological Chemistry*, pp 10156-10163.
42. Berggren, K., Chernokalskaya, E., Steinberg, T. H., Kemper, C., Lopez, M. F., Diwu, Z., Haugland, R. P., and Patton, W. F. (2000) Background-free, high sensitivity staining of proteins in one- and two-dimensional sodium dodecyl sulfate-polyacrylamide gels using a luminescent ruthenium complex, *ELECTROPHORESIS* 21, 2509-2521.
43. Lopez, M. F., Berggren, K., Chernokalskaya, E., Lazarev, A., Robinson, M., and Patton, W. F. (2000) A comparison of silver stain and SYPRO Ruby Protein Gel Stain with respect to protein detection in two-dimensional gels and identification by peptide mass profiling, *ELECTROPHORESIS* 21, 3673-3683.
44. Smejkal, G. B., Robinson, M. H., and Lazarev, A. (2004) Comparison of fluorescent stains: Relative photostability and differential staining of proteins in two-dimensional gels, *ELECTROPHORESIS* 25, 2511-2519.
45. Roth, A. F., Wan, J., Bailey, A. O., Sun, B., Kuchar, J. A., Green, W. N., Phinney, B. S., Yates, J. R., 3rd, and Davis, N. G. (2006) Global analysis of protein palmitoylation in yeast, *Cell* 125, 1003-1013.
46. Krishna, S. S., Majumdar, I., and Grishin, N. V. (2003) Structural classification of zinc fingers, pp 532-550.
47. Ducker, C. E., Stettler, E. M., French, K. J., Upson, J. J., and Smith, C. D. (2004) Huntingtin interacting protein 14 is an oncogenic human protein: palmitoyl acyltransferase, *Oncogene* 23, 9230-9237.
48. Cstorer, A., and Ménard, R. (1994) [33] Catalytic mechanism in papain family of cysteine peptidases, in *Methods in Enzymology* (Alan, J. B., Ed.), pp 486-500, Academic Press.
49. Zhou, X., Zhang, N., Liu, L., Walters, K. J., Hanna, P. E., and Wagner, C. R. (2009) Probing the catalytic potential of the hamster arylamine N-acetyltransferase 2 catalytic triad by site-directed mutagenesis of the proximal conserved residue, Tyr190, *FEBS J.* 276, 6928-6941.

50. Wang, H., Liu, L., Hanna, P. E., and Wagner, C. R. (2005) Catalytic Mechanism of Hamster Arylamine N-Acetyltransferase 2, *Biochemistry* 44, 11295-11306.
51. Sandy, J., Mushtaq, A., Holton, S. J., Schartau, P., Noble, M. E. M., and Sim, E. (2005) Investigation of the catalytic triad of arylamine N-acetyltransferases: essential residues required for acetyl transfer to arylamines, *Biochem. J.* 390, 115-123.

CHAPTER III

IDENTIFICATION OF PALMITOYLATION SITE(S) IN YEAST

PALMITOYLTRANSFERASE AKR1P

Introduction

DHHC protein family, a group of proteins containing a conserved DHHC (Asp-His-His-Cys) motif (1) has attracted much interest in recent years, as they have been shown to catalyze protein palmitoylation (2). In addition to catalyzing palmitoylation of substrate proteins, DHHC enzymes are also auto-palmitoylated (3-8), suggesting that a palmitoylated enzyme serves as a covalent intermediate in the reaction pathway. In the recent study of the Ras palmitoyltransferase Erf2p/Erf4p, Deschenes and colleagues developed assays to simultaneously monitor the kinetics of palmitoylation of both Erf2p and Ras2 substrate, and these data suggest that palmitoylation of Erf2p/Erf4p occurs by a two-step mechanism: the enzyme is first auto-palmitoylated to form a palmitoyl-Erf2p covalent intermediate, followed by the transfer of the palmitoyl moiety to the Ras2 substrate (9). The auto-palmitoylated intermediate is sensitive to cleavage by hydroxylamine, suggesting a labile thioester linkage (3). However, the detailed catalytic mechanism and the role of the conserved DHHC motif remain unknown. To investigate the catalytic

mechanism of palmitoylation, a critical step is characterization of the auto-palmitoylation site(s) in the enzyme to obtain more information about the potential intermediate in the palmitoylation reaction.

Akr1p, the yeast palmitoyltransferase being used in this study, is an integral membrane protein with 6 transmembrane domains (TMDs) that contains a total of 12 cysteines (4, 10-13), all of which could be potential auto-palmitoylation site(s). The DHHC motif of Akrlp (DHYC in this case) is located in the cytoplasm between the fourth and fifth TMDs (13). Previously Davis and colleagues have demonstrated that Akrlp catalyzes auto-palmitoylation, and mutations in the DHYC sequence (DH→AA and C→A) eliminate both catalytic activity and auto-palmitoylation (4). This correlation led to the proposal that the cysteine in the DHYC sequence is the site of auto-palmitoylation but there is no direct evidence for this hypothesis. Herein, we combine mutagenesis and acyl-biotinyl exchange (ABE) chemistry coupled with mass spectrometry to identify the auto-palmitoylation sites of Akrlp, demonstrating that the DHYC cysteine of Akrlp is palmitoylated.

In the past decade, mass spectrometry has become a versatile tool in protein chemistry and has been broadly used for the identification of posttranslational modifications (PTMs) (14-18). Electrospray ionization (ESI) and matrix-assisted laser desorption ionization (MALDI) sources can generate peptide ions that are detected by mass analyzers to determine the m/z value, while MS/MS analysis maps the protein sequence to identify the

corresponding PTMs (19-22). Many PTMs, including phosphorylation (23-25), glycosylation (26, 27), and acetylation (28, 29), have been successfully identified using mass spectrometry. Lipidation has gained increasing importance in biomedical research (30-37). Kast and colleagues have synthesized a variety of lipidated peptides (myristoylated, farnesylated, and palmitoylated), and analyzed them using different mass spectrometric methods such as ESI Q-TOF and MALDI-TOF-TOF (38). The results showed that for palmitoylation, MALDI generated a neutral loss of the precursor ion of $\text{CH}_3(\text{CH}_2)_{14}\text{COSH}$ (272 Da), while ESI provided a mass shift of 238 Da. These unique patterns allow identification of palmitoylation possible using mass spectrometric techniques. However, one major challenge of characterizing PTM by mass spectrometry is that the fraction of protein containing the modification is hard to estimate and may only be a small fraction of the total protein (14). This may be more problematic for palmitoylation since this modification is readily reversible (36). Therefore, successful identification of PTM by mass spectral analysis is usually achieved by including an affinity purification step to enrich the modified peptides.

To enrich palmitoylated peptides, we used the acyl-biotinyl exchange (ABE) chemistry to replace the palmitoyl group with a biotin followed by mass spectral analysis to identify the auto-palmitoylation sites of Akr1p. The ABE chemistry, first introduced by Drisdell and Green, consists of 3 steps (39, 40): 1. reduction of cysteine residues followed by reaction of all unmodified cysteines

in the protein with N-ethyl maleimide (NEM); 2. cleavage of the S-palmitoyl thioester linkage by reaction with hydroxylamine; and 3. labeling of the newly exposed cysteine with a biotinylation reagent (such as 1-biotinamido-4-[4'-(maleimidomethyl)cyclohexanecarbox-amido] butane) for enrichment using avidin affinity chromatography. The advantages of this method are that the labile thioester linkage is replaced with a more stable thioether bond to properly maintain the target modification, and biotinylation facilitates the enrichment of the target peptides, which is essential for detection by mass spectrometry. This method, coupled with a tandem-MS-based proteomic technology, was successfully used by Davis and colleagues to identify palmitoylated proteins in yeast (41), and was later modified by Freeman and colleagues (42) for both identification of palmitoylated proteins and the site of modification in lipid raft-enriched and non-raft membranes on a proteomic scale. Here, we use this method to demonstrate that the cysteine in the DHYC motif of Akr1p is the site of auto-palmitoylation *in vivo*, providing additional evidence for a covalent thioester intermediate in the catalytic mechanism of palmitoyltransferases.

Experimental Procedures

General methods

Mutagenesis of the cysteines in Akr1p, expression and purification of WT and mutant Akr1p and protein substrates, and the radioactive palmitoylation assay were carried out as described in the methods of Chapter II.

Acyl-Biotinyl Exchange (ABE) method (41, 42)

The C-terminal 3xHA/FLAG/6xHis-tagged Akr1p under the control of the *GAL1* promoter in plasmid pRS316 was transformed into *akr1Δ pep4Δ S. cerevisiae*. The yeast culture was grown in SRC-Ura medium at 30 °C until mid-log phase with an optical density (OD) of 1.0 and induced by addition of 4% galactose for 24 h. The cells were pelleted by centrifugation, and $\sim 1 \times 10^{11}$ cells were resuspended in 20 mL cold lysis buffer (50 mM Tris-HCl pH 7.4, 150 mM NaCl, 5 mM EDTA) containing 2 mM phenylmethylsulfonyl fluoride (PMSF) and 2x protease inhibitors (5 µg/mL of leupeptin, chymostatin, antipain, and pepstatin each). The cells were lysed using a bead beater at a 1:1 lysate/glass bead volume ratio with a 15 sec pulse for 10 times with a 1 min pause in between. The cell lysate were first centrifuged at low speed ($1000 \times g$) for 5 min to remove the cell debris, followed by ultracentrifugation ($100,000 \times g$) for 45 min at 4 °C to collect the total membrane fraction. Yeast membranes were solubilized by incubation with lysis buffer (50 mM Tris-HCl pH 7.4, 150 mM NaCl, 5 mM EDTA) containing 1 mM PMSF, 1x protease inhibitors and 1.7% Triton X-100 for 60 min at 4 °C. Following removal of the undissolved particulates by centrifugation, protein was precipitated by the chloroform-methanol precipitation method (43). The protein pellet was redissolved by incubation with SB (50 mM Tris-HCl, 4% SDS, 5 mM EDTA, pH 7.4) at 37 °C for 10 min, followed by dilution with 3 volumes of lysis buffer (50 mM Tris-HCl, pH 7.4, 150 mM NaCl, 5 mM EDTA) containing 0.2% Triton

X-100, 1 mM PMSF, and 1x protease inhibitors. The protein solution was incubated with end-over-end rotation for 30 min with 10 mM Tris(2-carboxyethyl) phosphine (TCEP) (Gold Biotechnology) to reduce disulfide bonds then incubated with 50 mM N-ethylmaleimide (NEM) (Sigma) for 2.5 h at room temperature (RT) to alkylate the thiol moieties. Excess NEM was removed by buffer exchange (5x) using Amicon Ultra-15 Centrifugal Filter Units (Millipore). This step is critical as the excess NEM will interfere with later steps. The protein solution is diluted with SB buffer to a final volume of 2 mL and divided into 2 equal samples. Each sample is mixed with 3 mL of freshly prepared 1.33 mM N-[6-(biotinamido)hexyl]-3'-(2'-pyridyldithio)propionamide (biotin-HPDP) (Pierce), 0.27% Triton X-100, 33.3% DMF, 1.33 mM PMSF, 1.33X protease inhibitors, pH 7.4, and either 1 M HA (experimental group; EXP) that reacts with thioesters to form free thiols or 50 mM Tris-HCl (control group; CON), followed by incubation at RT for 60 min with end-over-end rotation. Excess biotin-HPDP was removed by 3 sequential chloroform-methanol precipitations. Each protein pellet was dissolved in 0.5 mL TB (2% SDS, 50 mM Tris-Cl, 5 mM EDTA, pH 7.4), followed by a 20-fold dilution into the lysis buffer containing 0.2% Triton X-100, and 680 units of trypsin (Promega) was added to digest the protein and incubated at 58 °C for 60 min. Particulates were removed by centrifugation at 16,000 × g for 1 min, and the supernatant was incubated with 100 µL pre-equilibrated streptavidin agarose beads for 60 min at RT with end-over-end incubation. After binding, the beads were washed

5 times with 50 volumes of equilibrating buffer (50 mM Tris-HCl, 150 mM NaCl, 5 mM EDTA, 0.2% Triton X-100, 0.1% SDS, pH 7.4), and then washed 2 times with 50 volumes of 20% acetonitrile, 10 mM NH_4HCO_3 to remove the detergent. The target peptides were eluted by incubating with 5 volumes of 5 mM TCEP, 10 mM NH_4HCO_3 , 20% acetonitrile at 37 °C for 30 min to reduce the disulfide linkage with the biotin moiety. Samples were centrifuged at 2500 × *g* for 1 min to remove particulates, and the supernatant was dried using a Speed-Vac. The peptide samples were stored at -80 °C until mass spectral analysis.

Mass spectrometry

Peptide samples were reconstituted in 4:1 (v/v) H_2O :acetonitrile. Half of the solution was subjected to HPLC-ESI-MS analysis. HPLC was performed using an Agilent 1100 series system (Agilent Technologies) on a Phenomenex Synergi Hydro reverse phase C18 column (1.0 × 15 mm, Phenomenex). The gradient elution increased solvent B from 2% to 70% over 150 min. Solvent A was 0.1% formic acid in water and solvent B was acetonitrile with 0.1% formic acid. The HPLC eluent was infused online to a 7T Bruker Apex ESI-Q-FT-ICR mass spectrometer (Bruker Daltonics). LC-MS data was acquired by Hystar and ApexControl software (Bruker Daltonics). Extracted ion chromatograms (EICs) were calculated based on the accurate masses of peptides of interest and a 20 ppm error window. The elution time of peptides of interest was determined by the EICs. The remaining half of the sample was subjected to the same HPLC fractionation but the eluent was collected into fractions every 0.5

minutes. Fractions containing peptides of interest, based on the elution time, were infused into a 7T Bruker Solarix ESI-Q-FT-ICR mass spectrometer (Bruker Daltonics). Peptides of interest were fragmented in the gas phase by collisional induced dissociation (CID). Each spectrum was signal-averaged for approximately 10 minutes. Spectra were manually interpreted and peaks were assigned based on a 10 ppm mass error.

In vivo palmitoyl labeling

The C-terminal 3xHA/FLAG/6xHis-tagged WT and mutant Akr1p in plasmid pRS316 was transformed into *akr1Δ pep4Δ S. cerevisiae*. The cells were grown to an OD of 0.4 in YEP-Raffinose (2%) media. Expressions of WT and mutant Akr1p genes under the control of the *GAL1* promoter were induced by the addition of 2% galactose. After 1 h induction, Akr1p was labeled *in vivo* by addition of 25 μ M 17-octadecynoic acid (Cayman Chemicals), an analogue of palmitic acid with an alkyne group (44), to the media and incubation for 1 h at 30 °C. The cells from a 10 mL culture were harvested by centrifugation at 2500 x *g* for 5 min and resuspended in lysis buffer (50 mM Tris-HCl, 150 mM NaCl, 5 mM EDTA, pH 7.4) containing 2 mM PMSF and 2x protease inhibitors. Cells were lysed by vortexing vigorously with 100 μ L glass beads, with 5 x 45 sec blasts on the vortexer and 1 min rests on ice in between. The lysates were collected and solubilized by addition of 0.1% Triton X-100 and incubation at 4 °C for 30 min. The undissolved fraction was removed by centrifugation, and the protein in the supernatant was subjected to methanol-chloroform

precipitation. The protein pellet was then resuspended in 4 % SDS, 50 mM Tris-HCl, pH 7.4, 5 mM EDTA, and diluted with 39 volumes of lysis buffer containing 0.2 % Triton X-100, 1 mM PMSF and 1x protease inhibitors, followed by 30 min end-over-end incubation. The undissolved fraction was removed by centrifugation again. The supernatant was incubated with anti-FLAG M2 mAb-agarose for 1 h at 4°C, and washed 3 times by lysis buffer containing 0.1% SDS and 0.2% Triton. After adding 4% SDS, 50 mM triethanolamine (TEA) (Sigma), pH 7.4 to the agarose, Akr1p was eluted with incubation at 65 °C for 5 min.

Click chemistry

Click chemistry was used to react the alkyne of octadecynoic acid with an azide-labeled fluorophore to evaluate whether Akr1p was covalently labeled with the palmitate analog. Each 50 µL click chemistry reaction contains 27 µL reaction buffer (50 mM TEA, pH 7.4, 150 mM NaCl, 0.5% Triton X-100, 1mM PMSF, 1X protease inhibitors), 20 µL of the FLAG-immunoprecipitated protein extract containing Akr1p, 0.5 µL of 10 mM Alexa Fluor 647 azide (Invitrogen) in DMSO, 0.5 µl of 10 mM Tris[(1-benzyl-1*H*-1,2,3-triazol-4-yl)methyl]amine (TBTA) (Sigma) in DMSO, 1 µl of 50 mM TCEP (Gold Biotechnology), 1 µl of 50 mM CuSO₄. The reaction mixture was incubated in the dark at RT for 1 h. Then, 100 µL of 50 mM TEA, pH 7.4, 150 mM NaCl, 0.5% Triton X-100 was added and the mixture was subjected to methanol-chloroform precipitation. The protein pellet was then

redissolved in 25 μ L buffer (40 mM Tris-HCl, pH 6.8, 8 M urea, 5% SDS, 0.1 mM EDTA, 1% β -mercaptoethanol (BME)) and incubated at 65 °C for 5 min. The solution was then run on a SDS-PAGE gel and the fluorescent protein was visualized using a Typhoon-9410 phosphorimager.

Results

Mutagenesis of cysteine residues in Akr1p reveals possible auto-palmitoylation sites

Akr1p, under both *in vivo* and *in vitro* conditions, catalyzes palmitoylation of both exogenous proteins and itself (auto-palmitoylation) as previously demonstrated (4) and shown in Figure 2.4 in Chapter II. Palmitoylation of Akr1p has been proposed as either a catalytic intermediate or as a modification to alter membrane localization. To investigate the function and sites of the Akr1p auto-palmitoylation, we analyzed potential palmitoylation sites by alanine scanning mutagenesis of cysteine residues. There are 12 cysteine residues in Akr1p: C81, C209, C283, C443, C472, C500, C533, C554, C563, C598, C663, and C667. Based on the transmembrane topology data of Akr1p (Figure 3.1) (13), we ruled out cysteine side chains with a proposed location of buried in the membrane or positioned on the lumen side of Golgi, reasoning that only the cysteines with a cytoplasmic orientation would be modified with a palmitoyl group *in vivo*. Thus, eight single mutations (C81A, C209A, C283A, C443A, C472A, C500A, C598A, and C663A/C667A) in the

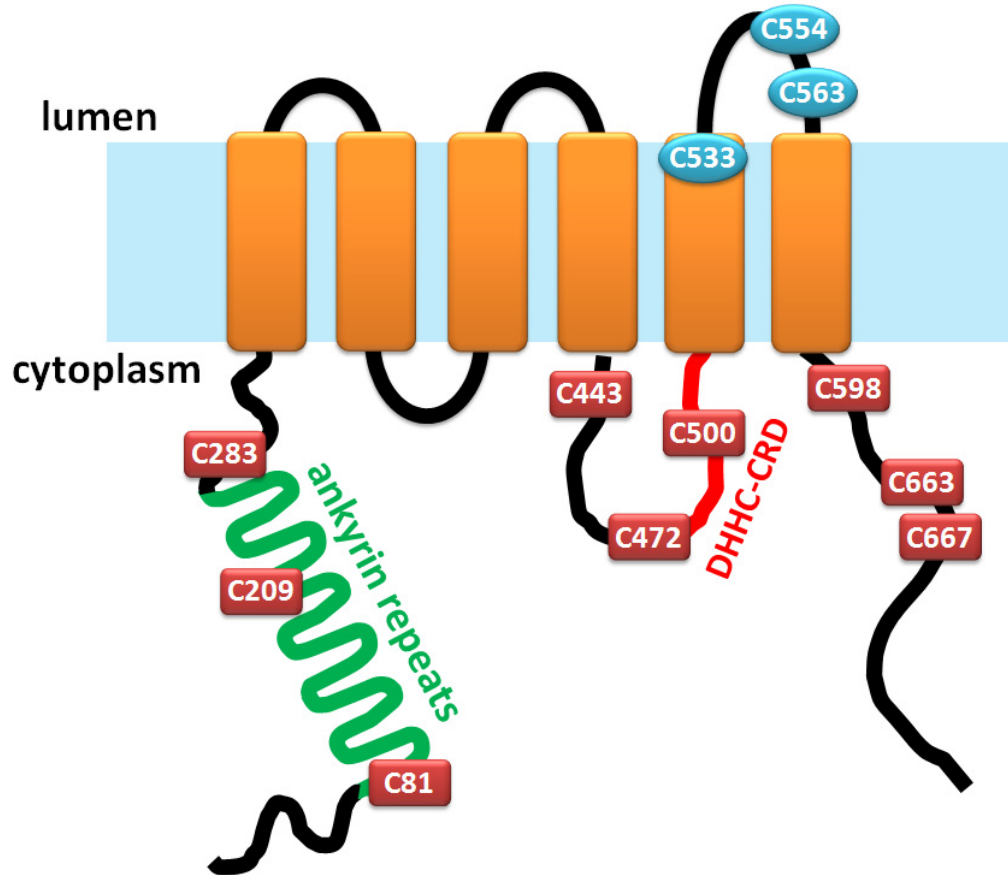


Figure 3.1: Schematic representation of Akrlp membrane topology showing the position of all its 12 cysteines. The 6 transmembrane domains are indicated in orange, and the DHHC-CRD sequence is labeled in red. 9 of the 12 cysteines are located in the cytoplasmic side (labeled in red square) and the other 3 cysteines are located either in the transmembrane domain or the lumen side (labeled in blue oval) (13).

Akrlp gene were prepared using site-directed mutagenesis. These mutant proteins were expressed in *S. cerevisiae* and purified as described for WT Akrlp (see Chapter II). Similar amounts of protein were obtained for the majority of proteins, with the exception of C598A and C663A/C667A double mutant where the yield was lower (see western blots shown in Figure 2.9, 3.2, and 3.3). The catalytic activity for both auto-palmitoylation and palmitoylation of Ypl199c was assayed with [³H]palmitoyl-CoA, using the method described in

Chapter II. The C500A mutation in the DHYC motif abolished catalysis of palmitoylation of Ypl199c as shown in Figure 2.9 in Chapter II. Alanine substitutions for C81, C209, C283, C443, C472, and C598 have no observable effect on either catalysis of auto-palmitoylation or palmitoylation of Ypl199c by Akr1p under these assay conditions (Figure 3.2). In contrast, the C500A mutation and the C663/667A double mutation greatly diminish the auto-palmitoylation of the enzyme (Figure 2.9 and 3.2). To further explore which cysteine in the C663/C667 double mutation causes this effect, we prepared the C663A and C667A single mutations in Akr1p and measured the palmitoylation activity. These data clearly shows that C663A has no observable effect on palmitoylation but C667A abolishes the auto-palmitoylation of Akr1p, indicating that C667 is likely palmitoylated in Akr1p (Figure 3.3). These results clearly indicate that both C500 and C667 affect auto-palmitoylation of Akr1p, and one or both could possibly be the site(s) where the palmitoyl thioester forms.

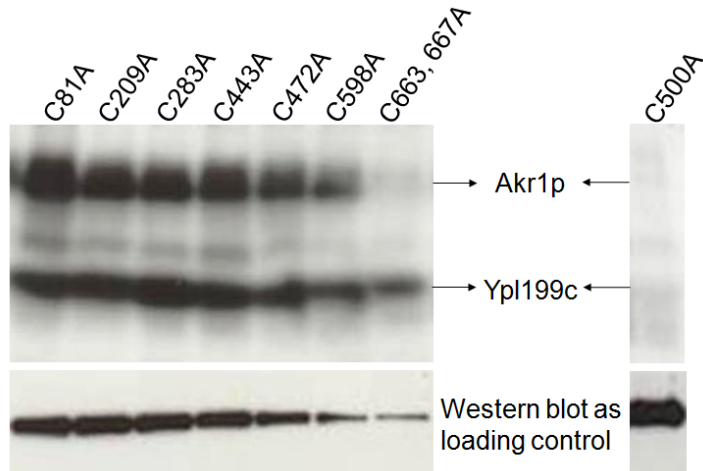


Figure 3.2: C663/667A double mutant abolishes the Akrlp auto-palmitoylation activity. Reactions are done *in vitro* using the radioactive palmitoylation assay. Each reaction contains 2.5 μM [^3H]palmitoyl-CoA, 10 μM Ypl199c, and ~ 60 nM cysteine mutant Akrlp expressed and purified from yeast. After a 1 h incubation at 30 $^\circ\text{C}$, reactions were methanol-chloroform precipitated, run on a SDS-PAGE gel, and then subjected to autoradiography to detect the level of protein labeling. Anti-HA western blotting is also shown to indicate that comparable level of HA-tagged Akrlp are obtained for the majority of mutants, except for C598A and C663A/C667A where the protein level is reduced for this purification. C500A data is cut from the gel in Figure 2.9 and shown on the right for easy comparison.

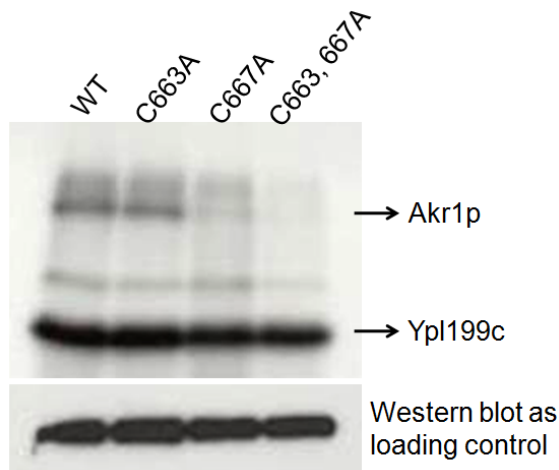


Figure 3.3: C667A mutant abolishes the Akrlp auto-palmitoylation activity but maintains the trans-palmitoylation activity, while C663A has no observable effect on catalysis. Palmitoylation assays were carried out as described in the legend of Figure 3.2.

The palmitoylation assays demonstrate that the C667A mutation, in contrast to the C500A mutation, has little effect on catalysis of palmitoylation of Ypl199c, as shown in Figure 3.3. These mutagenesis results indicate that the side chain of C500 plays a critical role for catalysis of both palmitoylation of substrate proteins and Akr1p, and could potentially be the auto-palmitoylation site in Akr1p. On the other hand, the role of C667 is more complicated. Although the C667A mutation decreases the level of palmitoylation, as indicated in Figure 3.3, this mutation does not significantly alter catalysis of palmitoylation of Ypl199c, suggesting that it is not essential for catalytic turnover at saturating palmitoyl-CoA. Hence, palmitoylation at this position has an alternative function such as acting as a storage site for palmitoyl group or an allosteric effector, or regulating the localization of Akr1p.

Mass spectral analysis demonstrates that the Cys500 in the DHYC motif of Akr1p is palmitoylated

To further examine the roles of C500 and C667 in the catalytic mechanism, we carried out the acyl-biotinyl exchange (ABE) chemistry to both replace the labile palmitoyl thioester with a more stable disulfide linkage with biotin and to enrich the modified peptide followed by mass spectral analysis to identify the site of modification. Akr1p has been shown to be auto-palmitoylated both *in vivo* and *in vitro*. Therefore, we first labeled Akr1p *in vitro*. FLAG-tagged Akr1p was expressed in yeast and purified using anti-FLAG agarose, followed by incubation with palmitoyl-CoA using the assay conditions as described

earlier. After the ABE chemistry and proteolysis no peptides were detected by mass spectral analysis, possibly due to a low fraction of the Akr1p labeled with a palmitoyl group which potentially could reflect a low level of active Akr1p reconstituted in the bovine lipids. Therefore, we examined the modification site using Akr1p labeled *in vivo*. Akr1p was expressed in yeast, cells were harvested and lysed using a bead beater, and the cell membrane fraction was collected by ultracentrifugation and subjected to ABE chemistry. The mixture, which contained total yeast membrane proteins, was digested by addition of trypsin in the presence of detergent followed by the enrichment of the target peptide using streptavidin agarose. The detailed procedure for MS sample preparation is shown in Figure 3.4. The key steps in the ABE chemistry are labeling all of the unmodified cysteines with NEM, reaction of labile thioester bond with hydroxylamine to form a free thiol followed by reaction of this thiol with a biotinylation reagent to form a disulfide bond. The biotinylated peptides are enriched by binding to streptavidin agarose and eluted from the column upon reduction of the disulfide bond.

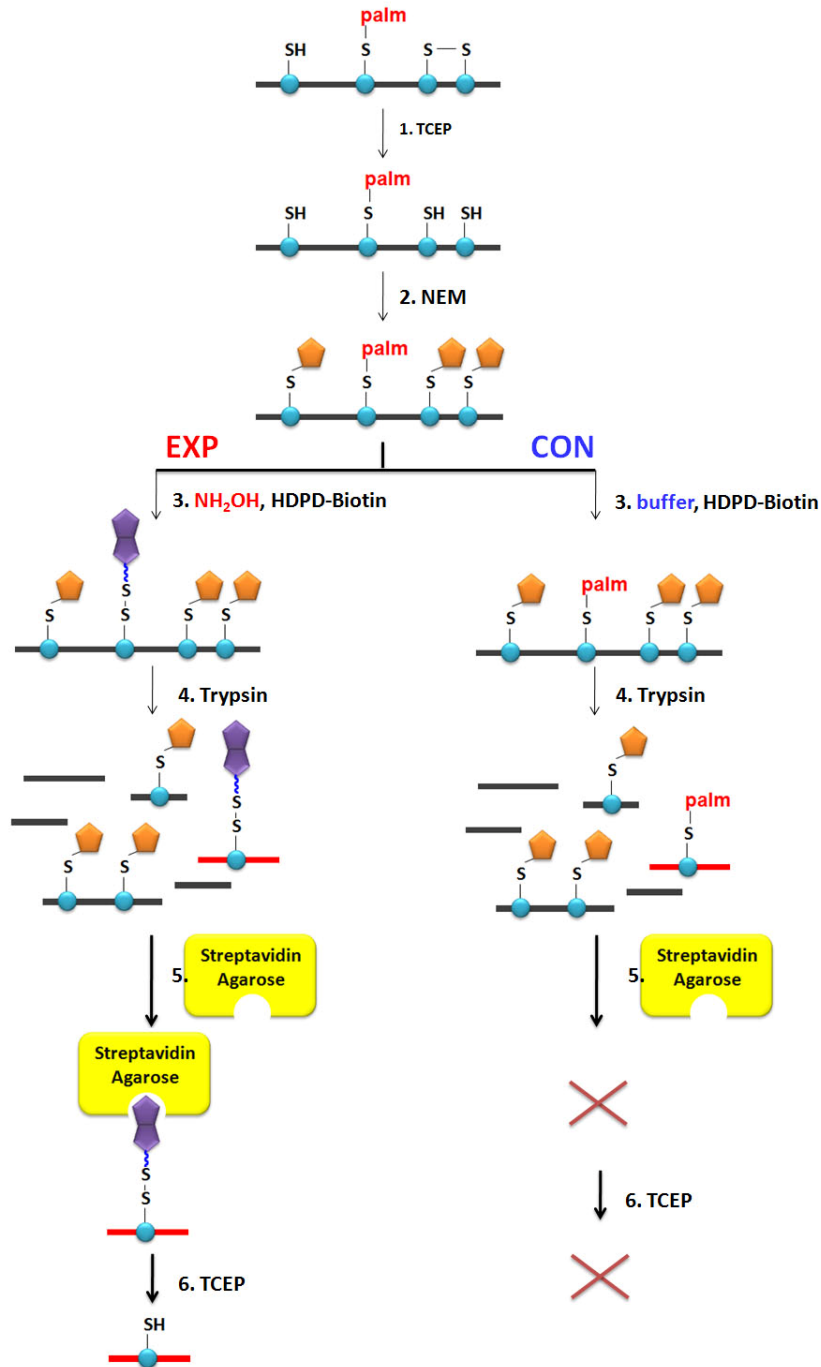


Figure 3.4: Schematic procedure of the acyl-biotinyl exchange (ABE) chemistry for the characterization of the Akrlp auto-palmitoylation site(s). *Top:* protection of the thiol groups by reduction with TCEP and alkylation with NEM; *Bottom left (EXP):* replacement of the S-palmitoyl group with the biotinyl moiety and enrichment of the S-palmitoylated peptides to localize the palmitoylation site(s); *Bottom right (CON):* control experiment where the sample is not treated with hydroxylamine to form cysteine from the thioester so the S-palmitoyl group is not replaced by a biotin.

To identify the modification site(s), the enriched peptide mixture was subjected to LC/ESI-FTICR-MS, and the peptide containing C500 (FDHYCPWIFNDVGLK, $m/z = 927$ at charge state of two) was detected in the sample treated with hydroxylamine (EXP) but not in the control sample (CON) (Figure 3.5(a)). In addition, MS/MS analysis of the 927 m/z peak was also performed, and the fragmentation pattern of the peptide completely matches with the target peptide. As shown in Figure 3.5(b), eleven fragments (y_4^+ , b_4^+ , b_5^+ , y_7^+ , y_{13}^{2+} , y_8^+ , b_8^+ , y_{10}^+ , y_{11}^+ , b_{11}^+ , and y_{12}^+) of the peptide confirm its sequence as FDHYCPWIFNDVGLK. These experiments were repeated and the C500 peptide was detected with comparable mass spectra. This evidence indicates that Akr1p is auto-palmitoylated on C500 in the DHYC motif. Additionally, we also looked for the other 10 peptides containing the rest of the 11 cysteines of Akr1p in the mass spectra (C663 and C667 end up in one peptide after the trypsin digestion). None of the m/z values of those peptides were detected by mass spectrometry except for the C663/C667 peptide, which indicates that those 9 cysteines are not palmitoylated *in vivo*. For the C663/667 peptide, we detected an 1165 m/z peak (corresponding to the doubly charged peptide with one free cysteine labeled by NEM) in the chromatograms of both the EXP sample and the CON sample (Figure 3.6 (a)); however, the MS/MS fragmentation did not match the peptide sequence TCFGVCYAVTGMDQWLAVIK (Figure 3.6 (b)). As peptides from many proteins are enriched by the ABE method when the starting sample is the

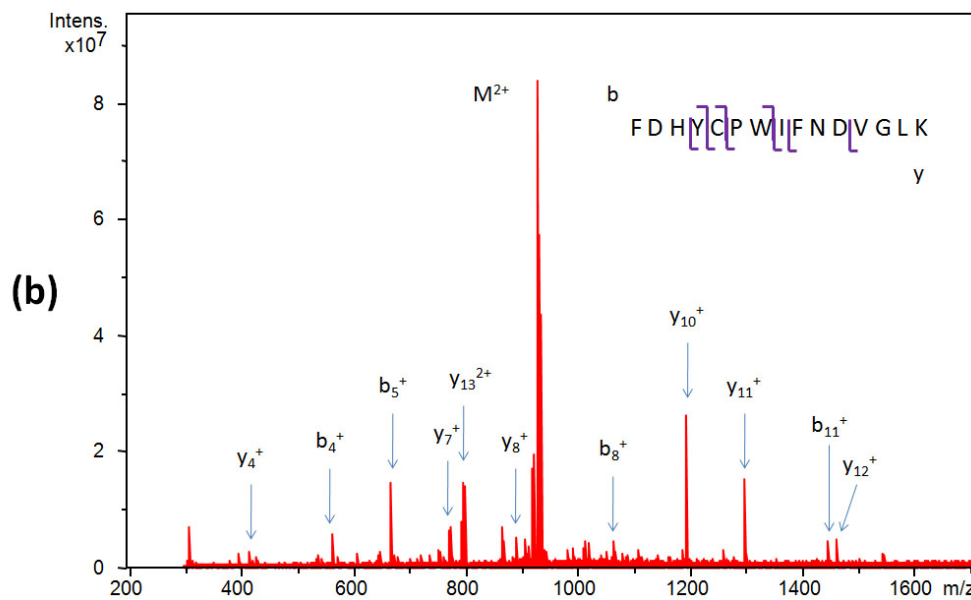
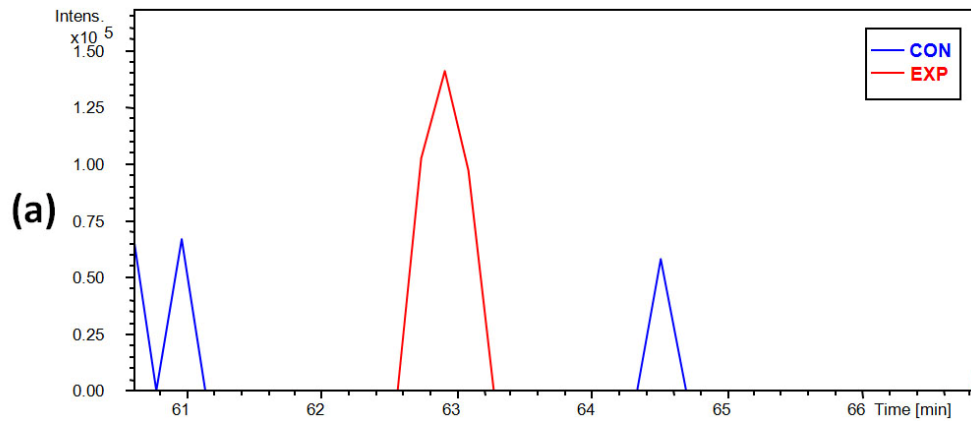


Figure 3.5: Extracted ion chromatograms of the doubly positively charged peptide FDHYCPWIFNDVGLK from HPLC-ESI-FTICR-MS of the EXP (red) and CON (blue) samples (a). A signal corresponding to the peptide containing the DHYC motif, FDHYCPWIFNDVGLK at $m/z=927.4376$, is detected at 62.9 min of elution for the EXP sample (red), but is not observed at the same elution time in the CON sample (blue). The observed signals in the CON samples at different elution times are verified as the second or third isotopes from other peptides with a similar m/z . MS/MS spectrum of the peptide with m/z of 927 collected from the HPLC fractions eluting between 62.5 - 63.0 min (b). Eleven fragments (y_4^+ , b_4^+ , b_5^+ , y_7^+ , y_{13}^{2+} , y_8^+ , b_8^+ , y_{10}^+ , y_{11}^+ , b_{11}^+ , and y_{12}^+) of the peptide confirm its sequence as FDHYCPWIFNDVGLK.

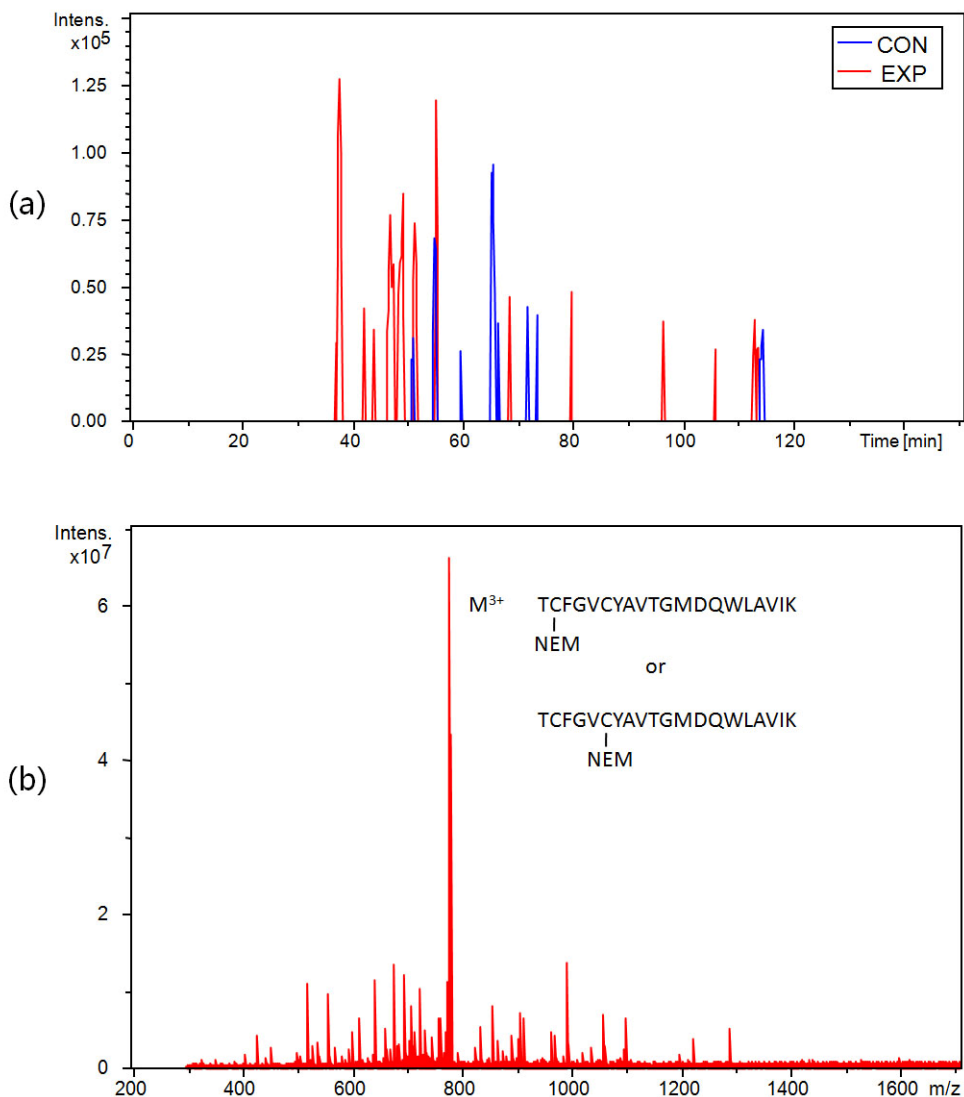


Figure 3.6: Extracted ion chromatograms of the doubly positively charged peptide TC(NEM)FGVCYAVTGMDQWLAVIK from the HPLC-ESI-FTICR-MS spectra of the EXP (red) and CON (blue) samples (a). A signal at 1165.5545 m/z was detected in multiple mass spectra across the entire chromatograms of both EXP (red) and CON (blue), as indicated by the multiple peaks in (a). However, the isotopic distribution and charge state of the peptide of interest were only found in the mass spectrum at 51.3 min. **MS/MS spectrum of 777 m/z collected by HPLC in fractions between 51.0 and 51.5 min (b).** In this HPLC fraction the doubly-charged form of the peptide of interest (1165 m/z) was not detected but 777 m/z, the triply-charged form was detected, possibly due to the difference between the two ESI sources used by LC-MS and MS/MS. However, none of the expected MS/MS fragments for the peptide sequence TC(NEM)FGVCYAVTGMDQWLAVIK were detected, suggesting that the signal is from another peptide with the same m/z value.

membrane fraction, what we were seeing in the LC-MS spectra is likely another peptide which has the same m/z value as our peptide of interest. We therefore concluded that although C667 plays an important role in our *in vitro* palmitoylation assay, it does not serve as an auto-palmitoylation site *in vivo*.

In summary, these data indicate that C500, not C667, is palmitoylated *in vivo*. This result confirms the catalytic importance of the DHYC motif and suggests that auto-palmitoylation could be an intermediate in the catalytic cycle.

To further examine the site of Akr1p auto-palmitoylation, we evaluated *in vivo* palmitoylation of Akr1p using the palmitic acid analog 17-octadecynoic acid (17-ODYA). Cultures of yeast transformed with plasmids encoding WT, C500A, and C667A Akr1p were induced by addition of 2% galactose and then incubated with 17-ODYA which replaces the palmitate modification *in vivo* (44). Click chemistry was then performed on each of the protein extracts to react the alkyne of 17-ODYA with Alexa Fluor 647 azide. The reaction mixtures were run on a protein gel and scanned for fluorescence using a phosphorimager. As shown in the SDS-PAGE gel (Figure 3.7), the *in vivo* auto-palmitoylation level of C500A mutant was greatly decreased compared to that of the WT, indicating that C500 is the site of auto-palmitoylation *in vivo* as well as *in vitro*. On the other hand, the C667A Akr1p mutant showed the same palmitoylation level as the WT protein, which suggests that this cysteine does not contribute to the auto-palmitoylation of Akr1p *in vivo*. This result is consistent with our findings

from the mass spectral experiment.

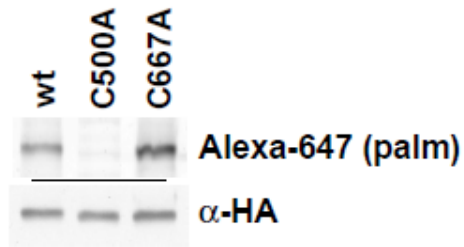


Figure 3.7: In vivo labeling of WT and mutant Akr1p with 17-ODYA to analyze auto-palmitoylation.³ Yeast cells were incubated with 17-ODYA to replace palmitoyl groups with this reagent *in vivo*. After lysis, the cell lysate was subjected to click chemistry to react 17-ODYA with Alexa Fluor 674 azide. Each reaction was then run on a SDS-PAGE gel and the fluorescence from Alexa Fluor 674 covalently attached to the protein was detected by scanning the gel using a phosphorimager. Anti-HA western blotting was also conducted to show that WT and mutant Akr1p were expressed at the same level. The C500A mutant, but not the C667A mutant, decreases labeling with 17-ODYA, indicative of decreased auto-palmitoylation.

Formation of the intermediate with C667A Akr1p in the presence and absence of Ypl199c substrate

To further examine the role of palmitoylation at C667 of Akr1p, we measured auto-palmitoylation of the C667A mutant of Akr1p in the presence and absence of the Ypl199c substrate. As previously noted, in the presence of Ypl199c, little auto-palmitoylation is observed in this mutant. However, upon the addition of substrate Ypl199c, the auto-palmitoylated intermediate of the C667A mutant is observed (Figure 3.8). In contrast, for WT Akr1p, the intermediate can be observed both in the presence and absence of Ypl199c (see Figure 2.4(a) in Chapter II). These results suggest that C667 enhances accumulation of the intermediate. When the C667 residue is mutated to alanine, the stabilization

³ Experiment carried out by Roth A. F.

effect from C667 no longer exists. When the substrate is absent, the palmitoyl moiety has nowhere to be transferred, so the intermediate can still be observed. However, when Ypl199c is added to the reaction, without the stabilizing effect from C667, the palmitoyl group is transferred from the intermediate to the substrate protein, and the intermediate is not sufficiently stable to accumulate in the reaction, and therefore the auto-palmitoylation species is not observed on our radioactive SDS-PAGE gel. On the other hand, the palmitoyl group stays on WT Akrlp due to the stabilizing effect from the C667 residue, so the intermediate can be sufficiently accumulated and therefore observed. In the *in vivo* 17-ODYA labeling experiment, the reason that we still see the auto-palmitoylation band for C667A is probably because the substrate level in the cell is relatively low, so the palmitoyl group stays on the enzyme without being transferred to the substrate.

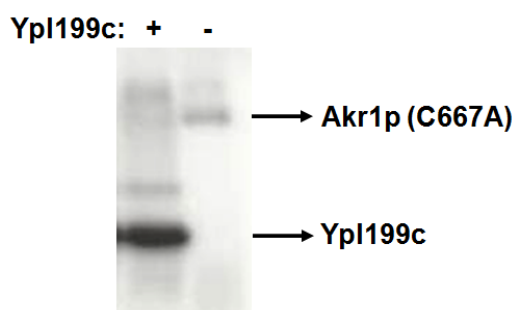


Figure 3.8: Palmitoylation assay of C667A Akrlp with and without substrate Ypl199c. Reactions are done *in vitro* using the radioactive assay. Each reaction contains [³H]palmitoyl-CoA, with or without the presence of Ypl199c, and C667A Akrlp purified from yeast. After 1h incubation at 30 °C, reactions were methanol-chloroform precipitated, run on a SDS-PAGE gel, and then subjected to autoradiography to detect the protein labeling level.

Discussion

C500 of the DHYC motif is palmitoylated

Previous studies have shown that mutation of the DHHC cysteine abolishes the palmitoylation activity of PATs (3, 4, 45, 46), leading to the hypothesis that this motif is the active site of these enzymes. However, up till now there was no clear indication of the role of C500 in catalysis and no direct evidence that this cysteine was palmitoylated. The combined mutagenesis and mass spectrometry data clearly demonstrate that C500 is covalently modified with a palmitoyl group upon auto-palmitoylation of Akr1p. Furthermore, mutations that decrease catalytic activity (D, H, C) also eliminate auto-palmitoylation, demonstrating that the formation of the intermediate is important for catalytic activity. In a recently published paper on the mechanism of the Ras palmitoyltransferase Erf2p/Erf4p (9), Deschenes and colleagues proposed a two-step catalytic mechanism, where the enzyme is auto-palmitoylated in the first step, followed by the transfer of the palmitoyl group from the enzyme to the substrate protein. Here we demonstrate that the auto-palmitoylated species is a covalent thioester linkage of a palmitoyl group with C500 of the DHYC cysteine. These data further validate the catalytic importance of a covalent thioester intermediate in the catalytic mechanism of Akr1p, and likely all PATs, since the DHH/YC motif is highly conserved.

To summarize our findings of the role of the DHYC motif using mutagenesis and mass spectrometry, we propose a detailed two-step

mechanism for Akr1p catalysis (Figure 3.9). In this model, the DHYC cysteine thiol is stabilized by the Asp and His residues to lower the pKa of the thiol group to form a thiolate at neutral pH, as shown in the catalytic triad model in Chapter II. The thiolate functions as a nucleophile to attack the palmitoyl-CoA thioester to form a tetrahedral intermediate followed by elimination of $-SCoA$ to form a covalent palmitoyl thioester intermediate at C500 of Akr1p. This is proposed to be the auto-palmitoylated Akr1p that we have observed both *in vivo* and *in vitro*. In the second step, the thiolate of the protein substrate attacks the carbonyl carbon of the palmitoyl-Akr1p intermediate, and reacts

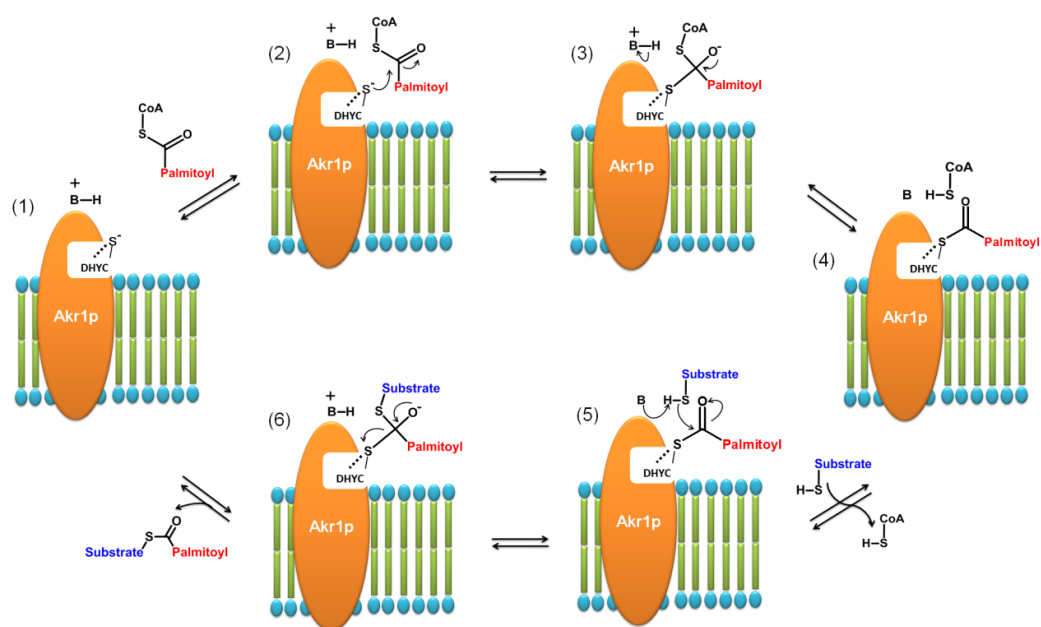


Figure 3.9: Scheme of the proposed Akr1p palmitoylation mechanism. (1): Akr1p with an activated thiol group; (2)-(4): formation of the auto-palmitoylated intermediate through attack of the reactive thiolate on the palmitoyl-CoA thioester to form a tetrahedral intermediate followed by elimination of CoA to form palmitoylated Akr1p intermediate; (4)-(6): the trans-palmitoylation step where the thioester of a substrate protein reacts with the palmitoylated Akr1p thioester to transfer the palmitoyl moiety to the substrate protein through an addition-elimination reaction followed by dissociation of the palmitoylated product.

with the palmitoyl moiety attached to Akr1p to finally form the product, a palmitoyl thioester on the substrate. Many of the details of the proposed mechanism still need to be tested.

The role of C667

In addition to the examination of the function of the DHYC motif, the functional role of C667 is also interesting and valuable. Mutagenesis data demonstrate that alanine substitution of C500 and C667 both impaired the level of auto-palmitoylation of Akr1p *in vitro*; however, the C667A mutation had no noticeable effect on the trans-palmitoylation activity with the Ypl199c substrate. Based on this result, two possible catalytic roles for C667 can be proposed: 1. C667 may act as a potential palmitoylation site, same as C500; 2. C667 is responsible for stabilizing the auto-palmitoylated intermediate. However, since the mass spectral results showed clear identification of auto-palmitoylation on C500 while there is no confirmed evidence for the formation of a palmitoyl linkage on C667, and *in vivo* labeling with 17-ODYA suggested little labeling of C667, the possibility that C667 is an auto-palmitoylation site is unlikely. The disparity between the *in vitro* and *in vivo* labeling of C667 could also suggest that palmitoylation of C667 is due to nonspecific reaction with palmitoyl-CoA. However, the observation of auto-palmitoylation in the absence of the protein substrate (Figure 3.8) suggests C667 functions to stabilize thioester intermediate at C500 of Akr1p.

The effect of C667 on the accumulation of C500 is also supported by the

spatial orientation of C500 and C667 on the membrane. Although the crystal structure of Akr1p is not available, Davis and colleagues have determined its membrane topology (Figure 3.1) (13), showing that C500 sits between TM 4 and 5 in the cytoplasm side, while C667 sits in the same side after TM 6 toward the C-terminus. Thus the effect of C667 on C500 could be an indirect effect, possibly by altering the relative ratio of formation and breakdown of the intermediate, or a direct effect of stabilizing the intermediate by forming a stabilizing hydrogen bond between the palmitoyl-Akr1p intermediate and C667, for example a hydrogen bond with the carbonyl of the thioester.

In summary, by using mutagenesis and mass spectrometry, we have identified the importance of the DHYC motif for the palmitoyltransferase activity of Akr1p, and directly showed that the DHYC cysteine is the site for formation of the palmitoylation intermediate. Although it has been agreed that the conserved DHHC motif of PATs is important for the palmitoylation mechanism, no direct evidence has yet been obtained to show the function of the DHHC motif. Here, for the first time, we demonstrated that the DHYC motif is the reaction site for auto-palmitoylation of Akr1p. As a step further, our results allow us to propose a detailed model of the Akr1p catalytic mechanism, leading to a better understanding towards the mechanism of all PATs. Taking the advantage of the methods described here, the auto-palmitoylation sites of other DHHC PATs could also be identified, and therefore the role of this protein family in palmitoylation reactions will be disclosed.

References

1. Putilina, T., Wong, P., and Gentleman, S. (1999) The DHHC domain: A new highly conserved cysteine-rich motif, *Molecular and Cellular Biochemistry* 195, 219-226.
2. Mitchell, D. A., Vasudevan, A., Linder, M. E., and Deschenes, R. J. (2006) Protein palmitoylation by a family of DHHC protein S-acyltransferases, *J. Lipid Res.* 47, 1118-1127.
3. Lobo, S., Greentree, W. K., Linder, M. E., and Deschenes, R. J. (2002) Identification of a Ras palmitoyltransferase in *Saccharomyces cerevisiae*, *J. Biol. Chem.* 277, 41268-41273.
4. Roth, A. F., Feng, Y., Chen, L., and Davis, N. G. (2002) The yeast DHHC cysteine-rich domain protein Akr1p is a palmitoyl transferase, *J. Cell. Biol.* 159, 23-28.
5. Swarthout, J. T., Lobo, S., Farh, L., Croke, M. R., Greentree, W. K., Deschenes, R. J., and Linder, M. E. (2005) DHHC9 and GCP16 Constitute a Human Protein Fatty Acyltransferase with Specificity for H- and N-Ras, *J. Biol. Chem.* 280, 31141-31148.
6. Smotrys, J. E., Schoenfish, M. J., Stutz, M. A., and Linder, M. E. (2005) The vacuolar DHHC-CRD protein Pfa3p is a protein acyltransferase for Vac8p, *J. Cell. Biol.* 170, 1091-1099.
7. Huang, K., Yanai, A., Kang, R., Arstikaitis, P., Singaraja, R. R., Metzler, M., Mullard, A., Haigh, B., Gauthier-Campbell, C., Gutekunst, C.-A., Hayden, M. R., and El-Husseini, A. (2004) Huntingtin-Interacting Protein HIP14 Is a Palmitoyl Transferase Involved in Palmitoylation and Trafficking of Multiple Neuronal Proteins, *Neuron* 44, 977-986.
8. Fukata, M., Fukata, Y., Adesnik, H., Nicoll, R. A., and Brecht, D. S. (2004) Identification of PSD-95 Palmitoylating Enzymes, *Neuron* 44, 987-996.
9. Mitchell, D. A., Mitchell, G., Ling, Y., Budde, C., and Deschenes, R. J. (2010) Mutational analysis of *Saccharomyces cerevisiae* Erf2 reveals a two-step reaction mechanism for protein palmitoylation by DHHC enzymes, *J. Biol. Chem.* 285, 38104-38114.
10. Givan, S. A., and Sprague, G. F., Jr. (1997) The ankyrin repeat-containing protein Akr1p is required for the endocytosis of yeast pheromone receptors, *Mol. Biol. Cell* 8, 1317-1327.

11. Feng, Y., and Davis, N. G. (2000) Akr1p and the type I casein kinases act prior to the ubiquitination step of yeast endocytosis: Akr1p is required for kinase localization to the plasma membrane, *Mol. Cell Biol.* **20**, 5350-5359.
12. Babu, P., Deschenes, R. J., and Robinson, L. C. (2004) Akr1p-dependent Palmitoylation of Yck2p Yeast Casein Kinase 1 Is Necessary and Sufficient for Plasma Membrane Targeting, *J. Biol. Chem.* **279**, 27138-27147.
13. Politis, E. G., Roth, A. F., and Davis, N. G. (2005) Transmembrane Topology of the Protein Palmitoyl Transferase Akr1, *J. Biol. Chem.* **280**, 10156-10163.
14. Jensen, O. N. (2006) Interpreting the protein language using proteomics, *Nat Rev Mol. Cell. Biol.* **7**, 391-403.
15. Mann, M., and Jensen, O. N. (2003) Proteomic analysis of post-translational modifications, *Nat. Biotechnol.* **21**, 255-261.
16. Schweppe, R. E., Haydon, C. E., Lewis, T. S., Resing, K. A., and Ahn, N. G. (2003) The characterization of protein post-translational modifications by mass spectrometry, *Acc. Chem. Res.* **36**, 453-461.
17. Witze, E. S., Old, W. M., Resing, K. A., and Ahn, N. G. (2007) Mapping protein post-translational modifications with mass spectrometry, *Nat. Methods* **4**, 798-806.
18. Farley, A. R., and Link, A. J. (2009) Identification and quantification of protein posttranslational modifications, *Methods Enzymol.* **463**, 725-763.
19. Andersen, J. S., Svensson, B., and Roepstorff, P. (1996) Electrospray ionization and matrix assisted laser desorption/ionization mass spectrometry: powerful analytical tools in recombinant protein chemistry, *Nat. Biotechnol.* **14**, 449-457.
20. Aebersold, R., and Goodlett, D. R. (2001) Mass spectrometry in proteomics, *Chem. Rev. (Washington, D. C.)* **101**, 269-295.
21. Wu, C. C., and Yates, J. R. (2003) The application of mass spectrometry to membrane proteomics, *Nat. Biotechnol.* **21**, 262-267.

22. Meng, F., Forbes, A. J., Miller, L. M., and Kelleher, N. L. (2005) Detection and localization of protein modifications by high resolution tandem mass spectrometry, *Mass Spectrom. Rev.* **24**, 126-134.
23. Mann, M., Ong, S.-E., Gronborg, M., Steen, H., Jensen, O. N., and Pandey, A. (2002) Analysis of protein phosphorylation using mass spectrometry: deciphering the phosphoproteome, *Trends Biotechnol.* **20**, 261-268.
24. McLachlin, D. T., and Chait, B. T. (2001) Analysis of phosphorylated proteins and peptides by mass spectrometry, *Curr. Opin. Chem. Biol.* **5**, 591-602.
25. Salih, E. (2005) Phosphoproteomics by mass spectrometry and classical protein chemistry approaches, *Mass Spectrom. Rev.* **24**, 828-846.
26. Burlingame, A. L. (1996) Characterization of protein glycosylation by mass spectrometry, *Curr. Opin. Biotechnol.* **7**, 4-10.
27. Marino, K., Bones, J., Kattla, J. J., and Rudd, P. M. (2010) A systematic approach to protein glycosylation analysis: a path through the maze, *Nat. Chem. Biol.* **6**, 713-723.
28. Mischerikow, N., and Heck, A. J. R. (2011) Targeted large-scale analysis of protein acetylation, *Proteomics* **11**, 571-589.
29. Zhang, K., Tang, J., and Jones, P. R. (2005) Qualitative and quantitative analysis of histone acetylation by mass spectrometry, *Curr. Pharm. Anal.* **1**, 319-328.
30. Sebti, S. M., and Hamilton, A. D. (2000) Farnesyltransferase and geranylgeranyltransferase I inhibitors and cancer therapy: lessons from mechanism and bench-to-bedside translational studies, *Oncogene* **19**, 6584-6593.
31. Winter-Vann, A. M., and Casey, P. J. (2005) Opinion: Post-prenylation-processing enzymes as new targets in oncogenesis, *Nat. Rev. Cancer* **5**, 405-412.
32. Selvakumar, P., Lakshmikuttyamma, A., Shrivastav, A., Das, S. B., Dimmock, J. R., and Sharma, R. K. (2006) Potential role of N-myristoyltransferase in cancer, *Prog. Lipid Res.* **46**, 1-36.

33. Bijlmakers, M.-J. (2009) Protein acylation and localization in T cell signaling (Review), *Mol. Membr. Biol.* 26, 93-103.
34. Sorek, N., Bloch, D., and Yalovsky, S. (2009) Protein lipid modifications in signaling and subcellular targeting, *Curr. Opin. Plant Biol.* 12, 714-720.
35. Linder, M. E., and Deschenes, R. J. (2007) Palmitoylation: policing protein stability and traffic, *Nat. Rev. Mol. Cell Biol.* 8, 74-84.
36. Fukata, Y., and Fukata, M. (2010) Protein palmitoylation in neuronal development and synaptic plasticity, *Nat. Rev. Neurosci.* 11, 161-175.
37. Nadolski, M. J., and Linder, M. E. (2007) Protein lipidation, *FEBS J.* 274, 5202-5210.
38. Hoffman, M. D., and Kast, J. (2006) Mass spectrometric characterization of lipid-modified peptides for the analysis of acylated proteins, *Journal of Mass Spectrometry* 41, 229-241.
39. Drisdell, R. C., and Green, W. N. (2004) Labeling and quantifying sites of protein palmitoylation, *Biotechniques* 36, 276-285.
40. Drisdell, R. C., Alexander, J. K., Sayeed, A., and Green, W. N. (2006) Assays of protein palmitoylation, *Methods* 40, 127-134.
41. Roth, A. F., Wan, J., Bailey, A. O., Sun, B., Kuchar, J. A., Green, W. N., Phinney, B. S., Yates, J. R., 3rd, and Davis, N. G. (2006) Global analysis of protein palmitoylation in yeast, *Cell* 125, 1003-1013.
42. Yang, W., Di Vizio, D., Kirchner, M., Steen, H., and Freeman, M. R. (2010) Proteome scale characterization of human S-acylated proteins in lipid raft-enriched and non-raft membranes, *Mol. Cell. Proteomics* 9, 54-70.
43. Wessel, D., and Flugge, U. I. (1984) A method for the quantitative recovery of protein in dilute solution in the presence of detergents and lipids, *Anal. Biochem.* 138, 141-143.
44. Martin, B. R., and Cravatt, B. F. (2009) Large-scale profiling of protein palmitoylation in mammalian cells, *Nat. Methods* 6, 135-138.
45. Raymond, F. L., Tarpey, P. S., Edkins, S., Tofts, C., O'Meara, S., Teague, J., Butler, A., Stevens, C., Barthorpe, S., Buck, G., Cole, J., Dicks, E.,

Gray, K., Halliday, K., Hills, K., Hinton, J., Jones, D., Menzies, A., Perry, J., Raine, K., Shepherd, R., Small, A., Varian, J., Widaa, S., Mallya, U., Moon, J., Luo, Y., Shaw, M., Boyle, J., Kerr, B., Turner, G., Quarrell, O., Cole, T., Easton, D. F., Wooster, R., Bobrow, M., Schwartz, C. E., Gecz, J., Stratton, M. R., and Futreal, P. A. (2007) Mutations in ZDHHC9, Which Encodes a Palmitoyltransferase of NRAS and HRAS, Cause X-Linked Mental Retardation Associated with a Marfanoid Habitus, *Am. J. Human Genet.* 80, 982-987.

46. Dighe, S. A., and Kozminski, K. G. (2008) Swf1p, a Member of the DHHC-CRD Family of Palmitoyltransferases, Regulates the Actin Cytoskeleton and Polarized Secretion Independently of Its DHHC Motif, *Mol. Biol. Cell.* 19, 4454-4468.

CHAPTER IV

CONSERVED AMINO ACIDS IN PROTEIN FARNESYLTRANSFERASE MODULATE PEPTIDE SUBSTRATE SELECTIVITY

Introduction

Protein prenylation, including both farnesylation and geranylgeranylation, is an important posttranslational modification catalyzed by protein farnesyltransferase (FTase) or protein geranylgeranyltransferase type I (GGTase-I), that enhances membrane localization of the modified proteins in the cell (1-3). FTase catalyzes modification of the protein substrate with a 15-carbon farnesyl group using farnesyl diphosphate (FPP) as a co-substrate, while GGTase-I catalyzes addition of a 20-carbon geranylgeranyl group from geranylgeranyl diphosphate (GGPP) to the protein substrate (2, 4). Both enzymes are $\alpha\beta$ heterodimers and they share a common 48 kDa α subunit with different β subunits. Both subunits are composed primarily of α helices, and the crescent-shaped α subunit is arranged around the barrel-shaped β subunits, with a catalytic zinc ion bound to the β subunit near the two-subunit interface (5-7).

More than 100 human proteins have been shown to be farnesylated, including G proteins γ subunit (8, 9), Ras (10-13), Rho (14-18), Rac (19), Rap

(20, 21), and Rab (22, 23) protein families, etc.. Furthermore, farnesylation of these proteins is important for the function of cellular pathways implied in a variety of diseases, such as cancer and parasitic infections (24-26). Many FTase inhibitors (FTIs) have been identified in preclinical studies and several are currently being evaluated in clinical studies for treatment of a variety of diseases. The FTIs basically fall in three categories: FPP analogues, peptide-competitive inhibitors, and bisubstrate mimics (27-32). Among these three types, the peptide-competitive inhibitors are the most promising and prevalent inhibitors (33-36); therefore, understanding substrate selectivity of FTase as well as the structural determinants of this selectivity will provide important information for the development of novel peptide-competitive FTIs and for the identification of novel FTase protein substrates.

FTase is proposed to recognize a C-terminal Ca_1a_2X sequence in protein substrates where “C” represents the cysteine residue that gets farnesylated through the thioether bond, while “a” refers to any aliphatic amino acids, and “X” is a subset of amino acids, including alanine, serine, glutamine, and methionine that contribute to FTase specificity (37-43). However, recent data suggest broader substrate recognition (44). Previous data indicate that FTase recognizes the a_2 residue of the Ca_1a_2X substrate by a combination of side chain hydrophobicity and volume (45). FTase displays a pyramidal dependence on the volume of the a_2 residue, with a peak reactivity volume at $\sim 140 \text{ \AA}^3$ (when $X=S$). However, recognition of the a_2 residue is dependent on

the identity of the X side chain; when X=M there is little dependence on the volume of the a_2 residue. Nonetheless, analysis of the reactivity of FTase with libraries of peptides implicates recognition of the a_2 side chain as a major determinant of substrate selectivity. The selectivity of the a_2 residue is presumably determined by the size and properties of the a_2 binding pocket. The crystal structure of the FTase•peptide complex illustrates that the a_2 binding pocket is formed by the side chains of W102 β , W106 β , and Y361 β , together with the third isoprenoid unit of the FPP co-substrate (46). These side chains are completely conserved in all FTases, although they are substituted with T49 β , F53 β , and L321 β in GGTase (6).

Previously mutation of Y361 β to leucine has been shown to enhance the affinity of the GCVLS peptide, a typical substrate for FTase, and this substitution also significantly decreases the FTase-catalyzed turnover number, reflecting a diminished product association rate (47). Here we demonstrate that mutation of either W102 β or W106 β with smaller or hydrophilic side chains has little effect on the steady-state kinetic parameters for farnesylation of the GCVa₂S peptides. This was an unexpected result since the residues are completely conserved and raises the question about the reason for this conservation. In this study, we analyze the reactivity of the mutant FTases with a library of peptide substrates demonstrating that these two conserved tryptophan side chains play important roles in regulating the substrate selectivity of FTase. These results provide insight into the structural

determinants of FTase required for efficient substrate recognition, and therefore shed light onto both potential protein substrates and the future design of FTIs.

Experimental procedures

Expression and purification of FTase

Wild-type rat FTase was recombinantly expressed in BL21(DE3) *E. coli* transformed with the pET23aPFT vector (48, 49) after induction by addition of isopropyl β -D-1-thiogalactopyranoside (IPTG) and incubation for 16 h at 25 °C. Cells were harvested by centrifugation, and lysed using a microfluidizer. FTase was purified by sequential DE53 DEAE-cellulose and POROS HQ-20 anion-exchange columns, with a NaCl gradient. The enzyme concentration was determined by active site titration using dansyl-GCVLS (48). FTase was then dialyzed into HT buffer (50 mM HEPES, pH 7.8, 2 mM tris(2-carboxyethyl) phosphine (TCEP) (Gold Biotechnology)), concentrated to 220 μ M, aliquoted, and stored at -80 °C.

Mutagenesis

Mutations at 102 β and 106 β in FTase were introduced into the pET23aPFT plasmid using QuikChange XL methodology (Stratagene). Following confirmation of the desired mutation by sequencing, mutant FTases were expressed and purified using the protocol described for WT FTase.

Preparation of WT and mutant FTase lysate

BL21(DE3) *E. coli* cells containing the pET23aPFT plasmid were grown in LB media containing 1 % glucose, 60 μ M IPTG, and 100 μ g/mL ampicillin for 22 h at 28 °C. WT and mutant FTase were overexpressed under auto-induction conditions. Cell lysates were prepared by mixing 900 μ L of cell culture with 100 μ L 10x FastBreak™ (Promega) lysis reagent containing 15 units benzonase, 2 mg/mL lysozyme, and 0.1 mg/mL phenylmethylsulfonyl fluoride (PMSF), followed by 20 min incubation in a shaker at 28 °C. Each enzymatic assay contained 2-4 μ L of lysate per 100 μ L reaction. SDS-PAGE analysis of the lysates confirmed that all mutants expressed at a level comparable to the WT FTase.

Peptide substrates

All peptides are conjugated with dansyl fluorophores at the N-terminus with a sequence of GCVa₂S, derived from the C-terminal H-Ras sequence (CVLS). An upstream glycine is introduced to prevent the inhibitory effect caused by an interaction between the N-terminal amine of the peptide and the FPP cosubstrate (50). Peptides were purchased from Sigma-Genosys (The Woodlands, TX) with >75% purities. The impurities, as shown by mass spectrometry, are mainly smaller peptide fragments which are not capable of being farnesylated. Peptides were dissolved in absolute ethanol with 10% (v/v) DMSO and stored at -80°C. Peptide concentrations were determined from the increase in absorbance at 412 nm after reaction of the peptide cysteine thiol

with 5,5'-dithiobis(2-nitrobenzoic acid) at pH 7.27, using an extinction coefficient of $14150 \text{ M}^{-1} \text{ cm}^{-1}$ (51).

Cell lysate activity assay

The activity of FTase was measured using clarified cell lysates. Each farnesylation reaction contains 0.1-10 μM dansylated peptide, 2-4 μL FTase lysate where the FTase concentration is more than 5-fold lower than the peptide concentration, 10 μM farnesyl diphosphate (FPP) (Sigma), 50 mM HEPPSO, pH 7.8, 5 mM TCEP, and 5 mM MgCl_2 , in a total volume of 100 μL . The assays were carried out at 25 °C in a 96-well plate (Corning). Peptides were pre-incubated in the reaction buffer containing TCEP for 15 min to ensure that all the peptides were reduced. FPP and FTase were incubated together for 10 min to form the enzyme-substrate complex. Reactions were initiated by the addition of the FTase/FPP mixture to the peptide. Upon farnesylation, the increase in the hydrophobicity near the dansyl group enhances the fluorescence signal (52, 53). The time-dependent increase in fluorescence was measured using a POLARstar Galaxy plate reader (BMG Labtechnologies, Durham, NC) with a λ_{ex} of 340 nm and a λ_{em} of 520 nm.

Steady State kinetic analysis

The initial velocity and the endpoint fluorescence for FTase-catalyzed farnesylation were measured as a function of peptide concentration. A conversion factor, which is defined as the ratio between the fluorescence units

and the product concentration, was calculated for each peptide by dividing the total fluorescence amplitude by the peptide concentration. Using this conversion factor, the linear initial velocity was converted from Δ fluorescence/sec to $\Delta\mu$ M peptide/sec. The Michaelis-Menten equation was fit to the dependence of the initial velocity on the peptide concentration to calculate values for V_{\max} , V_{\max}/K_M and K_M . Data analysis was conducted using Graphpad Prism (Graphpad Software, San Diego, CA).

Results

Substrate specificity of W102 β A and W106 β A mutant FTase

Preliminary mutagenesis studies (Hougland, unpublished results) suggested that substitution of W102 β and W106 β in FTase with random amino acids had little effect on either the recombinant expression levels or reactivity with the peptide dansyl-GCVLS. FTase mutants with alterations in both activity and substrate specificity were observed in a small library of variants with Trp at 102 β and 106 β each substituted with all 20 amino acids. Therefore to further explore the functional role of these two completely conserved Trp residues that interact with the a_2 side chain of the substrate CaaX sequence, we measured the reactivity of the W102 β A and W106 β A mutants with a panel of peptide substrates, dansyl-GCVa₂S, with varying a_2 residues. As shown in Figure 4.1, WT FTase selectivity (dashed lines) displays a pyramidal dependence on the volume of the side chain at a_2 ; for smaller side chains the volume of k_{cat}/K_M increases with side chain volume, likely reflecting enhanced Van der Waals

contact while the value of k_{cat}/K_M decreases with large side chains, presumably due to steric hindrance. The peak value for k_{cat}/K_M occurs for a side chain volume of $\sim 140 \text{ \AA}^3$, suggesting an ideal size of the a_2 binding pocket. Both W102 β A and W106 β A, shown in Figure 4.1(a) and (b) respectively, eliminate the FTase substrate selectivity against large side chains at the a_2 position (a_2 =M, I, L, F, W), presumably substitution of the large Trp with the small Ala residue increases the size of the a_2 binding pocket, relieving steric clash with the larger a_2 side chains. Additionally, the W106 β A, but not the W102 β A

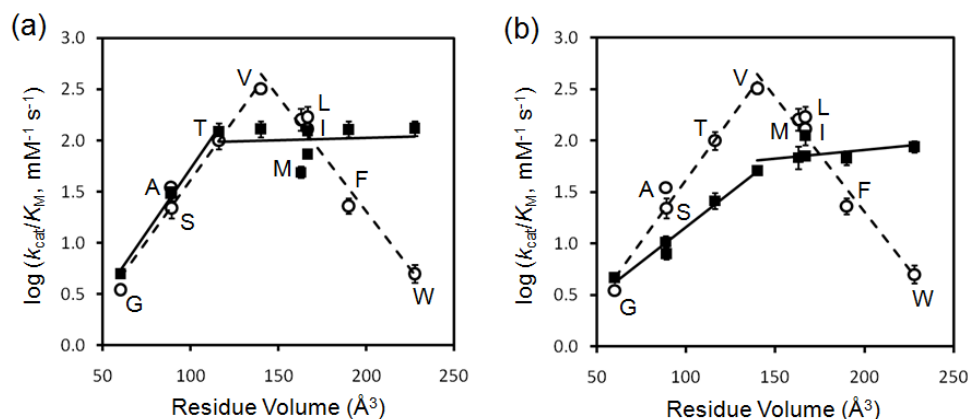


Figure 4.1: W102 β A and W106 β A FTase activity with peptide substrates dansyl-GCVa₂S.⁴ All data are obtained using purified enzymes. **(a)** Correlation of $\log(k_{cat}/K_M, \text{ mM}^{-1} \text{ s}^{-1})$ for farnesylation catalyzed by W102 β A FTase with the volume of side chains at the a_2 residue in GCVa₂S (a_2 =G, A, S, T, V, M, I, L, F, W). The open circles represent the values measured for WT FTase and are fit into two groups based on the a_2 residue volume (dashed line; left: slope = 0.024, $R^2 = 0.97$; right: slope = -0.022, $R^2 = 0.96$). The solid squares indicate the reactivity of W102 β A mutant and lines are fit to two groups of data (solid line; left: slope = 0.025, $R^2 = 0.99$; right: zero slope within error). **(b)** Dependence of $\log(k_{cat}/K_M, \text{ mM}^{-1} \text{ s}^{-1})$ on the volume of a_2 residues catalyzed by W106 β A FTase. The WT data (open circles) are identical to those described in (a) and the solid squares represent the value of k_{cat}/K_M measured for farnesylation of GCVa₂S peptides catalyzed by W106 β A FTase mutant. The data are fit based on two groups (solid line; left: slope = 0.014, $R^2 = 0.98$; right: zero slope within error).

⁴ Data obtained by Houglund et al.

mutation decreases the activation due to favorable contact with the a_2 residue.

Measuring W102 β A and W106 β A FTase activity using a cell lysate assay

To further explore the a_2 binding pocket, more W102 β and W106 β mutants were analyzed. To facilitate these experiments, we developed a cell lysate-based assay which allows a quantitative evaluation of the catalytic activity of the FTase mutants without purification. FTase mutants were expressed in *E. coli* using auto-induction conditions where cells were grown in LB media with 1 % glucose and 60 μ M IPTG for 22 h at 28 °C. The cells were lysed by incubation with the FastBreak™ lysis reagent. SDS-PAGE analysis of the lysates was carried out to examine expression levels (Figure 4.2); this gel illustrates comparable intensities of protein bands for all of the FTase mutants indicating that the protein concentration is comparable for each mutant.

To validate this assay, we remeasured the reactivity of the WT, W102 β A, and W106 β A FTases with the panel of dansyl-GCVa₂S peptides (a_2 =G, A, T, V, L, F, W), and values of V_{max}/K_M were obtained. As shown in Figure 4.3, using this cell lysate-based assay, all WT, W102 β A and W106 β A FTases showed the same trends in substrate specificity as using the purified protein (Figure 4.1). A comparison of the value of V_{max}/K_M measured using cell lysates and k_{cat}/K_M measured using purified enzymes is shown in Figure 4.1. V_{max}/K_M values were plotted with k_{cat}/K_M values, and the data show a linear correlation for both W102 β A and W106 β A FTases with a similar slope of ~ 10 nM, representing the FTase concentration used in the reaction from the cell lysate. These results

indicate that the cell lysate-based assay is a feasible tool to quantify the WT and mutant FTase activity without purifying a large number of proteins.

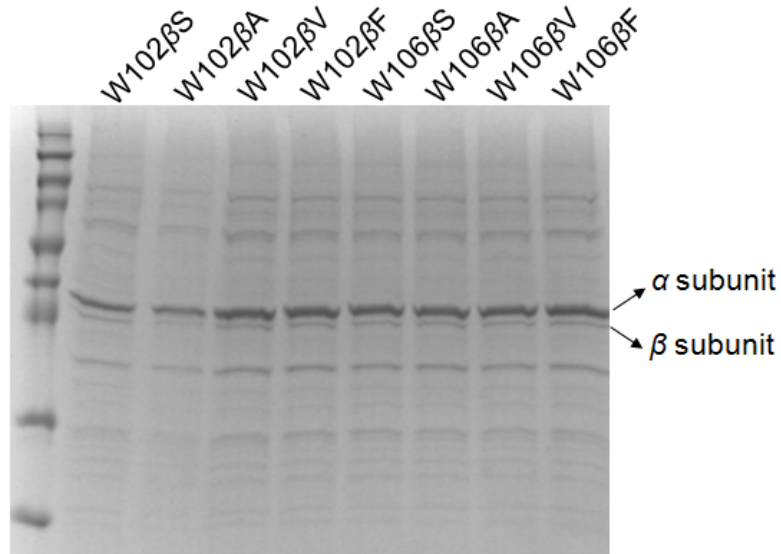


Figure 4.2: SDS-PAGE analysis of the lysates of FTase mutants. 6 μ L of the cell lysate was loaded onto each lane and fractionated by SDS-PAGE. The comparable size of protein bands representing α and β subunits of mutant FTases indicates that they all expressed to a similar level. W102 β A shows smaller intensities of the bands possibly due to loading errors, since the rest of the proteins in the lane are fainter as well.

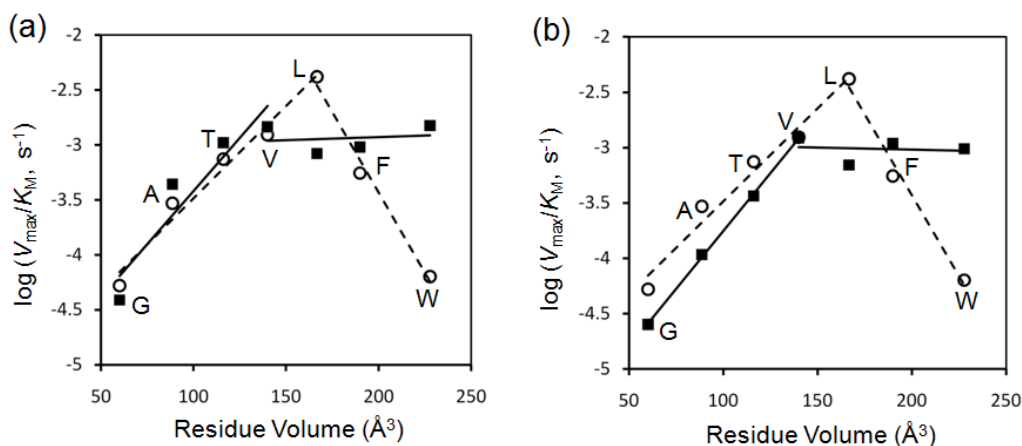


Figure 4.3: W102 β A and W106 β A FTase activity with peptide substrates dansyl-GCVa₂S using the cell lysate-based assay. These data show similar trends to those using the purified FTase. **(a)** Correlation of $\log(V_{\max}/K_M, \text{s}^{-1})$ for farnesylation catalyzed by W102 β A with the volume of the side chains at the a₂ residue in GCVa₂S (a₂=G, A, T, V, L, F, W). The open circles represent the values measured for WT FTase and are fit into two groups based on the a₂ residue volume (dashed line; left: slope = 0.017, $R^2 = 0.97$; right: slope = -0.029, $R^2 = 0.99$). The solid squares indicate the reactivity of W102 β A mutant and lines are fit to two groups of data (solid line; left: slope = 0.019, $R^2 = 0.88$; right: zero slope within error). **(b)** Dependence of $\log(V_{\max}/K_M, \text{s}^{-1})$ on the volume of a₂ residues catalyzed by W106 β A FTase. The WT data (open circles) are identical to those described in (a) and the solid squares represent the value of V_{\max}/K_M measured for farnesylation of GCVa₂S peptides catalyzed by W106 β A FTase. The data are fit based on two groups (solid lines; left: slope = 0.021, $R^2 = 1.00$; right: zero slope within error).

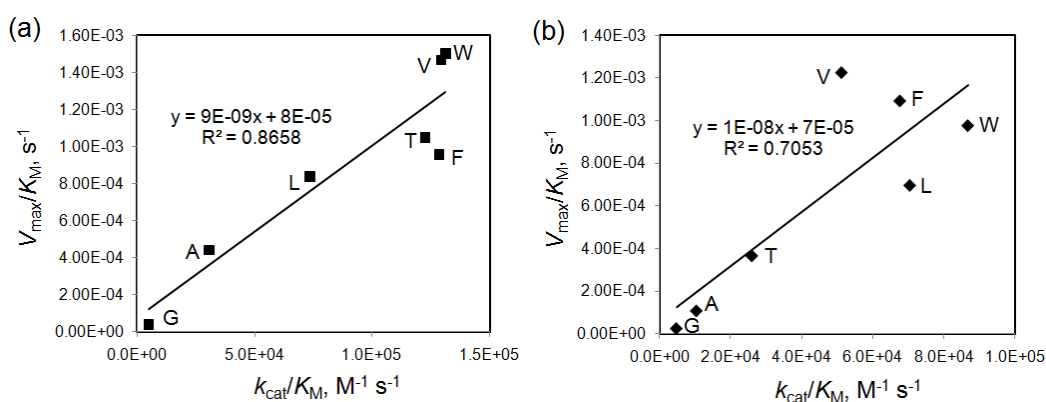


Figure 4.4: Validation of the cell lysate-based assay. **(a)** Correlation of V_{\max}/K_M , measured by the cell lysate-based assay with k_{cat}/K_M measured using purified W102 β A FTase with peptide substrates dansyl-GCVa₂S. Data points were fit with linear regression. **(b)** Same as described for (a) except that W106 β A cell lysate and purified enzyme were used.

Substrate selectivity of W102 β X and W106 β X mutant FTase

Using this robust cell lysate assay, we measured the reactivity with the substrates panel of six additional mutants at both the 102 β and 106 β positions, including W102 β S, W102 β V, W102 β F, W106 β S, W106 β V, and W106 β F. These amino acids substitutions provide a range of side chain volumes. For each FTase/substrate pair, the value of V_{\max}/K_M was determined using the cell lysate assay. The substrate selectivity of these mutants provides insight into recognition of the a_2 side chain. When Trp is substituted with Phe at 102 β position (Figure 4.5(a)), the dependence of the reactivity on the a_2 side chain volume is very similar to the WT pyramidal selectivity profile (Figure 4.3(a)) except that the activity peaks at Val rather than Leu. In contrast the W106 β F mutant has a selectivity profile similar to W102 β A FTase with substrate peptides containing a_2 with small side chains; however discrimination against large side chains at a_2 is eliminated (Figure 4.5(b)). This significant difference in the substrate selectivity pattern of W102 β F and W106 β F mutants indicates that W102 β and W106 β function differently in determining substrate selectivity of FTase, which will be discussed in detail in the discussion section.

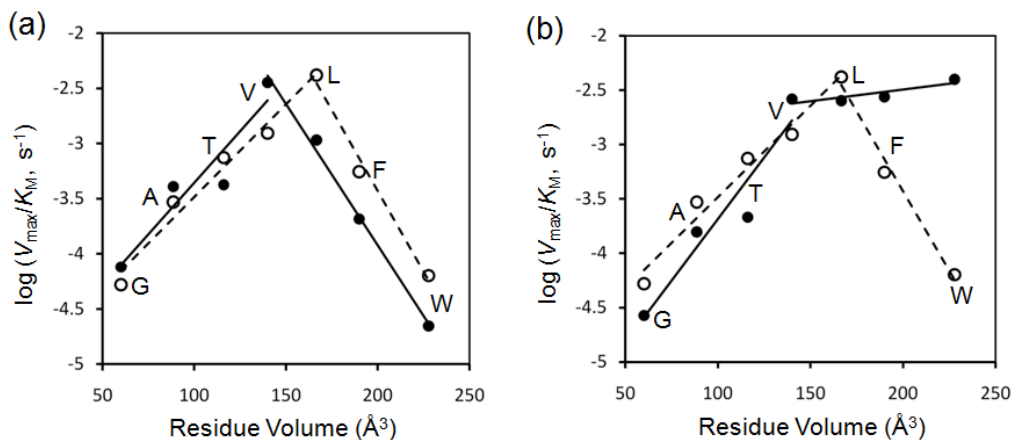


Figure 4.5: W102βF and W106βF FTase activity with peptide substrates dansyl-GCVa₂S. All data were obtained using the cell lysate-based assay. **(a)** Correlation of $\log (V_{\max}/K_M, s^{-1})$ for farnesylation catalyzed by W102βF FTase with the volume of side chain at the a₂ residue in GCVa₂S peptides (a₂=G, A, T, V, L, F, W). The open circles represent the values measured for WT FTase same as those in Figure 4.3, and the solid circles indicate the reactivity of W102βF mutant and lines are fit into two groups of data (solid line; left: slope = 0.019, $R^2 = 0.89$; right: slope = -0.026, $R^2 = 0.99$). **(b)** Dependence of $\log (V_{\max}/K_M, s^{-1})$ on the volume of a₂ residues catalyzed by W106βF FTase. The open circles indicate WT data and the solid circles represent the value of V_{\max}/K_M measured for farnesylation of GCVa₂S peptides catalyzed by W106βF FTase. The data were fit based on two groups (solid lines; left: slope = 0.023, $R^2 = 0.91$; right: zero slope within error).

Additional insights into the determinants of substrate selectivity of FTase are revealed by examining the specificity of additional mutants. The V_{\max}/K_M values for reaction of each FTase variant at position 102β (W, F, V, S and A) are measured and overlaid on a single graph (Figure 4.6 (a)). For these variants the catalytic activity for peptides containing small a₂ side chains (a₂ = G, A, T, V) are comparable, suggesting that the increased selectivity as the volume of the side chain increases is not due to contact with W102β. However, as the size of the side chain at position 102β increases, discrimination against substrates with large a₂ residues increases; i.e., both WT and W102βF FTases

display significant discrimination against reaction with substrates containing a_2 = Trp and Phe, while less selectivity is observed for the W102 β V and W102 β S FTases and no discrimination is observed for the W102 β A mutant. These data clearly indicate that W102 β side chain contributes significantly to steric discrimination without contributing to the Van der Waals contacts to enhance reactivity with moderate-sized a_2 residues.

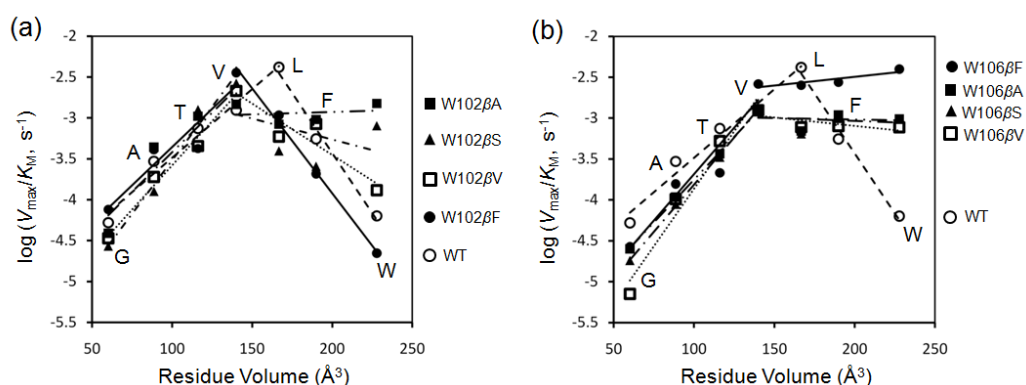


Figure 4.6: Overlay of W102 β X and W106 β X FTase activity with peptide substrates dansyl-GCVa₂S. All data were obtained using the cell lysate-based assay. **(a)** Correlation of $\log(V_{\max}/K_M, \text{s}^{-1})$ for farnesylation catalyzed by W102 β X (X=W, F, V, S, A) with the volume of the side chains at the a_2 residue in GCVa₂S peptides (a_2 =G, A, T, V, L, F, W). Each series of data are fit into two groups. WT is shown in open circles and fit with dashed line (---); W102 β F is shown in filled circles and fit with solid line (—) (as shown in Figure 4.5(a)); W102 β V is shown in open squares and fit with dotted line (····) (left: slope = 0.022, R^2 = 0.98; right: slope = -0.013, R^2 = 0.86); W102 β S is shown in filled triangles and fit with -·-·- (left: slope = 0.026, R^2 = 0.98; right: an almost flat slope = -0.005); W102 β A is shown in filled squares and fit with -·-·- (as shown in Figure 4.3(a)). **(b)** Dependence of $\log(V_{\max}/K_M, \text{s}^{-1})$ on the volume of a_2 residues catalyzed by W106 β X FTase. Each series of data were also fit into two groups as in (a). Open circles and dashed line (---) still indicate WT data; W106 β F is shown in filled circles and fit with solid line (—) (as shown in Figure 4.5(b)); W106 β V is shown in open squares and fit with dotted line (····) (left: slope = 0.028, R^2 = 0.96; right: zero slope within error); W106 β S is shown in filled triangles and fit with -·-·- (left: slope = 0.023, R^2 = 1.00; right: zero slope within error); W106 β A is shown in filled squares and fit with -·-·- (as shown in Figure 4.3(b)).

Residue W106 β , on the other hand, presents a very different result. The reactivity of WT, W106 β F, W106 β V, W106 β S, and W106 β A were all tested with the seven peptides and are overlaid on a single plot for comparison (Figure 4.6(b)). The enhanced reactivity with moderately sized a_2 side chains is largely unaffected by the mutations, as observed for of W102 β X FTase mutants (Figure 4.6(a)). However, for substrates with larger a_2 side chains, all of the W106 β mutations show a loss of substrate discrimination. This indicates that W106 β is not the main contributor to the steric discrimination; increasing the pocket size at this position (Trp to Phe) is sufficient to eliminate the steric hindrance.

Discussion

Conserved W102 β and W106 β regulate the substrate selectivity of FTase

The crystal structures of $-Ca_1a_2X$ peptides bound to FTase (46) illustrate that the a_2 side chain interacts with the indole rings of W102 β and W106 β as well as a phenol ring of Y361 β (Figure 4.7). These three amino acids are completely conserved in FTases, implying that they play an important role in protein function.

Mutagenesis studies demonstrate that these interactions are important for regulating the peptide substrate selectivity of FTase. The kinetic measurements of the reactivity of the W102 β A and W106 β A FTase mutants demonstrate that these Trp side chains limit reactivity with $-Ca_1a_2X$ substrates containing large a_2 side chains (Figure 4.1 and 4.3). For peptide substrates

with an a_2 side chain volume $\leq 140 \text{ \AA}^3$ (Gly (60.1 \AA^3), Ala (88.6 \AA^3), Thr (116.1 \AA^3) and Val (140 \AA^3) (54), the W102 β A and W106 β A FTase mutations have little or no effect on the reactivity and substrate selectivity compared to WT FTase. However when the a_2 residue is large ($> 170 \text{ \AA}^3$, Phe (189.9 \AA^3) and Trp (227.8 \AA^3)), the mutants at 102 β and 106 β lose all discrimination against the larger side chains.

Based on the crystal structure shown in Figure 4.7, the a_2 binding cavity formed by W102 β , W106 β , and Y361 β is estimated to be 180.1 \AA^3 according to the computational result using the POVME algorithm (55). Since this is smaller than the side chain volume of Trp or Phe, the discrimination observed in WT FTase is likely based on size. This conclusion is consistent with the loss of the selectivity against large a_2 residues where the size of the pocket is increased by substituting the smaller Ala (88.6 \AA^3) side chain for Trp (227.8 \AA^3) at W102 β or W106 β . The extra space accommodates a_2 side chains and leads to comparable reactivity with –CVVS, –CVLS, –CVFS, and –CVWS peptides. Previous studies have also demonstrated that Y361 β is important for selectivity but by a different mechanism. In this case, the Y361 β L mutation enhances the affinity of the peptide substrate (GCVLS) and leads to a substantial decrease in the rate for product dissociation (47).

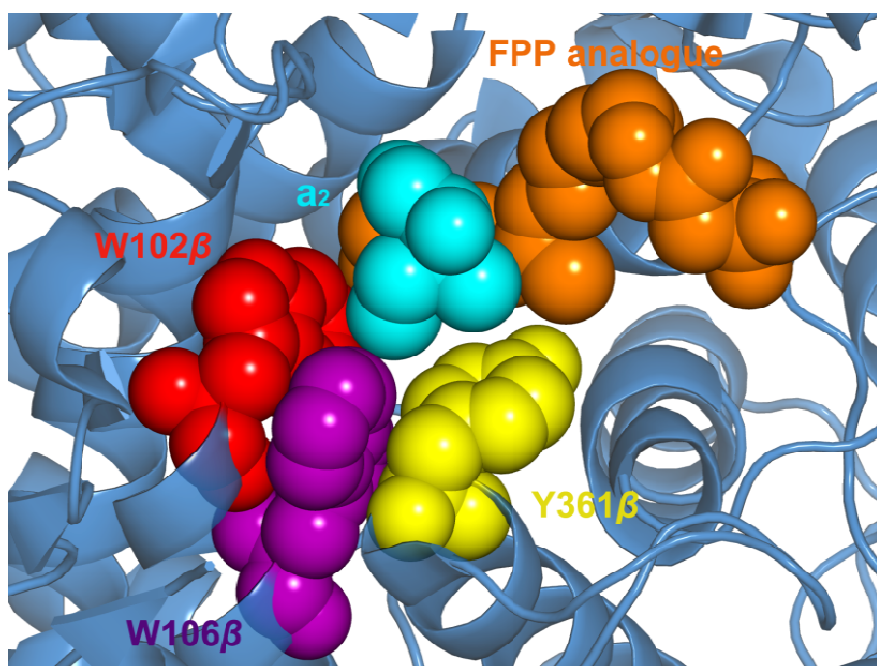


Figure 4.7: Crystal structure of FTase a_2 residue binding pocket. This figure is derived from PDB ID ID8D. The three FTase residues forming the Ca_1a_2X sequence a_2 binding site, W102 β , W106 β , and Y361 β , are highlighted in red, purple, and yellow respectively. The a_2 residue is shown in cyan, which is surrounded by the three hydrophobic residues together with the last isoprenoid unit of FPT-II-FPP analogue shown in orange.

W102 β and W106 β function differently for controlling the substrate selectivity of FTase

To further explore interactions between the a_2 side chain and the residues at position 102 β and 106 β important for controlling the substrate selectivity of FTase, we measured the specificity of W102 β and W106 β FTases containing smaller residues at these positions, including phenylalanine, valine, and serine. These data demonstrate that W102 β and W106 β have different contributions to the FTase substrate selectivity. For W102 β position, mutation of the large Trp residue (227.8 Å³) to smaller side chains (Phe (189.9 Å³), Val (140 Å³), and Ser (89 Å³)) (54), leads to a gradual decrease in the selectivity against

peptides with large a_2 groups (Figure 4.6(a)). Thus, the residue at the 102β position acts to fine tune the FTase substrate selectivity; the size of the $W102\beta$ side chain alters the volume of the a_2 binding pocket, which is reflected in enhanced reactivity for peptides with large a_2 groups. All mutations, including substitution of Trp (227.8 \AA^3) with Phe (189.9 \AA^3), completely abolish the discrimination of FTase against peptides with large a_2 residues. The Trp residue at 106β , on the other hand, behaves like a switch for the selectivity of FTase: only the bulky tryptophan is large enough to cap the size of the binding pocket and thereby allow steric discrimination of peptide substrates.

The different roles in substrate discrimination can be explained by the altered positions of $W102\beta$ and $W106\beta$ in the a_2 binding pocket. The crystal structure (Figure 4.7) demonstrates that the aromatic ring of $W102\beta$ has a facial interaction with the a_2 residue, forming one side of the binding pocket. Therefore substitution of Trp with other amino acids leads to a limited impairment of this interaction. In this way the substrate selectivity becomes less sensitive to the size of the a_2 side chain as the size of the $W102\beta$ amino acid decreases. However, the aromatic ring of $W106\beta$ is sandwiched between $W102\beta$ and $Y361\beta$, and therefore only interacts with the a_2 residue via the edge of the ring structure which leads to a defined requirement for the length of the side chain at 106β ; even a small decrease in length from Trp to Phe substitution is sufficient to eliminate substrate selectivity. It is also notable that the activity of $W106\beta$ F mutant is comparable to that of WT with the best

substrates and 3-4-fold higher than other mutations at this site. The Phe substitution may form an optimal binding pocket for the larger a_2 residue.

The majority of completely conserved residues in proteins are important for protein stability, catalytic activity, or high affinity substrate binding. However, in FTase, we demonstrated that the two tryptophans are conserved to preserve substrate recognition and therefore fine tune the reactivity of multiple protein substrates and non-substrates, which is crucial for *in vivo* functions of FTase.

In summary, the cell lysate-based assay has proven to be an efficient tool to rapidly measure the catalytic activity of FTase mutants. These data have delineated the crucial role of the two completely conserved tryptophan residues in tuning the substrate recognition of FTase. Future computational and structural analysis of the FTase mutants may provide more accurate information on the residue interactions within the a_2 binding pocket and therefore provide additional insight into the determinants of substrate selection. These studies will shed light on the design of novel peptidomimetics FTIs and prediction of *in vivo* protein farnesylation substrates.

References

1. Zhang, F. L., and Casey, P. J. (1996) Protein prenylation: molecular mechanisms and functional consequences, *Annu. Rev. Biochem.* 65, 241-269.
2. Benetka, W., Koranda, M., and Eisenhaber, F. (2006) Protein Prenylation: An (Almost) Comprehensive Overview on Discovery History, Enzymology, and Significance in Physiology and Disease, *Monatsh. Chem.* 137, 1241-1281.

3. Casey, P. J. (1994) Lipid modifications of G proteins, *Curr. Opin. Cell Biol.* 6, 219-225.
4. Casey, P. J., and Seabra, M. C. (1996) Protein Prenyltransferases, *J. Biol. Chem.* 271, 5289-5292.
5. Reiss, Y., Goldstein, J. L., Seabra, M. C., Casey, P. J., and Brown, M. S. (1990) Inhibition of purified p21ras farnesyl:protein transferase by Cys-AAX tetrapeptides, *Cell* 62, 81-88.
6. Reid, T. S., Terry, K. L., Casey, P. J., and Beese, L. S. (2004) Crystallographic Analysis of CaaX Prenyltransferases Complexed with Substrates Defines Rules of Protein Substrate Selectivity, *J. Mol. Biol.* 343, 417-433.
7. Lane, K. T., and Beese, L. S. (2006) Structural biology of protein farnesyltransferase and geranylgeranyltransferase type I, *J. Lipid Res.* 47, 681-699.
8. Lai, R. K., Perez-Sala, D., Canada, F. J., and Rando, R. R. (1990) The γ subunit of transducin is farnesylated, *Proc. Natl. Acad. Sci. U. S. A.* 87, 7673-7677.
9. Ray, K., Kunsch, C., Bonner, L. M., and Robishaw, J. D. (1995) Isolation of cDNA clones encoding eight different human G protein γ subunits, including three novel forms designated the γ_4 , γ_{10} , and γ_{11} subunits, *J. Biol. Chem.* 270, 21765-21771.
10. Ellis, C. A., Vos, M. D., Howell, H., Vallecorsa, T., Fults, D. W., and Clark, G. J. (2002) Rig is a novel Ras-related protein and potential neural tumor suppressor, *Proc. Natl. Acad. Sci. U. S. A.* 99, 9876-9881.
11. Der, C. J., and Cox, A. D. (1991) Isoprenoid modification and plasma membrane association: critical factors for ras oncogenicity, *Cancer Cells* 3, 331-340.
12. Carboni, J. M., Yan, N., Cox, A. D., Bustelo, X., Graham, S. M., Lynch, M. J., Weinmann, R., Seizinger, B. R., Der, C. J., and et, a. (1995) Farnesyltransferase inhibitors are inhibitors of Ras but not R-Ras2/TC21, transformation, *Oncogene* 10, 1905-1913.
13. Kontani, K., Tada, M., Ogawa, T., Okai, T., Saito, K., Araki, Y., and Katada, T. (2002) Di-Ras, a Distinct Subgroup of Ras Family GTPases with Unique Biochemical Properties, *J. Biol. Chem.* 277, 41070-41078.

14. Yamane, H. K., Farnsworth, C. C., Xie, H., Evans, T., Howald, W. N., Gelb, M. H., Glomset, J. A., Clarke, S., and Fung, B. K. K. (1991) Membrane-binding domain of the small G protein G25K contains an S-(all-trans-geranylgeranyl)cysteine methyl ester at its carboxyl terminus, *Proc. Natl. Acad. Sci. U. S. A.* *88*, 286-290.
15. Yoshida, Y., Kawata, M., Katayama, M., Horiuchi, H., Kita, Y., and Takai, Y. (1991) A geranylgeranyltransferase for rhoA p21 distinct from the farnesyltransferase for ras p21S, *Biochem. Biophys. Res. Commun.* *175*, 720-728.
16. Adamson, P., Marshall, C. J., Hall, A., and Tilbrook, P. A. (1992) Post-translational modifications of p21rho proteins, *J. Biol. Chem.* *267*, 20033-20038.
17. Nobes, C. D., Lauritzen, I., Mattei, M.-G., Paris, S., Hall, A., and Chardin, P. (1998) A new member of the Rho family, Rnd1, promotes disassembly of actin filament structures and loss of cell adhesion, *J. Cell Biol.* *141*, 187-197.
18. Hoffman, G. R., Nassar, N., and Cerione, R. A. (2000) Structure of the Rho family GTP-binding protein Cdc42 in complex with the multifunctional regulator RhoGDI, *Cell* *100*, 345-356.
19. Kinsella, B. T., Erdman, R. A., and Maltese, W. A. (1991) Carboxyl-terminal isoprenylation of ras-related GTP-binding proteins encoded by rac1, rac2, and ralA, *J. Biol. Chem.* *266*, 9786-9794.
20. Buss, J. E., Quilliam, L. A., Kato, K., Casey, P. J., Solski, P. A., Wong, G., Clark, R., McCormick, F., Bokoch, G. M., and Der, C. J. (1991) The carboxy-terminal domain of the Rap1A (Krev-1) protein is isoprenylated and supports transformation by an H-Ras:Rap1A chimeric protein, *Mol. Cell. Biol.* *11*, 1523-1530.
21. Farrell, F. X., Yamamoto, K., and Lapetina, E. G. (1993) Prenyl group identification of rap2 proteins: A ras superfamily member other than ras that is farnesylated, *Biochem. J.* *289*, 349-355.
22. Kinsella, B. T., and Maltese, W. A. (1992) rab GTP-binding proteins with three different carboxyl-terminal cysteine motifs are modified in vivo by 20-carbon isoprenoids, *J. Biol. Chem.* *267*, 3940-3945.
23. Farnsworth, C. C., Seabra, M. C., Ericsson, L. H., Gelb, M. H., and Glomset, J. A. (1994) Rab geranylgeranyl transferase catalyzes the

geranylgeranylation of adjacent cysteines in the small GTPases Rab1A, Rab3A, and Rab5A, *Proc. Natl. Acad. Sci. U. S. A.* *91*, 11963-11967.

24. Maurer-Stroh, S., Washietl, S., and Eisenhaber, F. (2003) Protein prenyltransferases: Anchor size, pseudogenes and parasites, *Biol. Chem.* *384*, 977-989.
25. Gelb, M. H., Van, V. W. C., Buckner, F. S., Yokoyama, K., Eastman, R., Carpenter, E. P., Panethymitaki, C., Brown, K. A., and Smith, D. F. (2003) Protein farnesyl and N-myristoyl transferases: piggy-back medicinal chemistry targets for the development of antitrypanosomatid and antimalarial therapeutics, *Mol. Biochem. Parasitol.* *126*, 155-163.
26. Chen, Z., Sun, J., Pradines, A., Favre, G., Adnane, J., and Sebti, S. M. (2000) Both farnesylated and geranylgeranylated RhoB inhibit malignant transformation and suppress human tumor growth in nude mice, *J. Biol. Chem.* *275*, 17974-17978.
27. Bell, I. M. (2004) Inhibitors of Farnesyltransferase: A Rational Approach to Cancer Chemotherapy?, *J. Med. Chem.* *47*, 1869-1878.
28. Doll, R. J., Kirschmeier, P., and Bishop, W. R. (2004) Farnesyltransferase inhibitors as anticancer agents: Critical crossroads, *Curr. Opin. Drug Discovery Dev.* *7*, 478-486.
29. Graaf, M. R., Richel, D. J., van, N. C. J. F., and Guchelaar, H.-J. (2004) Effects of statins and farnesyltransferase inhibitors on the development and progression of cancer, *Cancer Treat. Rev.* *30*, 609-641.
30. Sousa, S. F., Fernandes, P. A., and Ramos, M. J. (2008) Farnesyltransferase inhibitors: a detailed chemical view on an elusive biological problem, *Curr. Med. Chem.* *15*, 1478-1492.
31. Agrawal, A. G., and Somani, R. R. (2009) Farnesyltransferase inhibitor as anticancer agent, *Mini-Rev. Med. Chem.* *9*, 638-652.
32. Basso, A. D., Kirschmeier, P., and Bishop, W. R. (2006) Lipid posttranslational modifications. Farnesyl transferase inhibitors, *J Lipid Res.* *47*, 15-31.
33. Garcia, A. M., Rowell, C., Ackermann, K., Kowalczyk, J. J., and Lewis, M. D. (1993) Peptidomimetic inhibitors of Ras farnesylation and function in whole cells, *J. Biol. Chem.* *268*, 18415-18418.

34. Vogt, A., Qian, Y., Blaskovich, M. A., Fossum, R. D., Hamilton, A. D., and Sebti, S. M. (1995) A non-peptide mimetic of Ras-CAAX: selective inhibition of farnesyltransferase and Ras processing, *J. Biol. Chem.* **270**, 660-664.
35. Ohkanda, J., Lockman, J. W., Yokoyama, K., Gelb, M. H., Croft, S. L., Kendrick, H., Harrell, M. I., Feagin, J. E., Blaskovich, M. A., Sebti, S. M., and Hamilton, A. D. (2001) Peptidomimetic inhibitors of protein farnesyltransferase show potent antimalarial activity, *Bioorg. Med. Chem. Lett.* **11**, 761-764.
36. Dinsmore, C. J., and Bell, I. M. (2003) Inhibitors of farnesyltransferase and geranylgeranyltransferase-I for antitumor therapy: Substrate-based design, conformational constraint and biological activity, *Curr. Top. Med. Chem.* **3**, 1075-1093.
37. Casey, P. J., Thissen, J. A., and Moomaw, J. F. (1991) Enzymic modification of proteins with a geranylgeranyl isoprenoid, *Proc. Natl. Acad. Sci. U. S. A.* **88**, 8631-8635.
38. Moores, S. L., Schaber, M. D., Mosser, S. D., Rands, E., O'Hara, M. B., Garsky, V. M., Marshall, M. S., Pompliano, D. L., and Gibbs, J. B. (1991) Sequence dependence of protein isoprenylation, *J. Biol. Chem.* **266**, 14603-14610.
39. Reiss, Y., Stradley, S. J., Gierasch, L. M., Brown, M. S., and Goldstein, J. L. (1991) Sequence requirement for peptide recognition by rat brain p21ras protein farnesyltransferase, *Proc. Natl. Acad. Sci. U. S. A.* **88**, 732-736.
40. Yokoyama, K., Goodwin, G. W., Chomashchi, F., Glomset, J. A., and Gelb, M. H. (1991) A protein geranylgeranyltransferase from bovine brain: implications for protein prenylation specificity, *Proc. Natl. Acad. Sci. U. S. A.* **88**, 5302-5306.
41. Omer, C. A., Kral, A. M., Diehl, R. E., Prendergast, G. C., Powers, S., Allen, C. M., Gibbs, J. B., and Kohl, N. E. (1993) Characterization of recombinant human farnesyl-protein transferase: Cloning, expression, farnesyl diphosphate binding, and functional homology with yeast prenyl-protein transferases, *Biochemistry* **32**, 5167-5176.
42. Caplin, B. E., Hettich, L. A., and Marshall, M. S. (1994) Substrate characterization of the *Saccharomyces cerevisiae* protein farnesyltransferase and type-I protein geranylgeranyltransferase,

Biochim. Biophys. Acta, Protein Struct. Mol. Enzymol. 1205, 39-48.

43. Fu, H.-W., and Casey, P. J. (1999) Enzymology and biology of CaaX protein prenylation, *Recent Prog. Horm. Res.* 54, 315-343.
44. Hougland, J. L., Hicks, K. A., Hartman, H. L., Kelly, R. A., Watt, T. J., and Fierke, C. A. Identification of Novel Peptide Substrates for Protein Farnesyltransferase Reveals Two Substrate Classes with Distinct Sequence Selectivities, *J. Mol. Biol.* 395, 176-190.
45. Hougland, J. L., Lamphear, C. L., Scott, S. A., Gibbs, R. A., and Fierke, C. A. (2009) Context-dependent substrate recognition by protein farnesyltransferase, *Biochemistry* 48, 1691-1701.
46. Long, S. B., Casey, P. J., and Beese, L. S. (2000) The basis for K-Ras4B binding specificity to protein farnesyltransferase revealed by 2 Å resolution ternary complex structures, *Structure (London)* 8, 209-222.
47. Spence, R. A., Hightower, K. E., Terry, K. L., Beese, L. S., Fierke, C. A., and Casey, P. J. (2000) Conversion of Tyr361 β to Leu in Mammalian Protein Farnesyltransferase Impairs Product Release but Not Substrate Recognition, *Biochemistry* 39, 13651-13659.
48. Bowers, K. E., and Fierke, C. A. (2004) Positively Charged Side Chains in Protein Farnesyltransferase Enhance Catalysis by Stabilizing the Formation of the Diphosphate Leaving Group, *Biochemistry* 43, 5256-5265.
49. Zimmerman, K. K., Scholten, J. D., Huang, C.-C., Fierke, C. A., and Hupe, D. J. (1998) High-level expression of rat farnesyl protein transferase in *Escherichia coli* as a translationally coupled heterodimer, *Protein Expression Purif.* 14, 395-402.
50. Long, S. B., Hancock, P. J., Kral, A. M., Hellinga, H. W., and Beese, L. S. (2001) The crystal structure of human protein farnesyltransferase reveals the basis for inhibition by CaaX tetrapeptides and their mimetics, *Proc. Natl. Acad. Sci. U. S. A.* 98, 12948-12953.
51. Riddles, P. W., Blakeley, R. L., and Zerner, B. (1979) Ellman's reagent: 5,5'-dithiobis(2-nitrobenzoic acid) - a reexamination, *Anal. Biochem.* 94, 75-81.
52. Pompliano, D. L., Gomez, R. P., and Anthony, N. J. (1992) Intramolecular fluorescence enhancement: a continuous assay of Ras farnesyl:protein transferase, *J. Am. Chem. Soc.* 114, 7945-7946.

53. Cassidy, P. B., Dolence, J. M., and Poulter, C. D. (1995) Continuous fluorescence assay for protein prenyltransferases, *Methods Enzymol.* 250, 30-43.
54. Zamyatin, A. A. (1972) Protein volume in solution, *Progr. Biophys. Mol. Biol.* 24, 107-123.
55. Durrant, J. D., de Oliveira, C. A. F., and McCammon, J. A. POVME: An algorithm for measuring binding-pocket volumes, *J. Mol. Graph. Model.* 29, 773-776.

CHAPTER V

SUMMARY, CONCLUSIONS, AND FUTURE DIRECTIONS

Summary and Conclusions

Catalytic mechanism of protein palmitoyltransferase Akr1p

Protein palmitoyltransferases (PATs) catalyze S-palmitoylation of cysteines in proteins, contributing to membrane targeting, subcellular protein trafficking and function. Mutations in PATs are associated with a number of neurological diseases and cancer progression (1-6). Even though a number of PATs have been discovered (7-14), the understanding of the biological function, catalytic mechanism, and regulation is quite limited.

Akr1p is an 86 kDa yeast protein that has palmitoyltransferase activity (7, 15). It is an integral membrane protein, which makes it difficult to express and purify to a large quantity. This challenge has been partially solved by adding the detergent Triton X-100 and bovine liver lipids to solubilize and stabilize the membrane protein. Furthermore, expression of Akr1p using the *GAL1* promoter increases the expression level at least 10-fold compared to the natural yeast promoter. Through the optimization of an anti-FLAG affinity purification method (7), the active Akr1p containing a FLAG-tag was successfully purified from yeast. Using the purified enzyme, characterization of

its palmitoyltransferase activity was carried out. Akr1p-dependent palmitoylation activity is detected by the covalent modification of a substrate protein with a ^3H -labeled palmitoyl moiety in the presence of [^3H]-palmitoyl-CoA. Using this radioactive assay, I demonstrated that, in addition to the previously identified Akr1p substrate, yeast casein kinase 2 (Yck2) (16), Akr1p catalyzes palmitoylation of several other yeast proteins including Ypl199c, which is palmitoylated more rapidly by Akr1p. Use of this substrate facilitates the kinetic studies of Akr1p. Site-directed mutagenesis of the substrate, Ypl119c (Cys to Ser), reveals that two C-terminal cysteines (C233 and C235) are the sites of palmitoylation; Ypl119c containing either single mutation is palmitoylated by Akr1p but no palmitoylation is observed with simultaneous mutations (C233S/C235S).

Although the structure of Akr1p has not yet been solved, sequence homology among PATs suggests that a conserved DHHC (DHYC in Akr1p) motif may form a portion of the active site (17, 18). This sequence along with a conserved cysteine rich domain (CRD) is proposed to resemble a zinc finger domain (19), suggesting the possibility that Akr1p contains a functionally important metal binding site. However, the palmitoylation assays carried out with different metal chelators and different concentrations of zinc reveal that the Akr1p palmitoylation activity is not metal dependent.

To unravel the catalytic role of the DHYC motif in Akr1p, single mutations of each residue in this motif have been prepared, and their contributions to

both auto- and trans-palmitoylation activity were quantitatively evaluated. The results demonstrate that single mutations of D497, H498 or C500, which are strictly conserved across all known DHHC PATs, abolish the palmitoylation activity of Akr1p. However, mutation of Y499, which is normally a His in other PATs, causes a modest decrease in the activity of Akr1p. To sum up, the D497/H498 dyad is essential for catalytic activity. One possible catalytic role for these residues is to stabilize the nucleophilic thiolate anion in Akr1p for formation of the covalent thioester intermediate, similar to the thiol activation mechanism in thiol proteases and N-acetyltransferases (20-22).

To further explore the important residue(s) responsible for the palmitoylation activity of Akr1p and to identify the auto-palmitoylation site, an extensive mutagenesis study examining the importance of the majority of the cysteine residues of Akr1p has been carried out. These data demonstrate that two single alanine mutations, C500A and C667A abolish auto-palmitoylation of Akr1p. The C500A mutation also abolishes trans-palmitoylation activity while the C667A mutation has little effect on this activity. While either of these cysteines could be the site of auto-palmitoylation, palmitoylation at C667 cannot be an important catalytic intermediate. Furthermore, in the absence of the protein substrate, auto-palmitoylation of the C667A mutant is observed. This result argue that the cysteine at 667 plays a role in enhancing accumulation of the palmitoylated Akr1p, rather than being the site of auto-palmitoylation. Overall, the mutagenesis data suggest that C500 in the

DHYC motif is the most likely candidate for formation of a thioester intermediate in Akr1p.

To further evaluate the location of the palmitoylated cysteine in Akr1p, mass spectrometry has been applied to detect the palmitoylated peptide(s). To prevent the loss of the labile palmitoyl group on the protein during sample preparation, an acyl-biotinyl exchange (ABE) method was applied to the protein before mass spectral analysis (23-25). The palmitoylated peptides digested from Akr1p was enriched using the avidin resin and the sequence evaluated using ESI-FTICR-MS. The peptide containing C500 has been successfully detected, suggesting that C500 is indeed the palmitoylation site of Akr1p. However, there is no convincing mass spectral evidence supporting the palmitoylation on C667. Taken together these data suggest that the palmitoyl thioester at C500 is a reaction intermediate while C667 is not modified but may be responsible for stabilizing the auto-palmitoylated intermediate. This is the first time that the covalent palmitoylated intermediate has been identified, and the importance of the conserved DHHC cysteine has been clearly demonstrated.

These data lead to the proposal of a detailed two-step catalytic mechanism of Akr1p (Figure 3.9). First, the thiol group of C500, stabilized by the D497/H498 dyad, performs a nucleophilic attack to the palmitoyl-CoA thioester. Through an addition-elimination type of reaction, a covalent palmitoyl thioester forms with C500 of Akr1p. In the second step, the thiol of the protein

substrate reacts with the palmitoyl moiety attached to Akr1p through the same type of chemistry proposed in the first step, to form a palmitoyl thioester on the substrate. The enzyme is then released for another cycle of catalysis. Overall, these conclusions provide significant insight into the catalytic mechanism of Akr1p as well as the biological function of palmitoyltransferases.

Substrate selectivity of protein farnesyltransferase

Protein farnesylation is an important posttranslational modification in which a 15-carbon farnesyl group is modified onto the cysteine of substrate proteins resulting in their membrane localization (14, 26-32). Protein farnesyltransferase (FTase) catalyzes this process through recognition of a specific C-terminal "Ca₁a₂X" sequence of substrate proteins (33, 34). In chapter IV, using peptide substrates containing different a₂ residues, it has been discovered that completely conserved tryptophan residues in FTase, although not essential for maintaining the farnesylation activity, play an important role in modulating the substrate selectivity of FTase. A cell lysate-based fluorescent assay has been developed for fast analysis of a large number of FTase mutants. Detailed mutagenesis studies indicate that W102 β and W106 β both control substrate selectivity and the activity of FTase, and the selection patterns are mainly based on the size of the residues at the 102 β and 106 β positions. Mutations of the W102 β residue diminish the substrate selectivity against large amino acids (V, L, F, W) at the peptide a₂ position based on the size of the substituted amino acid, while mutation of W106 β to

Phe is sufficient to eliminate substrate selectivity. The complete conservation of these two amino acids suggests that maintenance of the exact substrate selectivity of FTase is crucial for the *in vivo* activity.

Future Directions

Substrate recognition of Akr1p

We propose to investigate the use of peptides as substrates for Akr1p to develop an assay to facilitate kinetic characterization of the enzyme. Myristoylated and farnesylated peptide substrates have previously been used to assay palmitoyltransferase activity in membrane fractions.

Recent studies of substrate specificity in other PATs suggest that regions distant from the palmitoylated cysteines are important for conferring specificity but are not essential for reactivity (35). Therefore, the model substrates to be developed will be useful for mechanistic studies of PATs and for identifying molecular recognition determinants near the cysteines. The availability of model peptide substrates and enhanced palmitoylation assays will facilitate future studies designed to further analyze substrate recognition and to develop robust high-throughput screens for inhibitors.

A dual cysteine motif is conserved near either the N- or C-terminus in all five known substrates of Akr1p, with sequence alignments revealing little additional residue or motif conservation. This suggests that the dual cysteine terminus may play an important role in the molecular recognition of Akr1p. Therefore, we propose to design peptide substrates for Akr1p based on the

C-terminus of Ypl199c: ${}^+H_3N-ACNCIQSLA-COO^-$. The peptides that could be tested for activity are listed in Table 5.1. The kinetics of palmitoylation of this peptide could be measured by incubation of Akr1p and [3H]palmitoyl-CoA with varying concentrations of peptide substrate under conditions identical to those used in assays with full-length substrate proteins. Control reactions with no added Akr1p or added Akr1p that has been inactivated by previous incubation with bromo-palmitate need to be included. Palmitoylation can be monitored either by thin layer chromatography or HPLC; addition of the hydrophobic palmitoyl group will lead to a change in peptide mobility. If Akr1p does not catalyze palmitoylation of the ACNCIQSLA peptide, the reactivity of longer peptides derived from the C-terminal sequence of Ypl199c (total length of 10, 15 and 20 amino acids) and addition of a lipid group to the peptide can be

Criteria for designing peptide library	Strategies for deriving peptides from AC(1)NC(2)IQSLA
Distance between the two cysteine residues	Insert different numbers of alanines between C(1) and N , as well as N and C(2)
Residues between the two cysteine residues	Change N to other amino acids
Distance of the cysteine residue(s) from the C-terminus	Insert different numbers of alanines after A
Residues close to the cysteine residue(s)	Change I , Q , S to other amino acids

Table 5.1: Peptide library designing criteria and sequence examples for studying the substrate recognition of Akr1p.

explored. The goal in these studies is to find the minimum requirements in a peptide to recover significant activity. These results will provide important information about molecular recognition in Akr1p, as well as produce reagents that will facilitate mechanistic biochemistry on PATs.

Catalytic mechanism of HIP14

As mentioned in the introduction chapter, HIP14 (huntingtin interacting protein 14), also known as DHHC17, is the mammalian homologue of Akr1p (1, 2, 32, 36, 37). HIP14 is known to palmitoylate several neuronal proteins including the huntingtin protein (htt) (2), PSD-95 (38), SNAP-25 (39), GAD65 (40), and synaptotagmin I (41-43). Palmitoylation of these proteins is required for their subcellular trafficking and function (44-46). One of the most noteworthy substrate protein is htt, as the palmitoylation of htt has been suggested to be related to the pathogenesis of Huntington's disease (HD) (37). Mutant htt, which contains 6-35CAG repeats encoding the polyQ expansion at its N-terminus, presents a reduced level of palmitoylation and shows less association with HIP14, and this is proposed to enhance aggregation of the protein (36). Therefore, further studies on the palmitoylation mechanism of HIP14 may disclose its exact pathophysiological roles in neurological disorders and may provide insights into potential ways of developing medical treatment for HD.

HIP14, like Akr1p, is also an integral membrane protein. The crystal structure of HIP14 is not available, but it contains 5 transmembrane domains

(TMDs), with the conserved DHHC sequence located between TMD 3 and 4. Studies have shown that HIP14 Δ DHHC, the DHHC-motif deletion version of the enzyme, loses its palmitoylation activity. Homologous to Akr1p, HIP14 also contains 5 ankyrin repeats in the upstream sequence. A schematic representation of the HIP14 sequence is shown in Figure 5.1.

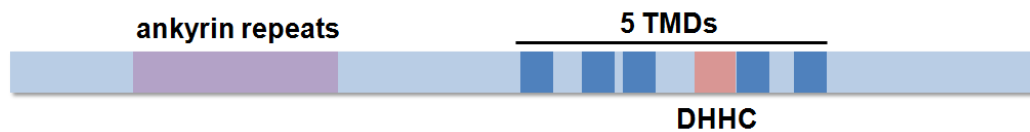


Figure 5.1: Schematic representation of the HIP14 sequence. Great similarity could be observed by comparing this scheme to that of Akr1p in Figure 1.2. HIP14 contains 5 TMDs (dark blue) with the conserved DHHC sequence (pink), and the ankyrin repeats (violet) sit close to the N-terminus.

To study the palmitoylation mechanism of HIP14, the first step will be to express and purify the active enzyme and conduct *in vitro* palmitoylation assays to confirm its activity. Expression clones for HIP14 and its pre-identified substrate PSD-95 have been purchased from GeneCopoeia Inc., and both clones are inserted in the pReceiver-B13 vector shown in Figure 5.2. PSD-95 was chosen at the protein substrate because it is one of the best-characterized proteins among all of the HIP14 substrates. Both HIP14 and PSD-95 have been expressed recombinantly in *E. coli* Rosetta (DE3) strain. We chose to use the bacterial strain because a previous study has reported obtaining small amount of active HIP14 expressed in bacteria (1). I demonstrated reasonable level of soluble expression of PSD-95 but little expression of HIP14 was observed. In the future, the expression conditions and codon usage could be optimized as well as switching to expression in other cell lines optimized for

expression of mammalian proteins. An initial purification of HIP14 and PSD-95 has been conducted. As shown in Figure 5.2, both proteins contain His₆-Sumo tags appended to their N-terminus, allowing for the Ni-affinity purification. The expressed proteins were loaded onto and eluted from a Ni-NTA column. Following addition of Sumo protease to cleave off the His₆-Sumo tag, the protein mixture was loaded onto a second Ni-NTA column. The His₆-Sumo tag should bind to the column while the recombinant protein should elute. However, in the initial attempt there was insufficient active Sumo protease, but this could be easily solved in the future.

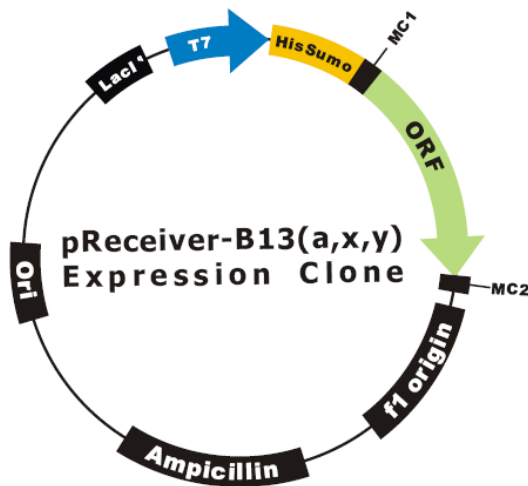


Figure 5.2: pReceiver-B13 vector information for HIP14 and substrate PSD-95. Both proteins are expressed under the control of T7 promoter and purified using the His₆-Sumo tag.

Following protein purification, *in vitro* palmitoylation assays could be performed with HIP14, PSD-95 and [³H]-palmitoyl-CoA, similar to those described with Akrlp. As DHHC motif is essential for HIP14 activity, and HIP14 has also been reported to be auto-palmitoylated, so it is reasonable to hypothesize that the catalytic mechanism of HIP14 is similar to that of Akrlp. If

the HIP14-dependent palmitoylation of PSD-95 is successfully observed, the mechanism could be examined by mutagenesis study and the ABE-coupled mass spectrometry to determine the auto-palmitoylation site(s), as described for Akr1p. If HIP14 can be overexpressed in bacteria, this would provide a significant advantage for studying palmitoylation since it might be possible to obtain large quantities of protein. Therefore many experiments, such as developing a better assay for detailed kinetic analysis, which are difficult to carry out due to the limited amount of the enzyme, will become feasible.

References

1. Huang, K., Yanai, A., Kang, R., Arstikaitis, P., Singaraja, R. R., Metzler, M., Mullard, A., Haigh, B., Gauthier-Campbell, C., Gutekunst, C.-A., Hayden, M. R., and El-Husseini, A. (2004) Huntingtin-interacting protein HIP14 is a palmitoyl transferase involved in palmitoylation and trafficking of multiple neuronal proteins, *Neuron* 44, 977-986.
2. Ohyama, T., Verstreken, P., Ly, C. V., Rosenmund, T., Rajan, A., Tien, A.-C., Haueter, C., Schulze, K. L., and Bellen, H. J. (2007) Huntingtin-interacting protein 14, a palmitoyl transferase required for exocytosis and targeting of CSP to synaptic vesicles, *J. Cell Biol.* 179, 1481-1496.
3. Baekkeskov, S., and Kanaani, J. (2009) Palmitoylation cycles and regulation of protein function, *Mol. Membr. Biol.* 26, 42-54.
4. Charollais, J., and Van Der Goot, F. G. (2009) Palmitoylation of membrane proteins, *Mol. Membr. Biol.* 26, 55-66.
5. Draper, J. M., and Smith, C. D. (2009) Palmitoyl acyltransferase assays and inhibitors (Review), *Mol. Membr. Biol.* 26, 5-13.
6. Ducker, C. E., Griffel, L. K., Smith, R. A., Keller, S. N., Zhuang, Y., Xia, Z. P., Diller, J. D., and Smith, C. D. (2006) Discovery and characterization of inhibitors of human palmitoyl acyltransferases, *Mol. Cancer Therap.* 5, 1647-1659.

7. Roth, A. F., Feng, Y., Chen, L., and Davis, N. G. (2002) The yeast DHHC cysteine-rich domain protein Akr1p is a palmitoyl transferase, *J. Cell Biol.* 159, 23-28.
8. Lobo, S., Greentree, W. K., Linder, M. E., and Deschenes, R. J. (2002) Identification of a Ras palmitoyltransferase in *Saccharomyces cerevisiae*, *J. Biol. Chem.* 277, 41268-41273.
9. Huh, W. K., Falvo, J. V., Gerke, L. C., Carroll, A. S., Howson, R. W., Weissman, J. S., and O'Shea, E. K. (2003) Global analysis of protein localization in budding yeast, *Nature* 425, 686-691.
10. Mukai, J., Liu, H., Burt, R. A., Swor, D. E., Lai, W. S., Karayiorgou, M., and Gogos, J. A. (2004) Evidence that the gene encoding ZDHHC8 contributes to the risk of schizophrenia, *Nat. Genetics* 36, 725-731.
11. Smotrys, J. E., Schoenfish, M. J., Stutz, M. A., and Linder, M. E. (2005) The vacuolar DHHC-CRD protein Pfa3p is a protein acyltransferase for Vac8p, *J. Cell Biol.* 170, 1091-1099.
12. Valdez-Taubas, J., and Pelham, H. (2005) Swf1-dependent palmitoylation of the SNARE Tlg1 prevents its ubiquitination and degradation, *Embo J.* 24, 2524-2532.
13. Sharma, C., Yang, X. H., and Hemler, M. E. (2008) DHHC2 affects palmitoylation, stability, and functions of tetraspanins CD9 and CD151, *Mol. Biol. Cell* 19, 3415-3425.
14. Roth, A. F., Wan, J., Bailey, A. O., Sun, B., Kuchar, J. A., Green, W. N., Phinney, B. S., Yates, J. R., III, and Davis, N. G. (2006) Global analysis of protein palmitoylation in yeast, *Cell* 125, 1003-1013.
15. Babu, P., Deschenes, R. J., and Robinson, L. C. (2004) Akr1p-dependent palmitoylation of Yck2p yeast casein kinase 1 is necessary and sufficient for plasma membrane targeting, *J. Biol. Chem.* 279, 27138-27147.
16. Babu, P., Bryan, J. D., Panek, H. R., Jordan, S. L., Forbrich, B. M., Kelley, S. C., Colvin, R. T., and Robinson, L. C. (2002) Plasma membrane localization of the Yck2p yeast casein kinase 1 isoform requires the C-terminal extension and secretory pathway function, *J. Cell Sci.* 115, 4957-4968.

17. Putilina, T., Wong, P., and Gentleman, S. (1999) The DHHC domain: A new highly conserved cysteine-rich motif, *Molecular and Cellular Biochemistry* 195, 219-226.
18. Mitchell, D. A., Vasudevan, A., Linder, M. E., and Deschenes, R. J. (2006) Protein palmitoylation by a family of DHHC protein S-acyltransferases, *J. Lipid Res.* 47, 1118-1127.
19. Bohm, S., Frishman, D., and Mewes, H. W. (1997) Variations of the C2H2 zinc finger motif in the yeast genome and classification of yeast zinc finger proteins, *Nucleic Acids Res.* 25, 2464-2469.
20. Sfakianos, M. K., Wilson, L., Sakalian, M., Falany, C. N., and Barnes, S. (2002) Conserved residues in the putative catalytic triad of human bile acid coenzyme A : amino acid N-acyltransferase, *J. Biol. Chem.* 277, 47270-47275.
21. O'Byrne, J., Hunt, M. C., Rai, D. K., Saeki, M., and Alexson, S. E. H. (2003) The human bile acid-CoA : amino acid N-acyltransferase functions in the conjugation of fatty acids to glycine, *J. Biol. Chem.* 278, 34237-34244.
22. Shonsey, E. M., Eliuk, S. M., Johnson, M. S., Barnes, S., Falany, C. N., Darley-Usmar, V. M., and Renfrow, M. B. (2008) Inactivation of human liver bile acid CoA : amino acid N-acyltransferase by the electrophilic lipid, 4-hydroxynonenal, *J. Lipid Res.* 49, 282-294.
23. Zhao, Z., Hou, J., Xie, Z., Deng, J., Wang, X., Chen, D., Yang, F., and Gong, W. (2010) Acyl-biotinyl exchange chemistry and mass spectrometry-based analysis of palmitoylation sites of in vitro palmitoylated rat brain tubulin, *Protein J.* 29, 531-537.
24. Drisdell, R. C., and Green, W. N. (2004) Labeling and quantifying sites of protein palmitoylation, *BioTechniques* 36, 276-282,284-285.
25. Yang, W., Di Vizio, D., Kirchner, M., Steen, H., and Freeman, M. R. (2010) Proteome scale characterization of human S-acylated proteins in lipid raft-enriched and non-raft membranes, *Mol. Cell. Proteomics* 9, 54-70.
26. Lane, K. T., and Beese, L. S. (2006) Structural biology of protein farnesyltransferase and geranylgeranyltransferase type I, *J. Lipid Res.* 47, 681-699.

27. Long, S. B., Casey, P. J., and Beese, L. S. (2002) Reaction path of protein farnesyltransferase at atomic resolution, *Nature* 419, 645-650.
28. Liang, P. H., Ko, T. P., and Wang, A. H. (2002) Structure, mechanism and function of prenyltransferases, *Eur. J. Biochem.* 269, 3339-3354.
29. Chakrabarti, D., Da Silva, T., Barger, J., Paquette, S., Patel, H., Patterson, S., and Allen, C. M. (2002) Protein farnesyltransferase and protein prenylation in *Plasmodium falciparum*, *J. Biol. Chem.* 277, 42066-42073.
30. Park, H. W., Boduluri, S. R., Moomaw, J. F., Casey, P. J., and Beese, L. S. (1997) Crystal structure of protein farnesyltransferase at 2.25 angstrom resolution, *Science* 275, 1800-1804.
31. Casey, P. J., and Seabra, M. C. (1996) Protein Prenyltransferases, *J. Biol. Chem.* 271, 5289-5292.
32. Yanai, A., Huang, K., Kang, R., Singaraja, R. R., Arstikaitis, P., Gan, L., Orban, P. C., Mullard, A., Cowan, C. M., Raymond, L. A., Drisdell, R. C., Green, W. N., Ravikumar, B., Rubinsztein, D. C., El-Husseini, A., and Hayden, M. R. (2006) Palmitoylation of huntingtin by HIP14 is essential for its trafficking and function, *Nat. Neurosci.* 9, 824-831.
33. Reid, T. S., Terry, K. L., Casey, P. J., and Beese, L. S. (2004) Crystallographic analysis of CaaX prenyltransferases complexed with substrates defines rules of protein substrate selectivity, *J. Mol. Biol.* 343, 417-433.
34. Fu, H.-W., and Casey, P. J. (1999) Enzymology and biology of CaaX protein prenylation, *Recent Prog. Horm. Res.* 54, 315-343.
35. Nadolski, M. J., and Linder, M. E. (2009) Molecular recognition of the palmitoylation substrate Vac8 by its palmitoyltransferase Pfa3, *J. Biol. Chem.* 284, 17720-17730.
36. Ducker, C. E., Stettler, E. M., French, K. J., Upson, J. J., and Smith, C. D. (2004) Huntingtin interacting protein 14 is an oncogenic human protein: palmitoyl acyltransferase, *Oncogene* 23, 9230-9237.
37. Singaraja, R. R., Hadano, S., Metzler, M., Givan, S., Wellington, C. L., Warby, S., Yanai, A., Gutekunst, C.-A., Leavitt, B. R., Yi, H., Fichter, K., Gan, L., McCutcheon, K., Chopra, V., Michel, J., Hersch, S. M., Ikeda, J.-E., and Hayden, M. R. (2002) HIP14, a novel ankyrin

domain-containing protein, links huntingtin to intracellular trafficking and endocytosis, *Hum. Mol. Genet.* 11, 2815-2828.

38. Fukata, M., Fukata, Y., Adesnik, H., Nicoll, R. A., and Brecht, D. S. (2004) Identification of PSD-95 Palmitoylating enzymes, *Neuron* 44, 987-996.
39. Veit, M. (2000) Palmitoylation of the 25-kDa synaptosomal protein (SNAP-25) in vitro occurs in the absence of an enzyme, but is stimulated by binding to syntaxin, *Biochem. J.* 345, 145-151.
40. Christgau, S., Aanstoot, H. J., Schierbeck, H., Begley, K., Tullin, S., Hejnaes, K., and Baekkeskov, S. (1992) Membrane anchoring of the autoantigen GAD65 to microvesicles in pancreatic β -cells by palmitoylation in the amino-terminal domain, *J. Cell Biol.* 118, 309-320.
41. El-Husseini, A. E.-D., Schnell, E., Dakoji, S., Sweeney, N., Zhou, Q., Prange, O., Gauthier-Campbell, C., Aguilera-Moreno, A., Nicoll, R. A., and Brecht, D. S. (2002) Synaptic strength regulated by palmitate cycling on PSD-95, *Cell* 108, 849-863.
42. El-Husseini, A. E., Craven, S. E., Chetkovich, D. M., Firestein, B. L., Schnell, E., Aoki, C., and Brecht, D. S. (2000) Dual palmitoylation of PSD-95 mediates its vesiculotubular sorting, postsynaptic targeting, and ion channel clustering, *J. Cell Biol.* 148, 159-171.
43. Heindel, U., Schmidt, M. F. G., and Veit, M. (2003) Palmitoylation sites and processing of synaptotagmin I, the putative calcium sensor for neurosecretion, *FEBS Lett.* 544, 57-62.
44. Kanaani, J., Patterson, G., Schaufele, F., Lippincott-Schwartz, J., and Baekkeskov, S. (2008) A palmitoylation cycle dynamically regulates partitioning of the GABA-synthesizing enzyme GAD65 between ER-Golgi and post-Golgi membranes, *J. Cell Sci.* 121, 437-449.
45. Kanaani, J., El-Din, E.-H. A. E.-D., Aguilera-Moreno, A., Diacovo, J. M., Brecht, D. S., and Baekkeskov, S. (2002) A combination of three distinct trafficking signals mediates axonal targeting and presynaptic clustering of GAD65, *J. Cell Biol.* 158, 1229-1238.
46. Solimena, M., Dirx, R., Jr., Radzynski, M., Mundigl, O., and De, C. P. (1994) A Signal Located within Amino Acids 1-27 of GAD65 Is Required for Its Targeting to the Golgi Complex Region, *J. Cell Biol.* 126, 331-341.